2012

Generation of singlet oxygen from fragmentation of monoactivated 1,1-dihydroperoxides

Jiliang Hang
University of Nebraska-Lincoln

Prasanta Ghorai
University of Nebraska-Lincoln

Solaire A. Finkenstaedt-Quinn
Macalester College

Ilhan Findik
Macalester College

Emily Sliz
Macalester College

See next page for additional authors

Hang, Jiliang; Ghorai, Prasanta; Finkenstaedt-Quinn, Solaire A.; Findik, Ilhan; Sliz, Emily; Kuwata, Keith T.; and Dussault, Patrick, "Generation of singlet oxygen from fragmentation of monoactivated 1,1-dihydroperoxides" (2012). *Patrick Dussault Publications.* 27.
http://digitalcommons.unl.edu/chemistrydussault/27

Authors

Jiliang Hang, Prasanta Ghorai, Solaire A. Finkenstaedt-Quinn, Ilhan Findik, Emily Sliz, Keith T. Kuwata, and Patrick Dussault

Generation of singlet oxygen from fragmentation of monoactivated 1,1-dihydroperoxides

Jiliang Hang[a], **Prasanta Ghorai**[a,§], **Solaire A. Finkenstaedt-Quinn**[b], **Ilhan Findik**[b], **Emily Sliz**[b], **Keith T. Kuwata**[b], and **Patrick H. Dussault**[*,a]

[a]Department of Chemistry, University of Nebraska–Lincoln, Lincoln, NE 68588-0304

[b]Department of Chemistry, Macalester College, Saint Paul, MN 55105-1899

Abstract
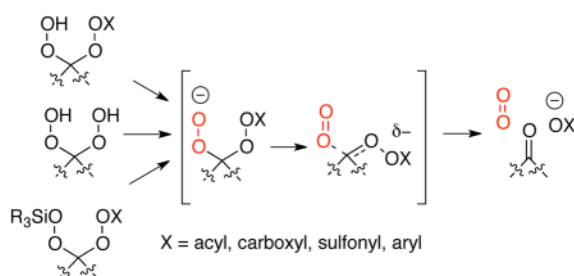
The first singlet excited state of molecular oxygen ($^1O_2$) is an important oxidant in chemistry, biology, and medicine. $^1O_2$ is most often generated through photosensitized excitation of ground state oxygen. $^1O_2$ can also be generated chemically through the decomposition of hydrogen peroxide and other peroxides. However, most of these "dark oxygenations" require water-rich media associated with short $^1O_2$ lifetimes, and there is a need for oxygenations able to be conducted in organic solvents. We now report that monoactivated derivatives of 1,1-dihydroperoxides undergo a previously unobserved fragmentation to generate high yields of singlet molecular oxygen ($^1O_2$). The fragmentations, which can be conducted in a variety of organic solvents, require a geminal relationship between a peroxyanion and a peroxide activated towards heterolytic cleavage. The reaction is general for a range of skeletal frameworks and activating groups and, via in situ activation, can be applied directly to 1,1-dihydroperoxides. Our investigation suggests the fragmentation involves rate-limiting formation of a peroxyanion that decomposes via a Grob-like process.

INTRODUCTION

Singlet molecular oxygen ($^1O_2$ is an important oxidant in chemistry, biology, and medicine, and the source of energy for chemical oxygen-iodine (COIL) lasers.[1a–c] Several typical reactions are illustrated in Scheme 1.[2,3,4]

corresponding author: pdussault1@unl.edu.
§Current address: Department of Chemistry, Indian Institute of Science and Education Research, Bhopal, India.

Supporting Information

Details regarding experimental procedures, spectral listings for new molecules, ^1H and ^{13}C NMR data for new compounds, thermal analysis for **1a** and **1c**, conformational analysis of model monoperoxyacetate and monopercarbonate structures, and optimized coordinates of calculated structures described in the paper. This material is available free of charge via the Internet at http://pubs.acs.org.

$^1O_2$ is most commonly generated through dye-sensitized excitation of ground state dioxygen $(^3O_2)$[1b, 5] However, preparative application can be limited by the need for high-volume photoreactors, as well as by safety issues associated with reactions under oxygen.[6] Following the discovery of the chemical generation of $^1O_2$ from the reaction of hydrogen peroxide and bleach,[7] a number of methods for "dark oxygenation" have been reported based upon decomposition of ozone,[8] hydrogen peroxide,[1a, 9,10,11,12,13] hydrotrioxides,[14,15] and several inorganic peroxides.[16,17] The majority of these methods require the use of water-enriched media, conditions associated with a very short $^1O_2$ lifetime.[18] However, preparative oxidations have been achieved for relatively reactive substrates using biphasic or emulsion conditions.[19] Generation of $^1O_2$ in organic solvents has been achieved through thermal decomposition of calcium peroxide (suspension),[16] arene endoperoxides,[20] phosphite ozonides,[21] silyl hydrotrioxides,[14] and alkyl hydrotrioxides.[15] However, the latter class of reagents are often thermally unstable and must be prepared immediately prior to reaction. Major classes of reagents for chemical generation of $^1O_2$ are overviewed below.
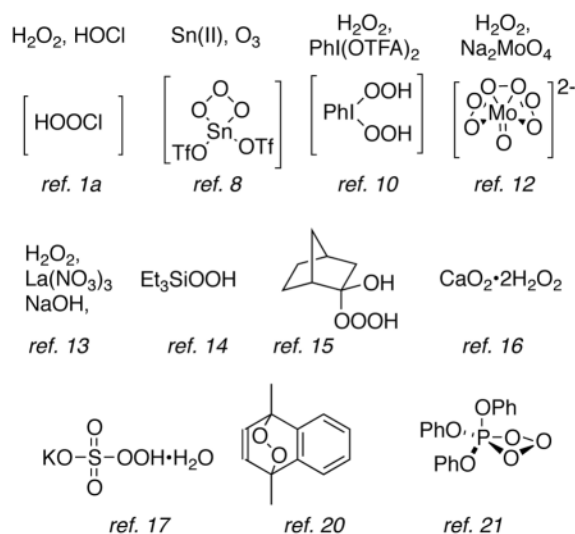
Our interest in this area arose during investigations of a "reductive ozonolysis" of alkenes.[22] This transformation was hypothesized to involve nucleophilic addition of amine N-oxides to short-lived carbonyl oxides to generate peroxyanion/oxyammonium acetals. These previously unknown intermediates were surmised to undergo fragmentation to generate the observed "reduction" products, along with a molecule of $^1O_2$, and a molecule of amine (eq. 1). Reasoning that a similar fragmentation should be possible for any species featuring a geminal relationship between a peroxyanion and a heterolytically activated O-X bond, we explored the reactivity of monoperesters of readily available 1,1-dihydroperoxides. Deprotonation of these species resulted in rapid fragmentation accompanied by highly efficient liberation of $^1O_2$ (eq. 2).[23] We now describe our investigations into the scope and mechanism of this process.
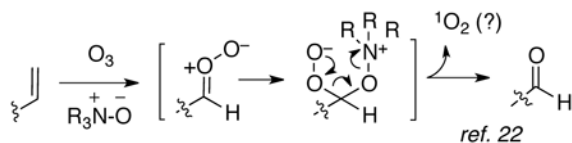
(1)
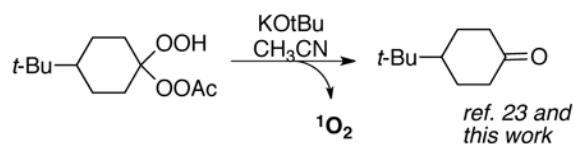
(2)

RESULTS

### Range of acetal/ketal scaffolds

1,1-Bishydroperoxides **1a**–**8a** were prepared through Re(VII)-promoted acetalization of the corresponding ketones (Scheme 2).[24] Monoacetylation with acetic anhydride and pyridine furnished isolable monoperesters (**1b**–**4b**, **6b**–**8b**); [25] the exception was adamantanone dihydroperoxide (**5a**), which instead underwent ring expansion to a lactone. 1,1-Dihydroperoxides derived from aldehydes (not shown) reacted to form highly polar byproducts, presumably reflecting E_1cb fragmentation of peresters bearing an adjacent C-H.[26]

Thermal stability

Dihydroperoxide **1a**, which melts without decomposition at 78–80 °C and is not detonated by a sharp hammer blow, undergoes a highly exothermic decomposition when heated beyond 100 °C. Monoacetate **1b** is stable for prolonged periods at freezer temperature and for days at room temperature, but undergoes an exothermic decomposition beginning at approximately 76 °C (Figure 1). Monocarbonate **1d** undergoes partial decomposition within days at room temperature to form a substituted caprolactone and undergoes exothermic decomposition when heated above 70 °C.

Assay for $^1O_2$

The release of $^1O_2$ was quantified by chemical reaction with terpinene (**T**) or diphenylisobenzofuran (DPBF, **D**). Terpinene (**T**) undergoes addition of $^1O_2$ to form the stable endoperoxide ascaridole (**T-O$_2$** eq. 3).[27] Furan **D** undergoes an even faster addition to generate diketone D-O$_2$ via an unstable endoperoxide (eq 4). **T-O$_2$** and **D-O$_2$** are easily quantified through isolation or by NMR or GC/MS analysis in the presence of an internal standard. Details are provided in Supporting Information.
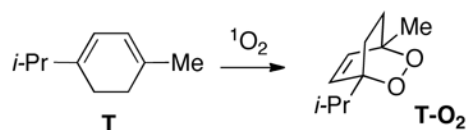
(3)
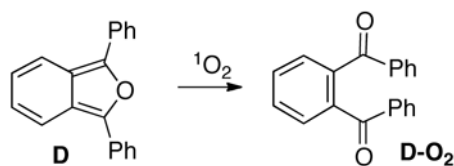
Variation of the bisperoxyacetal skeleton

We next investigated the generality of the fragmentation across a range of peroxyacetal skeletons. Solutions of monoesters **1b**–**4b**, and **6b**–**8b** were decomposed with TBAF in the presence of 0.5 equiv of terpinene (Table 1); the relative stoichiometry was chosen to facilitate product separation. Addition of base was accompanied by the disappearance (TLC) of the monoesters and the appearance of the corresponding ketone and **T-O$_2$**. The yield of trapped $^1O_2$ varied little with peroxyacetal structure. By comparison, a 1,1-dihydroperoxide (**1a**) did not react under the reaction conditions.

Influence of peroxyacetal backbone on relative reactivity

The decomposition of mixtures of dihydroperoxide monoesters in the presence of a limiting amount of TBAF revealed little difference in reactivity between acyclic and cyclic substrates or between cyclic substrates possessing different amounts of ring strain (Scheme 3).

Influence of Solvent

Decomposition of monoester **1b** in a number of solvent systems (Table 2) revealed the yield of dioxygen transfer (as **T-O$_2$**) to be increased in solvents associated with greater $^1O_2$ lifetime.[18] The exception was for perfluorinated media, in which reaction appeared limited by reagent solubility. However, improved yields were possible in fluorocarbon/CH$_3$CN mixtures.

Order of addition

In early experiments involving decomposition of monoperester **1b**,[23] we had observed the yield of $^1O_2$ to vary with the relative order of addition of KOtBu and perester, suggesting the possibility of disproportionation to form poorly reactive bisperesters (vida infra). However, a reinvestigation of the phenomenon using peracetate **1b** and TBAF revealed insignificant differences (Table 3).

Range of activating groups

Base-promoted decomposition of a perbenzoate (**1c**) and a percarbonate (**1d**) proceeded rapidly to furnish yields of trapped $^1O_2$ similar to those observed for the peracetate (Table 4). Attempts to prepare the analogous percarbamate or persulfonate led only to ring-expansion.

Influence of Base/Counterion

As shown in Table 5, the decomposition of **1b** in the presence of LiN(TMS)$_2$ resulted in much lower yields of $^1O_2$ trapping compared to reactions involving the comparably basic KOtBu or TBAF.

Effect of temperature and rate of addition

The base-promoted decomposition of the 1,1-dihydroperoxide monoesters is rapid; for example, rapid (1–2 sec) injection of 1*M* THF solution of TBAF into a rapidly stirring solution of monoester **1a** (1M in THF) results in immediate effervescence. Although the decomposition of monoperester **1b** proceeds significantly faster at higher temperatures, the yield of trapped $^1O_2$ is improved at lower temperatures (Table 6, entries 1–4). Slowing the rate of reagent addition resulted in a significant increase in the yield of trapped $^1O_2$ (entries 5 and 6).

Attempted gas-phase transfer

The inverted relationship between the yield of oxygen transfer and the rate of peroxide decomposition (Table 6, entries 5 and 6) led us to investigate whether $^1O_2$ could be escaping into the gas phase. The headspace of a septum-covered flask containing an acetonitrile solution of perester **1b** was exhausted via a short Teflon tube into an acetonitrile solution of terpinene (**T**). Rapid (≤ 10 sec) addition of TBAF/THF into the solution of monoester led to vigorous effervescence and net efflux of a high volume of gas through the receiving solution. However, no significant amount of ascaridole (**T-O₂**) was detected.

Generation of the peroxyanion via nucleophilic desilylation

We investigated an alternative route to the presumed peroxyanion intermediate through nucleophilic desilylation. Monotrialkylsilylated substrates were readily available via silylation of the monoesters (Scheme 4). Curiously, the perester carbonyl remained invisible by ^{13}C NMR despite use of pulse delays (≥ 5 sec) or the addition of Ni(acac)$_2$ as a relaxation agent.[28] The perester carbonyl could be observed as a single sharp signal at 167.8 ppm if spectra were acquired at ≤ 40 °C (9a, 9b, 11). We are unsure as to the basis of this phenomenon, which was not encountered with either the monoperesters (e.g. **1b**) or a bisperester (**16**, vida infra).

Reaction of the silylated monoesters with TBAF in the presence of a trapping agent resulted in yields of transferred $^1O_2$ equal to or exceeding those observed through deprotonation of the dihydroperoxide monoesters (Table 7).

Reactivity of bissilyl and bisacyl derivatives

Preparation of bissilyl and bisacyl derivatives of dihydroperoxide **1a** are illustrated in Scheme 5. The bistriethylsilyl derivative (**15**) was an oily compound that decomposed at ~ 140 °C. The bisacyl derivative (**16**) was a solid that melted without decomposition at 54–56 °C.[29] Saponification of **16** with cesium hydroxide in CH₃CN resulted in reformation of the parent ketone and generation of $^1O_2$. Bissilyl ether **15** was decomposed by n-Bu₄NF without apparent transfer of oxygen.

Tandem activation and fragmentation

Intrigued by the possibility of generating and decomposing the monoactivated bisperoxide intermediate *in situ*, we investigated the reactivity of dihydroperoxide **1a** towards four classes of activating agents: an electron-poor nitrile, a heteroaromatic known to undergo S$_N$Ar reaction with tertiary hydroperoxides,[30] a sulfonyl chloride, and an acid anhydride. Our initial assay qualitatively monitored the formation of ketone upon addition of base to solutions containing the dihydroperoxide and the individual additive (Table 8). In each case, the addition of stoichiometric electrophile and excess KOtBu resulted in rapid conversion of **1a** to 4-*tert*-butylcyclohexanone without any evidence of intermediates. Although these reactions should in theory require only two equivalents of base, we found that four equivalents were invariably required to achieve complete consumption of the dihydroperoxide.

We next reinvestigated the most promising conditions in the presence of a trapping agent. The yields of oxygen transfer, which were as good as those obtained from the dihydroperoxide monoesters, were similar regardless of activating agent (Table 9).

Preparative Reactions

Our experiments until this point had focused on the yield of liberated oxygen. We next investigated the amount of reagent necessary to completely consume a trapping reagent

using either the fragmentation of a preformed perester (**1b**, **8b**) or the tandem activation/ fragmentation of dihydroperoxide **1a**. As illustrated in Table 10, complete consumption of terpinene was generally possible with as little as 5 equiv. of reagent.

Reaction order and apparent rate constant

The base-promoted decomposition of monoperbenzoate **1c** was monitored at 272 nm (Figure 2). In the first experiment, rapidly stirred THF solutions (0.5 mM) of dihydroperoxide monoester **1c** were mixed with THF solutions of TBAF ranging in concentration from 0.50 to 2.00 m*M*. The reaction solutions were then placed in the UV spectrophotometer, and the absorbance at 272 nm monitored for 1.0 minute. Plotting the log[TBAF]$_{initial}$ against the $-\log(\Delta_{abs})$ revealed an apparent reaction order of 0.94 in TBAF and a calculated rate constant of 10^2 L/mol-sec; details are provided in the Supporting Information. Repeating the experiment with a constant concentration of TBAF and varying concentrations of **1c** indicated an order of 1.2 in peroxide and a calculated rate constant of 10^2 L/mol-sec. Overall, the results support a mechanism that is first-order in both peroxide and base.

Theoretical investigations of the putative fragmentation step

The base-promoted fragmentation of the monoactivated 1,1-dihydroperoxides could conceivably involve either a concerted Grob-like fragmentation of a zwitterion or the formation and decomposition of an intermediate trioxetane.[31ab] The latter pathway cannot be simply disregarded. Dioxetanes are readily formed by intramolecular nucleophilic displacements of β–halo alkylhydroperoxides,[32] while dioxiranes are generated with good efficiency from intramolecular attack of a hemiacetal oxygen on an electrophilically activated peroxide. [33] We therefore turned to density functional theory (specifically, the B3LYP hybrid functional and the 6–31+G(d,p) basis set) to investigate each transition state (**TS**) and intermediate (**MIN**) involved in the decomposition of the monoactivated dihydroperoxides. We focused our efforts on heterolytic processes as fragmentations involving radical intermediates would be expected to generate $^3O_2$ and not $^1O_2$.

Decomposition of the monoperester

Comparison of the predicted zero-point corrected relative energies for transition states and intermediates in the decomposition of a peroxyanion found a concerted fragmentation to offer the lowest energy pathway for generation of $^1O_2$ and a carbonyl (Scheme 6). The alternative pathway is disfavored by the strain in the trioxetane intermediate, presumably reflecting electron pair repulsions, and by the high barrier for loss of $^1O_2$. (The combined energy of the trioxetane and acetate is 6.5 kcal/mol *higher* than the trioxetane formation transition state. This reflects the existence of an exit channel complex of the trioxetane and acetate that is bound by 16.3 kcal/mol.) For simplicity, calculations were performed on an unsubstituted acetal framework. Repeating the computations on a more substituted acetal framework (not shown) lowered the energies of most intermediates and transition states on the order of 5 kcal/mole but did not, in general, alter the relative energies of the transition states The exception was the transition state for trioxetane formation, which increased significantly in energy for the more substituted scaffold. Optimized coordinates for calculated structures are provided in the Supporting Information.

Conformational analysis of the peroxyanion

Figure 3 shows the optimized geometries of two of the 12 possible conformers of the peroxyanion in the unsubstituted acetate system. There is a striking difference in energy between conformers **MIN-1a** (and the structurally and energetically similar **MIN-1b**, not shown) versus the remaining ten conformers, exemplified by **MIN-1c**, all of which lie at least 8 kcal/mol higher in energy.[34]

The most stable conformer (**MIN-1a**, Figure 3a) possesses two pairs of synclinal O-O and C-O bonds, allowing for hyperconjugation of oxygen lone pairs from O_2 and O_3 into neighboring C-O antibonding orbitals (C_1-O_3; C_1-O_2) The antiperiplanar orientation of the C_2-O_5 and O_3-O_4 bonds minimizes the repulsion between the lone pairs on O_3 and O_5. Several lines of evidence suggest the presence of a stabilizing intramolecular hydrogen bond between the anionic oxygen (O_1) and the C_3-H_1 bond. The O_1---H_1 distance is less than 1.9 Å, and the C_3-H_1 bond is 0.03 Å longer than the other two methyl C-H bonds. The C_3-H_1 bond also vibrates at a much lower frequency (2693 cm^{-1}) compared with the other hydrogen atoms on C_3 (~3100 cm^{-1}). These data support a normal hydrogen bond in which electron density from the peroxyanion is delocalized into the sigma antibonding orbital of the C-H bond. There is precedence for normal C-H hydrogen bonds in the literature.[35] Conformer **MIN-1b** (not shown) is structurally very similar to **MIN-1a**. In particular, **MIN-1b** also possesses an intramolecular hydrogen bond, with an O_1---H_1 distance of 1.851 Å. In contrast, the O_1-O_2 and C_1-O_3 bonds in conformer **MIN-1c** are antiperiplanar instead of synclinal (Fig. 3b). This difference deprives **MIN-1c** of the intramolecular hydrogen bond and removes one of the hyperconjugative interactions, raising the energy of **MIN-1c** by 7–8 kcal/mol.[34]

Conformational analysis of the Grob-like transition states

The lowest energy conformer of the transition state for Grob fragmentation, **TS-2** (Figure 4a), is predicted to lie only 6.7 kcal/mol higher in energy than the ground state reactant conformer; **TS-2** benefits from antiperiplanar O_2-C_1 and O_3-O_4 bonds. As described by Grob,[31a,b] this arrangement facilitates fragmentation since electron density in the O_2-C_1 bond can be donated into the sigma antibonding orbital of the O_3-O_4 bond. Intrinsic reaction coordinate calculations reveal that **TS-2** does not correlate directly with any of the reactant conformers (see the Supporting Information), but rather the unnumbered van der Waals complex shown in Figure 4b. This complex lies only 0.4 kcal/mol below the transition state in energy, and the excess −1 charge in the complex is evenly distributed between the $OOCH_2O$ and $OC(O)CH_3$ moieties.

Another fragmentation transition state, **TS-2*** (Figure 4c), which is only 0.7 kcal higher in energy than **TS-2,** is derived from the most stable peroxyanion conformer, **MIN-1a** (Figure 3a). **TS-2*** lacks antiperiplanar O_2-C_1 and O_3-O_4 bonds but is stabilized by a weak intramolecular hydrogen bond between O_1 and H_1: the C_3-H_1 bond is 0.01 Å longer than the other two methyl C-H bonds, and the C_3-H_1 stretch is ~200 cm^{-1} to the red of the other methyl C-H stretches.

For a more substituted system (methine rather than methylene acetal), the two lowest energy transition states are structurally analogous to those shown in Figures 3 and 4. However, the methylated transition state lacking antiperiplanar O_2-C_1 and O_3-O_4 bonds, but possessing an intramolecular hydrogen bond, is slightly (0.8 kcal/mol) lower in energy than the one possessing antiperiplanar O_2-C_1 and O_3-O_4 bonds.

Pathways for fragmentation of the monopercarbonate

We were interested in whether the pathways for fragmentation varied with the nature of the electrophilic activating group. Scheme 7 shows calculated zero-point corrected relative energies for selected intermediates and transition states in the decomposition of a peroxyanion derived from a dihydroperoxide monopercarbonate, as modeled for the unsubstituted (formaldehyde acetal) backbone.[34] The methyl carbonate nucleofuge in the percarbonate stabilizes negative charge more effectively than the acetate leaving group in the perester, as indicated by a calculated *E* of decomposition ~6 kcal/mol more exothermic than in the acetate series (compare Schemes 6 and 7). The two lowest energy pathways for

liberation of $^1O_2$ from the deprotonated monocarbonate are illustrated in Scheme 7. A third pathway involving an intermediate trioxetane, analogous to one illustrated in Scheme 6 for the monoperester, was predicted to involve a very high energy transition state and is not described here.

Concerted fragmentation of the most stable conformer of the acyclic peroxyanion of the dihydroperoxide monocarbonate is calculated to occur with a significantly lower activation barrier (4.3 vs. 6.7 kcal/mol) compared with the corresponding transformation of the perester (Scheme 6). We note that bond breaking in **TS-4** (see Figure 5) is significantly less advanced than in the most stable transition state for the acetate system (**TS-2**, Figure 4a), and is comparable to the bond breaking that exists in the second most stable acetate conformer (**TS-2***, Figure 4c). As is the case for the most stable peracetate transition state conformer, **TS-4** (Figure 5) benefits from antiperiplanar O_2-C_1 and O_3-O_4 bonds. However, overlap of the $\sigma(O_2$-$C_1)$ and $\sigma^*(O_3$-$O_4)$ orbitals is not optimal, since the dihedral angle between the O_2-C_1 and O_3-O_4 bonds is significantly less than 180°.

The peroxyanion derived from the dihydroperoxide monocarbonate can also undergo decomposition via a six-membered ring intermediate (Scheme 7). The barrier for cyclization to the 1,2,4,5-tetroxan-3-oxide is predicted to be nearly identical to that for fragmentation of the acyclic peroxyanion. The preference for the cyclic isomer is substantial: the ground state conformer of the tetroxane oxide (**MIN-3a**) is over 9 kcal/mol lower in energy that the most stable acyclic conformation (**MIN-3d**).[34] reflecting the significant number of hyperconjugative interactions between C-O sigma antibonding orbitals and oxygen lone pairs in the chair-like conformation of the cyclic isomer. Figure 5b shows the transition state, **TS-5**, for the fragmentation of the cyclic peroxide to generate a carbonyl, $^1O_2$, and a methyl carbonate anion. The activation barrier for fragmenting the cyclic structure, while greater than that for fragmenting the acyclic peroxyanion (9.6 vs. 4.3 kcal/mol), is still lower than that for ring opening to the acyclic form. As was the case in the monoester series, fragmentation of a more substituted acetal is predicted to be more favorable by ~ 5 kcal/mol; however, there is predicted to be a minimal impact, typically less than 1 kcal/mol, on the relative energies of individual pathways.

Comparison with intermediates in "reductive" ozonolysis

We also modeled analogous intermediates and transition states postulated to be involved in the fragmentation of zwitterionic peroxy/ammonium acetals during reductive ozonolyses (Scheme 8).[22] As a result of a stabilizing electrostatic interaction, the zwitterionic acetal is predicted to strongly favor a ground-state conformation with a gauche O-C-O-O. The low-energy transition state for fragmentation lies less than 5 kcal/mol above the ground state; the fragmentation itself is predicted to be significantly downhill. (These calculations are based upon a zwitterionic acetal incorporating a fully substituted nitrogen; repeating these calculations on a species containing one or more N-H bonds predicted proton transfer would take place in preference to fragmentation).

DISCUSSION

The reactions described here constitute a new class of fragmentations involving a peroxyanion geminally linked to an electrophilically activated peroxide.[36] The peroxyanion can be generated via deprotonation, desilylation, or deacylation. The higher yields observed in the presence of tetraalkylammonium or potassium counterions vs. lithium point to the potential importance of anion dissociation, but must be interpreted with caution given the potential for different levels of $^1O_2$ quenching by the different bases and their protonated byproducts. The data from competition reactions suggests that deprotonation may be rate limiting.
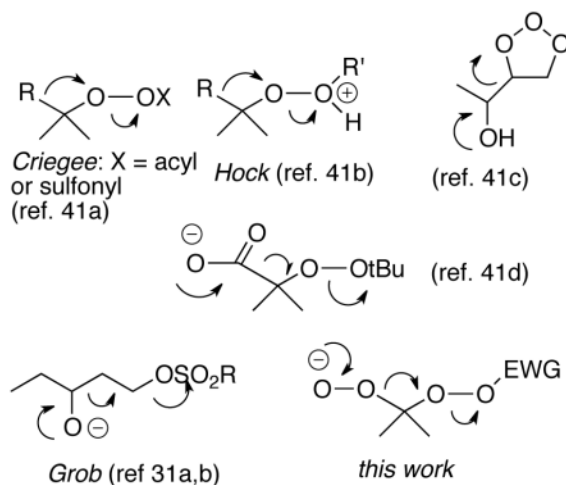
The ability to achieve tandem activation and fragmentation of readily available 1,1-dihydroperoxides is noteworthy. Hydroperoxyimidates, while not isolable, have been postulated as short-lived intermediates in epoxidations.[37] Alkylperoxytriazenes, which have been prepared from tertiary hydroperoxides via S_NAr reactions, have mainly been of interest as radical initiators.[30]

Relationship between reaction conditions and efficiency of $^1O_2$ transfer

The observation of more efficient oxygen transfer in deuterated or halogenated solvents is in keeping with the enhanced lifetime of $^1O_2$ in solvents lacking C-H, O-H, or N-H bonds.[18] The failure of the results to scale linearly to $^1O_2$ lifetime results from the presence of the trapping substrate, by definition a potent quenching agent. The observation of improved trapping yields at reduced reaction temperatures is not unexpected. While the lifetime of $^1O_2$ in organic solvents varies little with temperature,[38] reaction of $^1O_2$ with electron-rich alkenes has a near-zero enthalpy of activation and a strongly negative entropy of activation;[39] photosensitized oxygenations are often quite rapid even at low temperatures.[5] However, the observation of increased yields from a slower rate of fragmentation is not easily explained. Although rapid injection of reactants was associated with significant effervescence, we could detect no evidence for transfer of $^1O_2$ into the gas phase. We therefore suspect that yields of oxygen transfer under conditions associated with higher $^1O_2$ flux are limited by self-quenching.[40]

Relationship to known fragmentations

A number of heterolytic fragmentations involve formation of a new C-O bond through migration of a C-C sigma bond with cleavage of an activated O-O bond.[41a-d] These include the Criegee rearrangement of peresters,[41a] the Hock rearrangement of protonated or Lewis acid-complexed peroxides,[41b] the fragmentation of primary ozonides derived from allylic alcohols,[41c] and the fragmentation of 2-hydroperoxycarboxylates.[41d] Overall, the new fragmentation bears a close topological resemblance to the Grob fragmentation, an extended elimination reaction in which formation of C=O and C=C pi systems drives the cleavage of C-C and C-X sigma bonds.[31ab] The fragmentations described above are likely to require a similar antiperiplanar alignment of the breaking peroxyanion C-O with the activated O-O bond.

Criegee: X = acyl or sulfonyl (ref. 41a)   Hock (ref. 41b)   (ref. 41c)

(ref. 41d)

Grob (ref 31a,b)   this work

CONCLUSIONS

The decomposition of monoactivated derivatives of 1,1-dihydroperoxides is established as a new peroxide fragmentation that provides an efficient means for preparative generation of $^1O_2$ in organic media.

EXPERIMENTAL SECTION

Standard procedure for synthesis of 1,1-dihydroperoxides

1,1-Dihydroperoxides were prepared by a reported procedure.[24]

1,1-Dihydroperoxy-4-*tert*-butylcyclohexane (1a)—84%, white solid, mp 81–83°C, R_f = 0.33 (30% EA/Hex), other physical data were identical to literature reports.[24]

1,1-Dihydroperoxycycloheptane (2a)—83%, white solid, mp 59–61°C, R_f = 0.33 (30% EA/Hex), other physical data were identical to literature reports. [24]

1,1-Dihydroperoxycyclooctane (3a)—58%, colorless oil, R_f = 0.33 (30% EA/Hex), other physical data were identical to literature reports.[24]

4-Phenyl-2,2-dihydroperoxybutane (4a)—72%, white solid, mp 61–63°C, R_f = 0.36 (40% EA/Hex), other physical data were identical to literature reports.[24]

1,1-Dihydroperoxyadamantane (5a)—88%, white solid, mp 148–150°C, R_f = 0.30 (30% EA/Hex), other physical data were identical to literature reports.[24]

5,5-Dihydroperoxynonane (6a)—75%, colorless oil. R_f = 0.25 (20% EA/Hex), other physical data were identical to literature reports.[24]

1,1-Dihydroperoxy-3-*tert*-butylcyclopentane (7a)—84%, colorless oil. R_f = 0.30 (30% EA/Hex), IR: 3420, 2956, 2870, 1365, 1104, 963 cm^{-1}; ^{1}H NMR δ 9.83 (s, 2H), 2.05 (m, 2H), 1.9 (m, 2H), 1.7 (m, 2H), 1.47 (m, 1H), 0.85 (s, 9H); ^{13}C NMR δ 121.7, 49.2, 34.5, 32.6, 31.5, 27.4, 25.6; HRMS (ESI, MeOH/H$_2$O, NaOAc), calc. for $C_9H_{18}NaO_4$ (M+Na)$^+$: 213.1103; found 213.1110

1,1-Dihydroperoxycyclododecane (8a)—93%, colorless oil, R_f = 0.33 (30% EA/Hex), other physical data were identical to literature reports.[24]

Standard procedure for preparation of 1,1-dihydroperoxide monoacetate (illustrated for 1b)

To a solution of 4-*tert*-butylcyclohexyl-1,1-dihydroperoxide **1a** (1.48 g, 7.2 mmol) in CH$_2$Cl$_2$ (15 mL), was added DMAP (0.09 g, 0.75 mmol), and pyridine (0.57 g, 7.2 mmol). The reaction mixture was cooled to 0 °C and a solution of Ac$_2$O (0.74 g, 7.2 mmol) in CH$_2$Cl$_2$ (10 mL) was added dropwise over 10 min. Upon completion of addition, the reaction was stirred for 30 min at 0 °C, and then diluted with CH$_2$Cl$_2$ (100 mL). The solution was washed with saturated NaHCO$_3$ (20 mL), water (20 mL), brine (20 mL), and then dried over anhydrous Na$_2$SO$_4$. The residue obtained upon removal of the solvent *in vacuo* was purified by silica flash chromatography (5% EA/Hex) to give a white solid (1.47 g, 84% yield). The acid anhydride could be replaced by acid chloride (peresters) or ethoxycarbonyl chloride (percarbonates) without any other change.

1-Acetyldioxy-1-hydroperoxy-4-*tert*-butylcyclohexane (1b)—84%, white solid, mp 35–37°C. R_f = 0.33 (10% EA/Hex); other physical data were identical to literature reports.[23]

1-Acetyldioxy-1-hydroperoxycycloheptane (2b)—76%, colorless oil. R_f = 0.33 (10% EA/Hex); IR: 3345, 2930, 2859, 1756, 1425, 1171, 1006, 899 cm^{-1}; ^{1}H NMR δ 10.13 (s, 1H), 2.09 (2, 3H), 1.92 (m, 4H), 1.54 (br, 8H); ^{13}C NMR δ 171.7, 117.4, 32.5, 29.6, 22.6, 17.5; HRMS (ESI, MeOH/H$_2$O, NaOAc), calc. for C$_9$H$_{16}$NaO$_5$ (M+Na)$^+$: 227.0895; found 227.0898

1-Acetyldioxy-1-hydroperoxycyclooctane (3b)—73%, colorless oil. R_f = 0.33 (10% EA/Hex); IR: 3340, 2924, 1756, 1409, 1200, 1078, 898 cm^{-1}; ^{1}H NMR δ 10.13 (s, 1H), 2.15 (s, 3H), 2.00 (m, 2H), 1.89 (m, 2H), 1.63 (br, 4H), 1.57 (br, 6H); ^{13}C NMR δ 171.7, 116.8, 27.8, 27.4, 24.9, 21.8, 17.6; HRMS (ESI, MeOH/H$_2$O, NaOAc), calc. for C$_{10}$H$_{18}$NaO$_5$ (M+Na)$^+$: 241.1052; found 241.1046

4-Phenyl-1-acetyldioxy-1-hydroperoxybutane (4b)—86%, colorless oil. R_f = 0.33 (10% EA/Hex); IR: 3340, 2988, 2900, 1758, 1378, 1066, 899, 748, 698 cm^{-1}; ^{1}H NMR δ 10.39 (s,1H), 7.35 (m, 2H), 7.28 (m, 3H), 2.86 (m, 2H), 2.24 (dd, J = 5.46, 12.9 Hz, 1H), 2.20 (s, 3H), 2.09 (dd, J = 5.46, 12,2 Hz, 1H), 1.61 (s, 3H); ^{13}C NMR δ 171.7, 141.0, 128.6, 128.4, 126.3, 113.7, 34.9, 30.2, 18.1, 17.6; HRMS (ESI, MeOH/H$_2$O, NaOAc), calc. for C$_{12}$H$_{16}$NaO$_5$ (M+Na)$^+$: 263.0895; found 263.0899

5-Acetyldioxy-5-hydroperoxynonane (6b)—76%, colorless oil. R_f = 0.33 (10% EA/Hex); IR: 3350, 2960, 2873, 1760, 1198, 1056, 899 cm^{-1}; ^{1}H NMR δ 10.13 (s, 1H), 2.12 (s, 3H), 1.73 (m, 2H), 1.56 (m, 2H), 1.34 (m, 8H), 0.90 (t, J = 7.15 Hz, 3H); ^{13}C NMR δ 171.6, 116.0, 28.9, 25.6, 22.7, 17.4, 13.8; HRMS (ESI, MeOH/H$_2$O, NaOAc), calc. for C$_{11}$H$_{22}$NaO$_5$ (M+Na)$^+$: 257.1365; found 257.1361

1-Acetyldioxy-1-hydroperoxy-3-*tert*-butylcyclopentane (7b)—84%, colorless oil. R_f = 0.33 (10% EA/Hex); IR: 2959, 2869, 1758, 1365, 1184, 1070, 962; ^{1}H NMR δ 10.516/10.501 (two s, totaling 1H), 2.17 (s, 3H), 2.0 (m, 4H), 1.75 (m, 2H), 1.54 (m, 1H), 0.88 (s, 9H); ^{13}C NMR δ 171.6, 122.9, 122.8, 49.3, 49.2, 34.6, 34.5, 32.7, 32.6, 31.6, 27.38, 27.36, 25.6, 17.6; HRMS (ESI, MeOH/H$_2$O, NaOAc), calc. for C$_{11}$H$_{20}$NaO$_5$ (M+Na)$^+$: 255.1208; found 255.1199

1-Acetyldioxy-1-hydroperoxycyclododecane (8b)—81% colorless oil. R_f = 0.33 (10% EA/Hex);. IR: 3307, 2946, 2851, 1748, 1426, 1190, 997, 850 cm^{-1}; ^{1}H NMR δ 10.22 (s, 1H), 2.17 (s, 3H), 1.76 (m, 2H), 1.59(m, 6H), 1.39 (br, 14H); ^{13}C NMR δ 171.7, 116.8, 26.1, 25.9, 25.8, 22.1, 21.8, 19.3, 17.7; HRMS (ESI, MeOH/H$_2$O, NaOAc), calc. for C$_{14}$H$_{26}$NaO$_5$ (M+Na)$^+$: 297.1678; found 297.1679

1-Benzoyldioxy-1-hydroperoxy-4-*tert*-butylcyclohexane (**1c**), 37%, white solid, mp 76–78 °C, R_f = 0.43 (10% EA/hex), other physical data were identical to literature reports.[23]

4-*tert*-Butyl-1-hydroperoxycyclohexyl ethyl carbonoperoxoate (**1d**), 76%, colorless oil, R_f = 0.22 (10% EA/Hex), other physical data were identical to literature reports.[23]

Standard procedure for preparation of monosilylated peresters (illustrated for 8a)

To a solution of monoacetate **1b** (2.46 g, 10 mmol) in CH$_2$Cl$_2$ (150 mL), was added DMAP (0.24 g, 2.0 mmol), and Et$_3$N (2.7 ml, 20 mmol), The reaction mixture was cooled to 0 °C and a solution of TESCl (1.5 g, 10 mmol) in CH$_2$Cl$_2$ (50 mL) was added dropwise over 10 min. The reaction was stirred for 30 min at 0 °C, and then the solvent was removed in vacuo. The residue obtained was purified by silica flash chromatography (5% EA/Hex) to give a colorless oily product (2.09 g, 58% yield).

1-Acetyldioxy-1-triethylsilyldioxy-4-*tert*-butylcyclohexane (9a)—58%, colorless oil, R_f = 0.65 (20% EA/Hex); IR 2954, 1777, 1366, 1180, 865 cm^{-1}; ^{1}H NMR δ 2.33 (d, J = 14.48Hz, 2H), 2.15 (s, 3H), 1.70 (d, J = 13.2Hz, 2H), 1.46 (dt, J = 3.78, 13.8Hz, 2H), 1.30 (m, 2H), 1.05 (m, 1H), 0.98 (t, J = 7.69Hz, 9H), 0.87 (s, 9H), 0.69 (dd, J = 7.55, 16.27Hz, 6H); ^{13}C NMR (233K) δ 167.9, 110.6, 47.2, 32.5, 30.4, 27.7, 23.2, 18.3, 7.0, 3.4; HRMS (ESI, MeOH/H$_2$O, NaOAc), calc. for C$_{18}$H$_{36}$NaO$_5$Si (M+Na)$^+$: 383.2230; found 383.2224

1-Acetyldioxy-1-*tert*-butyldimethylsilyldioxy-4-*tert*-butylcyclohexane (9b)—TESCl was replaced by TBSCl without any other change, 65%, colorless oil. R_f = 0.65 (20% EA/Hex); IR: 2954, 2859, 1777, 1365, 1178, 873, 830, 784 cm^{-1}; ^{1}H NMR δ 2.33 (m, 2H), 2.14 (s, 3H), 1.68 (m, 2H), 1.46 (dt, J = 3.85, 13.63Hz, 2H), 1.29 (m, 2H), 1.05 (m, 1H), 0.93 (s, 9H), 0.87 (s, 9H), 0.14 (s, 6H); ^{13}C NMR (233K) δ 167.9, 110.7, 47.2, 32.5, 30.4, 27.7, 26.3, 23.2, 18.6, 18.3; HRMS (ESI, MeOH/H$_2$O, NaOAc), calc. for C$_{18}$H$_{36}$NaO$_5$Si (M+Na)$^+$: 383.2230; found 383.2235

1-Acetyldioxy-1-triethylsilyldioxycycloheptane (10)—81%, colorless oil. R_f = 0.65 (20% EA/Hex); IR: 2969, 1776, 1409, 1170, 1056, 796 cm^{-1}; ^{1}H NMR δ 2.08 (s, 3H), 1.95 (m, 4H), 1.55 (br, 8H), 0.97 (t, J = 7.86 Hz, 9H), 0.68 (q, 6H); ^{13}C NMR δ 115.9, 33.0, 30.2, 22.8, 17.8, 6.6, 3.7; HRMS (ESI, MeOH/H$_2$O, NaOAc), calc. for C$_{15}$H$_{30}$NaO$_5$Si (M+Na)$^+$: 341.1760; found 341.1759

1-Acetyldioxy-1-triethylsilyldioxycyclooctane (11)—70%, colorless oil. R_f = 0.65 (20% EA/Hex); IR: 2956, 1776, 1363, 1184, 1066, 833, 729 cm^{-1}; ^{1}H NMR δ 2.10 (s, 3H), 1.97 (m, 4H), 1.56 (br, 10H), 0.97 (t, J = 7.63 Hz, 9H), 0.68 (q, 6H); ^{13}C NMR (233K) δ 168.1, 115.0, 27.8, 27.2, 24.7, 22.0, 18.2, 7.0, 3.7; HRMS (ESI, MeOH/H$_2$O, NaOAc), calc. for C$_{16}$H$_{32}$NaO$_5$Si (M+Na)$^+$: 355.1917; found 355.1906

4-Phenyl-1-acetyldioxy-1-triethylsilyldioxybutane (12)—79%, colorless oil. R_f = 0.65 (20% EA/Hex); IR: 2957, 1780, 1182, 1103, 825, 698 cm^{-1}; ^{1}H NMR δ 7.31 (m, 2H), 7.23 (m, 2H), 2.78 (t, J = 8.95 Hz, 2H), 2.15 (m, 5H), 1.57 (s, 3H), 1.04 (t, J = 7.95 Hz, 9H), 0.75 (q, 6H); ^{13}C NMR δ 141.3, 128.5, 128.3, 126.1, 111.9, 35.5, 30.4, 18.5, 17.8, 6.7, 3.7; HRMS (ESI, MeOH/H$_2$O, NaOAc), calc. for C$_{18}$H$_{30}$NaO$_5$Si (M+Na)$^+$: 377.1760; found 377.1756

1-Acetyldioxy-1-triethylsilyldioxynonane (13)—73%, colorless oil. R_f = 0.65 (20% EA/Hex); IR: 2959, 1781, 1409, 1184, 1066, 802, 729 cm^{-1}; ^{1}H NMR δ 2.04 (s, 2H), 1.69 (m, 2H), 1.30 (br, 8H), 0.93 (t, J = 7.85 Hz, 9H), 0.85 (t, J = 6.35Hz, 6H), 0.63 (q, 6H); ^{13}C NMR δ 114.1, 29.6, 25.5, 22.7, 17.7, 13.7, 6.5, 3.6; HRMS (ESI, MeOH/H$_2$O, NaOAc), calc. for C$_{18}$H$_{30}$NaO$_5$Si (M+Na)$^+$: 377.1760; found 377.1768

1-Acetyldioxy-1-triethylsilyldioxycyclododecane (14)—80%, colorless oil. R_f = 0.65 (20% EA/Hex); IR: 2929, 1779, 1470, 1186, 1003, 851, 728 cm^{-1}; ^{1}H NMR δ 2.08 (s, 3H), 1.73 (m, 4H), 1.37 (br, 18H), 0.96(t, J = 7.96 Hz, 9H), 0.66 (q, 6H); ^{13}C NMR δ 114.9, 26.7, 26.1, 26.0, 22.3, 21.9, 19.4, 6.7, 3.7; HRMS (ESI, MeOH/H$_2$O, NaOAc), calc. for C$_{20}$H$_{40}$NaO$_5$Si (M+Na)$^+$: 411.2543; found 411.2536

1,1-Triethylsilyldioxy-4-*tert*-butylcyclohexane (15)—To a solution of 4-*tert*-butylcyclohexyl-1,1-dihydroperoxide **1a** (0.50 g, 2.5 mmol) in DMF (30 mL), was added Et$_3$N (0.76 ml, 5.4 mmol), The reaction mixture was cooled to −40 °C and TESCl (0.91 ml, 5.4 mmol) was added. The reaction was stirred for 1 hour at −40 °C, then quenched with brine (100 mL). The solution was extracted with hexane (50 ml) three times and the combined organic layer was dried over anhydrous Na$_2$SO$_4$. The residue obtained upon

removal of the solvent *in vacuo* was purified by silica flash chromatography (5% EA/Hex) to give colorless oil. (0.57g, 53%), R_f = 0.80 (20% EA/Hex), other physical data were identical to literature reports.[42]

1,1-Diacetyldioxy-4-*tert*-butylcyclohexane (16)—To a solution of 4-*tert*-butylcyclohexyl-1,1-dihydroperoxide **1a** (1.48 g, 7.2 mmol) in CH_2Cl_2 (15 mL), was added DMAP (0.09 g, 0.75 mmol), and pyridine (0.57 g, 7.2 mmol). The reaction mixture was cooled to 0 °C and a solution of Ac_2O (1.48 g, 14.4 mmol) in CH_2Cl_2 (10 mL) was added dropwise over 10 min. Upon completion of addition, the reaction was stirred for 30 min at 0 °C, and then diluted with CH_2Cl_2 (100 mL). The solution was washed with saturated $NaHCO_3$ (20 mL), water (20 mL), brine (20 mL), and then dried over anhydrous Na_2SO_4. The residue obtained upon removal of the solvent *in vacuo* was purified by silica flash chromatography (10% EA/Hex) to give a white solid (1.55 g, 75% yield). mp 54–56 °C; R_f = 0.30 (20% EA/Hex); IR: 2960, 2869, 1785, 1361, 1187, 1057, 896 cm^{-1}; ^{1}H NMR δ 2.34 (d, J = 12.81 Hz, 2H), 2.08 (s, 3H), 2.07 (s, 3H), 1.75 (d, J = 14.12 Hz, 2H), 1.62 (m, 2H), 1.31 (m, 2H), 1.09 (m, 1H), 0.86 (s, 9H); ^{13}C NMR δ 167.5, 167.4, 111.5, 47.1, 32.2, 30.1, 27.5, 23.2, 17.5, 17.4; HRMS (ESI, MeOH/H$_2$O, NaOAc), calc. for $C_{14}H_{24}NaO_6$ (M+Na)$^+$: 311.1471; found 311.1467

Standard procedure for fluoride-mediated decomposition of silylated monoesters

To a solution of **9a** (77 mg, 0.2 mmol) and 1,3-diphenylisobenzofuran (DPBF, **D**, 27 mg, 0.1 mmol) in CH_3CN (2 ml), was added TBAF (1M in THF, 0.24 ml, 0.24 mmol) over a period of 5 seconds (syringe injection). The resulting reaction mixture was stirred at room temperature for 5 minutes. Then solvent was removed by vacuum, and the residue was purified by column chromatography on silica gel to give the pure product **D-O$_2$** (19 mg, 66%).

NMR method for quantification of oxygen transfer (illustrated for dioxygenation of terpenine)

To a solution of **1b** (50 mg, 0.2 mmol) and α-terpinene (**T**, 90%, 15 mg, 0.1 mmol) in CH_3CN (2 ml), TBAF (1M in THF, 0.24 ml, 0.24 mmol) was injected within 5 seconds, and the reaction mixture stirred at room temperature for 5 minutes. Then solvent was removed by vacuum. Internal standard 1,2- dichloroethane was added and **T-O$_2$** was measured by NMR. The alkene peak at 6.3 ppm (dd, J = 8.56, 25.93Hz) of T-O$_2$ will be used for calculation via following equations:

$$\text{Actual Mole}_{T-O2} = \text{Mole}_{standard} * 2 * \text{Area}_{T-O2} / \text{Area}_{standard}$$

Therefore, the calculated %yield = 100*Actual MoleT-$_{O2}$/Theoretical MoleT-$_{O2}$
Alternatively, quantification of **T-O$_2$** can be conducted by GC/MS using a reported procedure[5]

GC/MS quantification of relative reactivity of dihydroperoxide monoesters (Illustrated for 1b and 4b)

Prepare a standard solution of 4-*tert*-butylcyclohexanone (1 mmol) and benzylacetone (1 mmol) in CH_3CN (2 ml). The standard ratio α = Area$_{4\text{-}tert\text{-butylcyclohexanone standard}}$/Area$_{benzylacetone\ standard}$. The mole ratio of the ketone products from the competitive reaction is Area$_{4\text{-}tert\text{-butylcyclohexanone actual}}$/(α*Area$_{benzylacetone\ actual}$)

Standard procedure for tandem activation and decomposition of 1,1-dihydroperoxides (Illustrated for CCl$_3$CN activator)

To a solution of **1a** (41 mg, 0.2 mmol), CCl$_3$CN (29 mg, 0.2 mmol) and 1,3-diphenylisobenzofuran (DPBF, **D**, 27 mg, 0.1 mmol) in CH$_3$CN (2 ml), was added KOtBu (90 mg, 0.8 mmol). The reaction was monitored by TLC and stirred at room temperature for 5 minutes. Then solvent was removed by vacuum, and the residue was purified by column chromatography on silica gel to give the pure product **D-O$_2$** (21 mg, 72% yield based upon **D** or 36% based upon consumed 1,1-dihydroperoxide).

Standard procedure for preparation of 1,1-dihydroperoxide monoacetates (illustrated for 1b)—To a solution of 4-*tert*-butylcyclohexyl-1,1-dihydroperoxide **1a** (1.48 g, 7.2 mmol) in CH$_2$Cl$_2$ (15 mL), was added DMAP (0.09 g, 0.75 mmol), and pyridine (0.57 g, 7.2 mmol). The reaction mixture was cooled to 0 °C and a solution of Ac$_2$O (0.74 g, 7.2 mmol) in CH$_2$Cl$_2$ (10 mL) was added in a dropwise manner over 10 min. Upon completion of addition, the reaction was stirred for 30 min at 0 °C, and then diluted with CH$_2$Cl$_2$ (100 mL). The solution was washed with saturated NaHCO$_3$ (20 mL), water (20 mL), brine (20 mL), and then dried over anhydrous Na$_2$SO$_4$. The residue obtained upon removal of the solvent *in vacuo* was purified by silica flash chromatography (5% EA/Hex) to give a white solid (1.47 g, 84% yield). The acid anhydride could be replaced by acid chloride (peresters) or ethoxycarbonyl chloride (percarbonates) without any other change.

Sample procedure for oxygen transfer (illustrated for decomposition of 1b and dioxygenation of *terpenine*)—To a solution of **1b** (50 mg, 0.20 mmol) and α-terpinene (**T**, 90%, 15 mg, 0.10 mmol) in CH$_3$CN (2 ml) was added via syringe a solution of TBAF (nominally 1M in THF, 0.24 ml, 0.24 mmol) over 5 seconds. The reaction mixture was stirred at room temperature for 5 minutes and then the solvent was removed under vacuum. 1,2- Dichloroethane was added as an internal standard and **T-O$_2$** determined by NMR, GC/MS, or isolation, as described in the Supporting Information.

Standard procedure for preparation of monosilylated peresters (illustrated for 8a)—To a solution of monoacetate **1b** (2.46 g, 10 mmol) in CH$_2$Cl$_2$ (150 mL), was added DMAP (0.24 g, 2.0 mmol), and Et$_3$N (2.7 ml, 20 mmol), The reaction mixture was cooled to 0 °C and a solution of Et$_3$SiCl (1.5 g, 10 mmol) in CH$_2$Cl$_2$ (50 mL) was added dropwise over 10 min. The reaction was stirred for 30 min at 0 °C, and then the solvent was removed in vacuo. The residue was purified by silica flash chromatography (5% EA/Hex) to give **8a** as a colorless oil (2.09 g, 58% yield).

Standard procedure for fluoride-mediated decomposition of silylated monoesters—To a solution of **9a** (77 mg, 0.2 mmol) and 1,3-diphenylisobenzofuran (DPBF, **D**, 27 mg, 0.10 mmol) in CH$_3$CN (2 ml), was added via syringe a solution of TBAF (nominally 1*M* in THF, 0.24 ml, 0.24 mmol) and the reaction mixture stirred at room temperature for 5 minutes. Then solvent was removed by vacuum, and the residue was purified by column chromatography on silica gel to give the pure product **D-O$_2$** (19 mg, 66%)

Standard procedure for tandem activation and decomposition of 1,1-dihydroperoxides (Illustrated for trichloroacetonitrile)—To a solution of **1a** (41 mg, 0.2 mmol), CCl$_3$CN (29 mg, 0.2 mmol) and 1,3-diphenylisobenzofuran (DPBF, **D**, 27 mg, 0.1 mmol) in CH$_3$CN (2 ml), was added KOtBu (90 mg, 0.8 mmol). The reaction was monitored by TLC and stirred at room temperature for 5 minutes. Then solvent was removed by vacuum, and the residue was purified by column chromatography on silica gel to give the

pure product **D-O$_2$** (21 mg, 72% yield based upon **D** or 36% based upon consumed 1,1-dihydroperoxide).

Calculation Methods—The B3LYP/6-31+G(d,p) model chemistry was used in all calculations. Differences in electronic energies were corrected by inclusion of zero-point vibrational energies scaled by 0.9806. Because B3LYP is based on a single Slater determinant, it cannot rigorously describe either singlet molecular oxygen or transition structures in which singlet O$_2$ is a distinct moiety. The standard approximate treatment is to relax the restriction that and orbitals be identical. While this allows B3LYP to provide a qualitatively correct description of the electronic structure, this treatment also introduces triplet character into the wave function. We corrected for this spin contamination using the approach of Houk and co-workers.[43] This approach predicts a singlet-triplet gap for molecular oxygen of 20.8 kcal/mol, in fair agreement with the experimental value of 22.5 kcal/mol.[1a] Individual conformers within the monoperacetate and monopercarbonate systems, along with optimized coordinates for each minimized structure or transition state, are described in the Supporting Information.

Supplementary Material

Refer to Web version on PubMed Central for supplementary material.

Acknowledgments

References

1. a) Foote, CS.; Clennan, EL. Active Oxygen in Chemistry. Foote, CS.; Valentine, JS.; Greenberg, A.; Liebman, JF., editors. Blackie Academic and Professional; London: 1995. p. 105b) Clennan E, Pace A. Tetrahedron. 2005; 61:6665.c Endo M. Russ J Phys Chem A. 2007; 81:1497.

2. Gollnick, K.; Kuhn, HJ. Singlet Oxygen. Wasserman, HH.; Murray, RW., editors. Academic Press; New York: 1979. p. 287-427.

3. Clennan EL, L'Esperance RP. Tetrahedron Lett. 1983; 24:4291.

4. Sheu C, Kang P, Khan S, Foote CS. J Am Chem Soc. 2002; 124:3905. [PubMed: 11942827]

5. Schmidt R. Photochem Photobiol. 2006; 82:1161. [PubMed: 16683906]

6. Wootton RCR, Fortt R, de Mello AJ. Org Proc Res Dev. 2002; 6:187.

7. Foote CS, Wexler S, Ando W, Higgins R. J Am Chem Soc. 1968; 90:975.Greer A. Acc Chem Res. 2006; 39:797. [PubMed: 17115719]

8. Jary WG, Ganglberger T, Pöchlauer P, Falk H. Monat Chem. 2005; 136:537.Ganglberger T, Jary WG, Pöchlauer P, Aubry JM, Nardello V, Falk H. Monat Chem. 2004; 135:501.

9. Adam W, Kazakov DV, Kazakov VP. Chem Rev. 2005; 105:3371. [PubMed: 16159156] Wahlen J, De Vos DE, Jacobs PA, Alsters PL. Adv Synth Catal. 2004; 346:152.

10. Catir M, Kilic H, Nardello-Rataj V, Aubry JM, Kazaz C. J Org Chem. 2009; 74:4560. [PubMed: 19449850]

11. Sels BF, De Vos DE, Jacobs PA. J Am Chem Soc. 2007; 129:6916. [PubMed: 17488006]

12. Nardello V, Barbillat J, Marko J, Witte PT, Alsters PL, Aubry JM. Chem Eur J. 2003; 9:435. [PubMed: 12532292]

13. Renirie R, Pierlot C, Aubry JM, Hartog AF, Schoemaker HE, Alsters PL, Wever R. Adv Synth Cat. 2003; 345:849.

14. Corey EJ, Mehrotra MM, Khan AU. J Am Chem Soc. 1986; 108:2472. [PubMed: 22175617] Posner GH, Weitzberg M, Nelson WM, Murr BL, Seliger HH. J Am Chem Soc. 1987; 109:278.Cerkovnik J, Tuttle T, Kraka E, Lendero N, Plesnicar B, Cremer D. J Am Chem Soc. 2006; 128:4090. [PubMed: 16551118]

15. Deslongchamps P, Atlani P, Fréhel D, Malaval A, Moreau C. Can J Chem. 1974; 52:3651.Abdrakhmanova AR, Khalitova LR, Spirikhin LV, Dokichev VA, Grabovskiy SA, Kabal'nova NN. Russ Chem Bull Int Ed. 2007; 56:271.

16. Pierlot C, Nardello V, Schrive J, Mabille C, Barbillat J, Sombret B, Aubry JM. J Org Chem. 2002; 67:2418. [PubMed: 11950282]

17. Carreño MC, González-Lopez M, Urbano A. Angew Chem Int Ed. 2006; 45:2737.

18. The half-life of $^1O_2$ ranges from 1–2 μsec in H_2O to 60 usec in CH_3CN to nearly msec in perhalogenated solvents. See ref. 1a and Wilkinson F, Helman WP, Ross AB. J Phys Chem Ref Data. 1995; 24:663.

19. See, for example: Aubry J-M, Adam W, Alsters PL, Borde C, Queste S, Marko J, Nardello V. Tetrahedron. 2006; 62:10753.Caron L, Nardello V, Alsters PL, Aubry J-M. J Mol Cat, A. 2006; 251:194.

20. Aubry JM, Pierlot C, Rigaudy J, Schmidt R. Acc Chem Res. 2003; 36:668–675. [PubMed: 12974650]

21. Thompson QE. J Am Chem Soc. 1961; 83:845.Mendenhall, GD. Advances in Oxygenated Processes. Baumstark, AL., editor. Vol. 2. JAI; Greenwich: Connecticut: 1990. p. 203

22. Schwartz C, Raible J, Mott K, Dussault PH. Org Lett. 2006; 8:3199. [PubMed: 16836365] Tetrahedron. 2006; 62:10747.

23. Ghorai P, Dussault PH. Org Lett. 2009; 11:4572. [PubMed: 19772310]

24. Ghorai P, Dussault PH. Org Lett. 2008; 10:4577. [PubMed: 18783232]

25. Cudden RCP, Hewlett C. J Chem Soc C. 1968:2983.Dihydroperoxide monoesters have been investigated as radical initiators: Van de Bovenkamp-Bouwman AG, Van Gendt JWJ, Meijer J, Hogt AH, Van Swieten AP. PCT Int Appl. 1999WO 9932442 A1 19990701.

26. Dussault, PH. Active Oxygen in Chemistry. Foote, CS.; Valentine, JS.; Greenberg, A.; Liebman, JF., editors. Blackie A&P; London: 1995. p. 141-203.

27. The rate constants for reaction of $^1O_2$ with terpinene and 1,3-Diphenylisobenzofuran (DPBF, D) are on the order of 10^8 and 10^9 L/mol-sec, respectively; see ref. 18. *Caution:* DPBF is both an efficient $^1O_2$ trap and a visible photosensitizer. In control reactions, we found that stirring a solution of 1b with DPBF in an unlit fume hood gave little oxidized product (D-O_2) over the typical period (≤ 0.5 h) of these reactions. In contrast, care had to be taken to prevent extensive formation of D-O_2 during chromatographic purification of reaction mixtures under normal lab lighting. See: Nowakowska M. J Chem Soc, Faraday Trans 1. 1984; 80:2119.Howard JA, Mendenhall GD. Can J Chem. 1975; 53:2199.No precautions were required with terpinene (T).

28. Miller J, Abernathy S, Sharp R. J Phys Chem A. 2000; 104:4839.

29. Bis perester derivatives of 1,1-dihydroperoxides have been prepared (Criegee R, Schnorrenberg W, Becke J. Annalen. 1949; 565:7.Warnant J, Joly R, Mathieu J, Velluz L. Bull Soc Chim Fr. 1957:331.Milas NA, Golubovic A. J Am Chem Soc. 1959; 81:6461.and also investigated as polymerization initiators: Van de Bovenkamp-Bouwman AG, Van Gendt JWJ, Meijer J, Hogt Andreas H, Van Swieten AP. (Akzo Nobel N V, Neth) PCT Int Appl. 1999:42.CODEN: PIXXD2 . WO 9932442 A1 19990701.

30. Davies AG, Sutcliffe RJ. J Chem Soc, Perkins Trans 2. 1981; 1512

31. a Grob CA, Bolleter M, Kunz W. Angew Chem, Int Ed Engl. 1980; 19:708.b Grob CA. Angew Chem, Int Ed Engl. 1969; 8:535.

32. Baader, WJ. Science of Synthesis. Berkessel, A., editor. Vol. 38. Georg Thieme Verlag; Stuttgart: 2009. p. 323-344.Four-Membered Ring Cyclic Peroxides

33. Adam W, Curci R, Edwards JO. Acc Chem Res. 1989; 22:205.Murray RW. Chem Rev. 1989; 89:1187.

34. All identified conformers are described within the Supporting Information

35. Tâme Parreira RL, Galembeck SE, Hobza P. Chem Phys Chem. 2007; 8:87. [PubMed: 17121408]

36. The successful alkylation of 1,1-dihydroperoxides using CsOH also demonstrates the stability of 1,1-dihydroperoxides and 1-alkyldioxy-1-hydroperoxyalkanes towards strongly basic conditions, although it is interesting to note that ketones are obtained as minor byproducts in these reactions: Hamada Y, Tokuhara H, Masuyama A, Nojima M, Kim H-S, Ono K, Ogura N, Wataya Y. J Med Chem. 2002; 45:1374–1378. [PubMed: 11882006]

37. Payne GB. Tetrahedron. 1962; 18:763.Payne GB, Deming PH, Williams PH. J Org Chem. 1961; 26:659.

38. Long CA, Kearns DR. J Am Chem Soc. 1975; 97:2018.

39. Frimer AA. Chem Rev. 1979; 79:359.Gorman AA, Gould IR, Hamblet I. J Am Chem Soc. 1982; 104:7098.

40. Matheson IBC, Lee J, Yamanashi BS, Wolbarsht ML. Chem Phys Lett. 1974; 27:355.

41. Criegee: a) Goodman RM, Kishi Y. J Am Chem Soc. 1998; 120:9392.Criegee R. Lieb Ann. 1948; 560:127.Kropf H. Kropf H. Methoden der Organischen Chemie (4). ThiemeStuttgart1988; E13:1095–1099.Hock: b) Hock H, Kropf H. Angew Chem. 1957; 69:313.Dussault PH, Lee HJ, Liu X. Perkin 1. 2000:3006.Anomalous ozonolysis: c) Jung ME, Davidov P. Org Lett. 2001; 3:627. [PubMed: 11178842] Fragmentation of 2-hydroperoxyacids: d) Richardson WH, Smith RS. J Am Chem Soc. 1967; 89:2230.

42. Ramirez A, Woerpel KA. Org Lett. 2005; 7:4617. [PubMed: 16209493]

43. Goldstein E, Beno B, Houk KN. J Am Chem Soc. 1996; 118:6036.
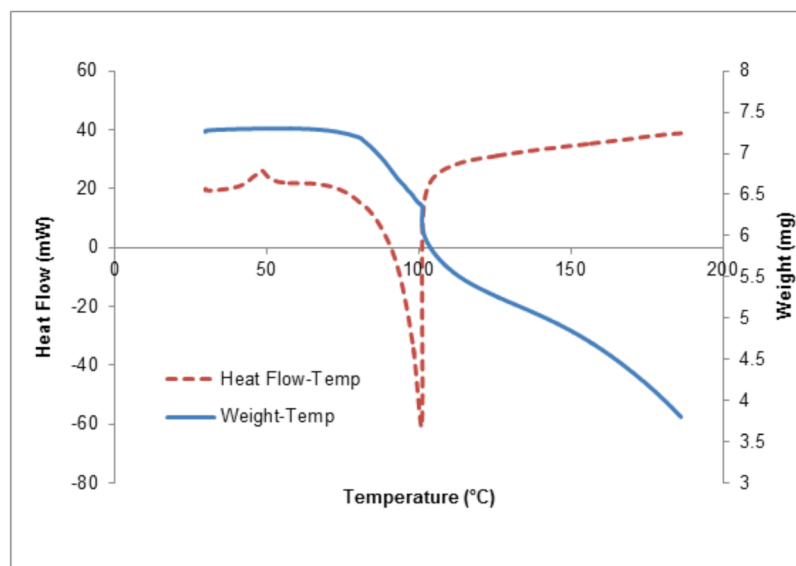
Figure 1.
Thermal stability of dihydroperoxide monoester 1b
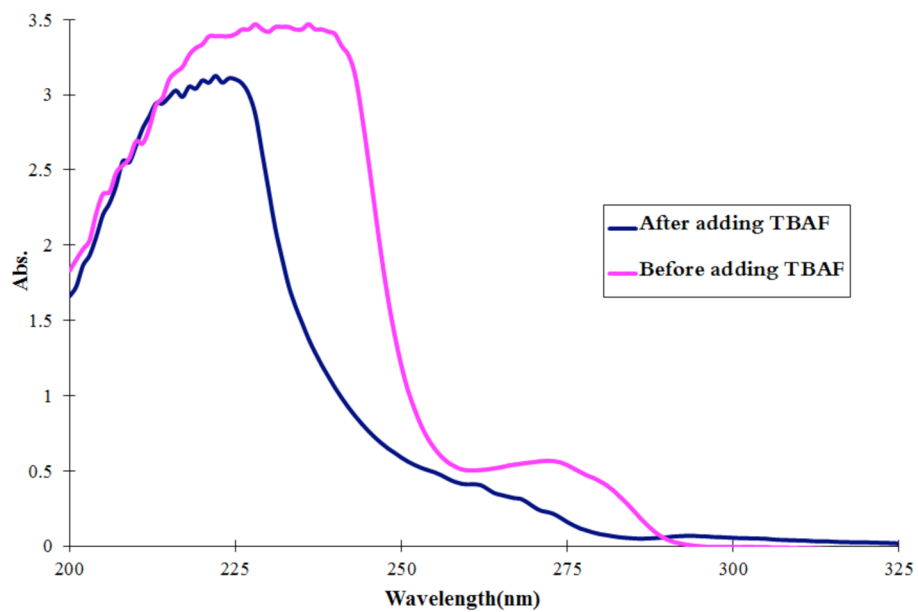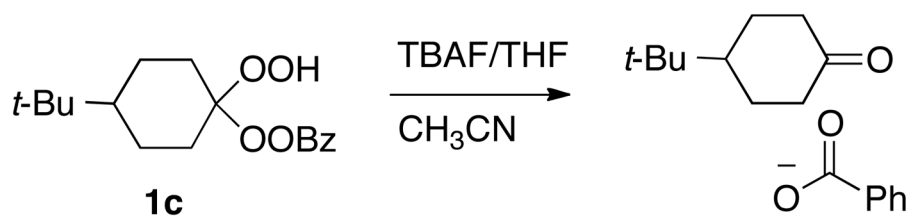
Figure 2.
Monitoring rate of decompositions
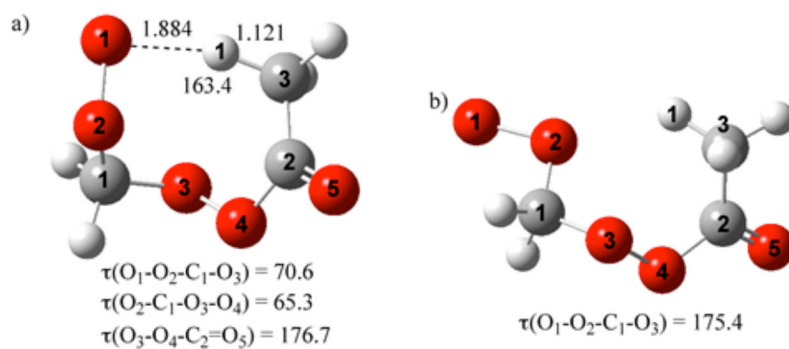
Figure 3.
a) The optimized geometry of the ground state conformer, **MIN-1a**. b) The optimized geometry of conformer **MIN-1c**. Bond lengths are in Å, and bond angles and dihedral angles are in degrees.
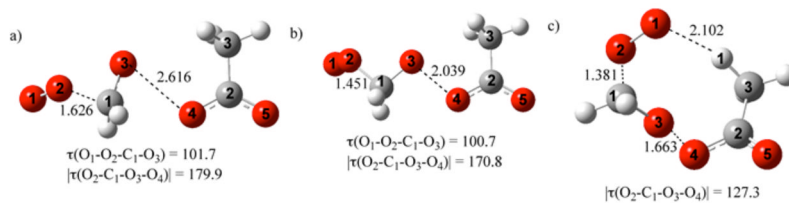
Figure 4.
a) The optimized geometry of the most stable conformer of **TS-2**. b) The optimized geometry of the reactant complex leading to the most stable conformer of **TS-2**. c) The optimized geometry of the second most stable transition state conformer, **TS-2***.
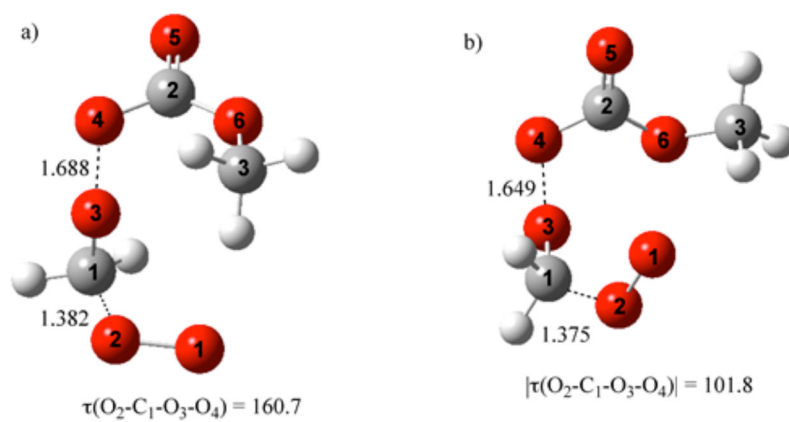
Figure 5.
The optimized geometries of the most stable conformers of: a) **TS-4**; b) **TS-5.** Bond lengths are in Å, and bond angles and dihedral angles are in degrees.
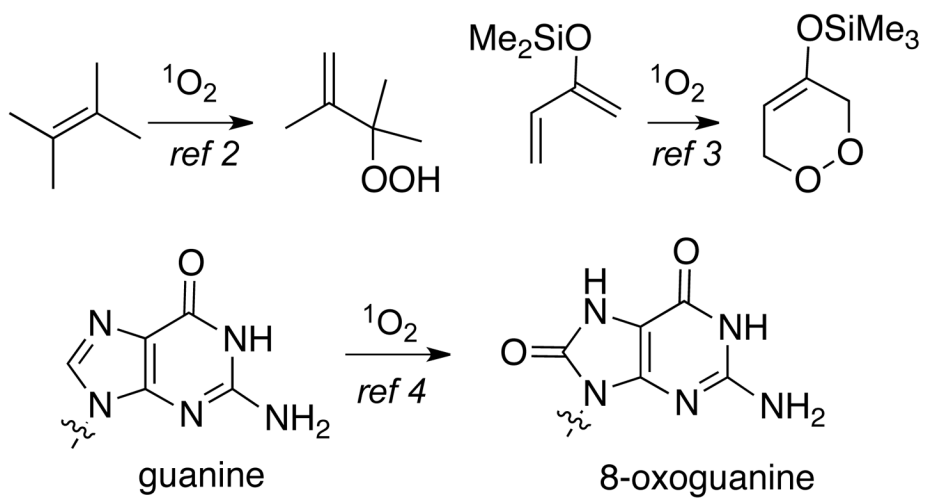
Scheme 1.
Examples of $^1O_2$ reactivity
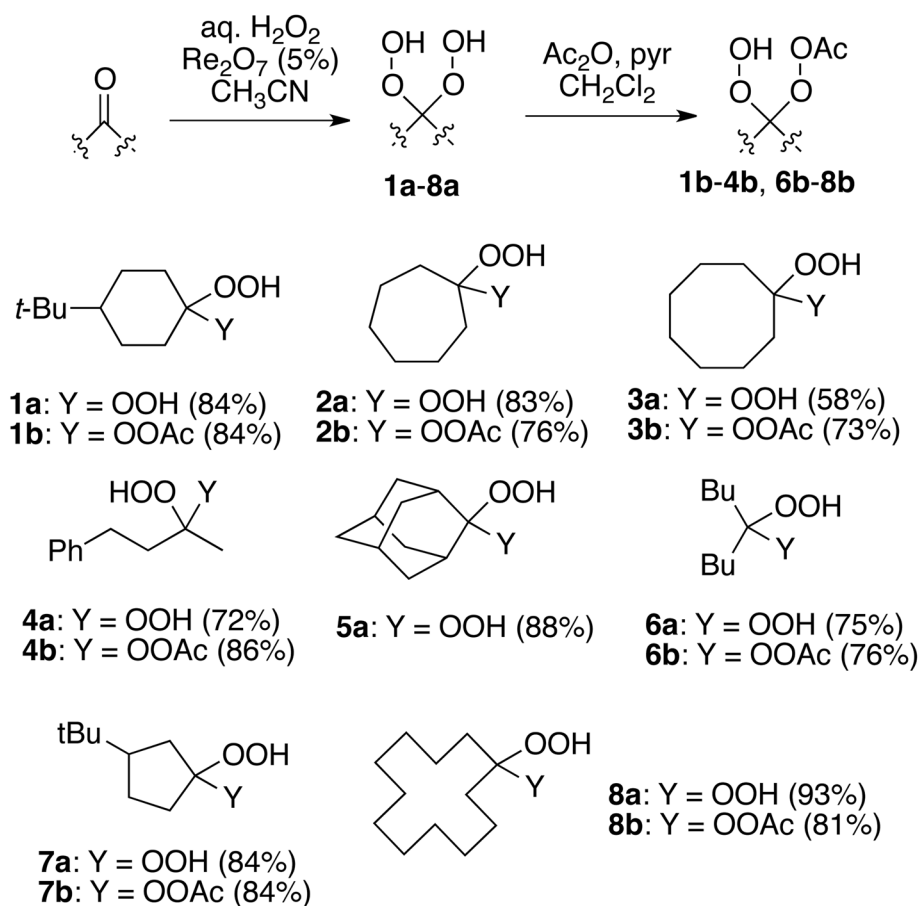
Scheme 2.
Synthesis of 1,1-dihydroperoxides and derived monoperesters

1b (1.0 eq)
4b (1.0 eq)

n-Bu₄NF (1.0 eq)

CH₃CN, 0 °C, 0.5 h

45:55

1b (1.0 eq)
7b (1.0 eq)

nBu₄NF (1 equiv.)

CH₃CN, 0 °C, 0.5 h

53:47
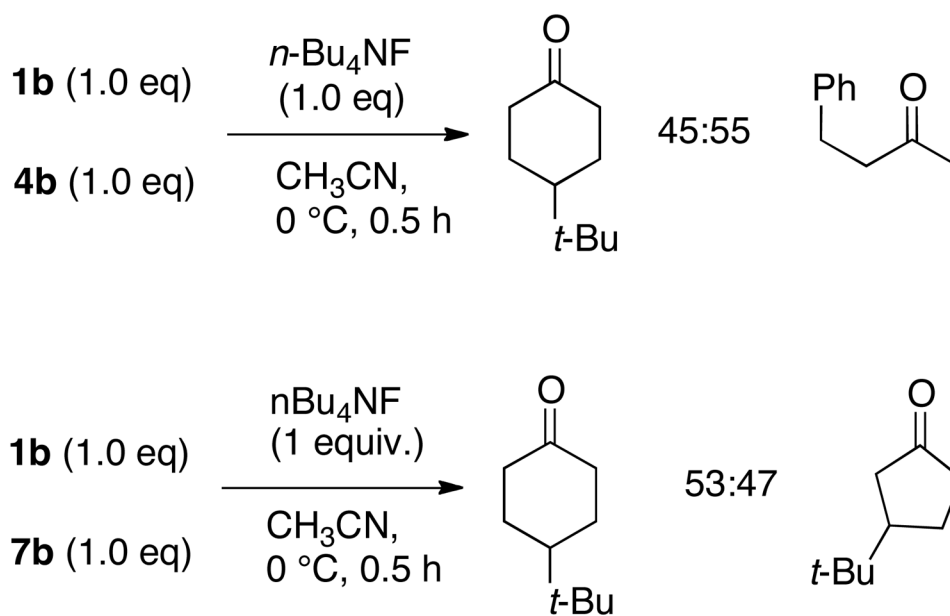
Scheme 3. Influence of scaffold on reactivity
[a]Products analyzed by GC/MS.
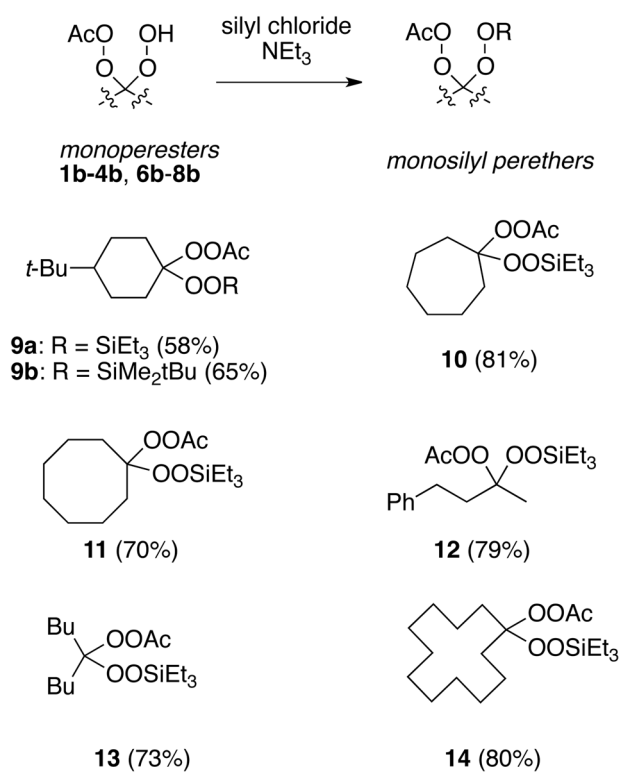
Scheme 4.
Synthesis of silylated peresters
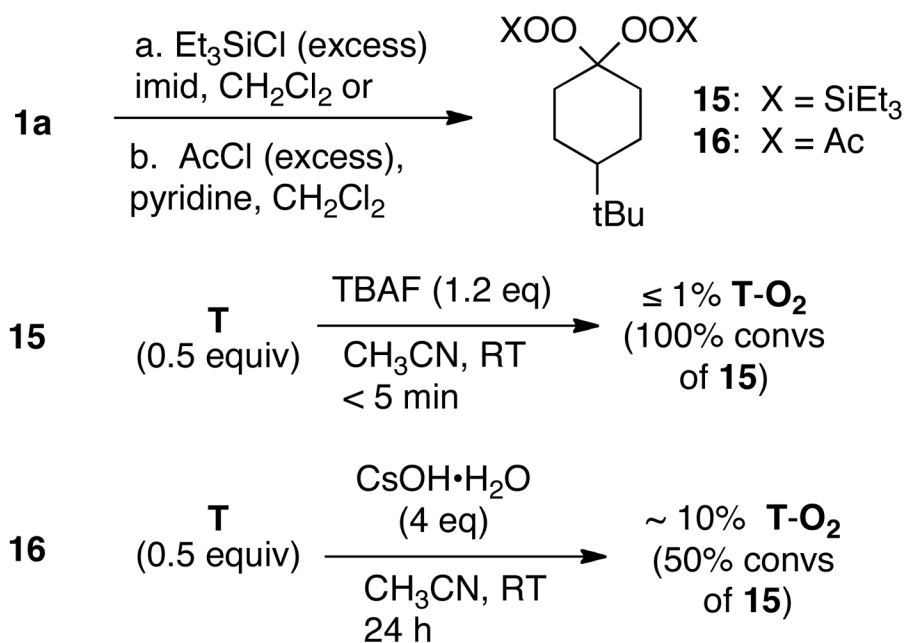
Scheme 5.
Reactivity of bissilyl and bisacyl derivatives of 1,1-dihydroperoxides
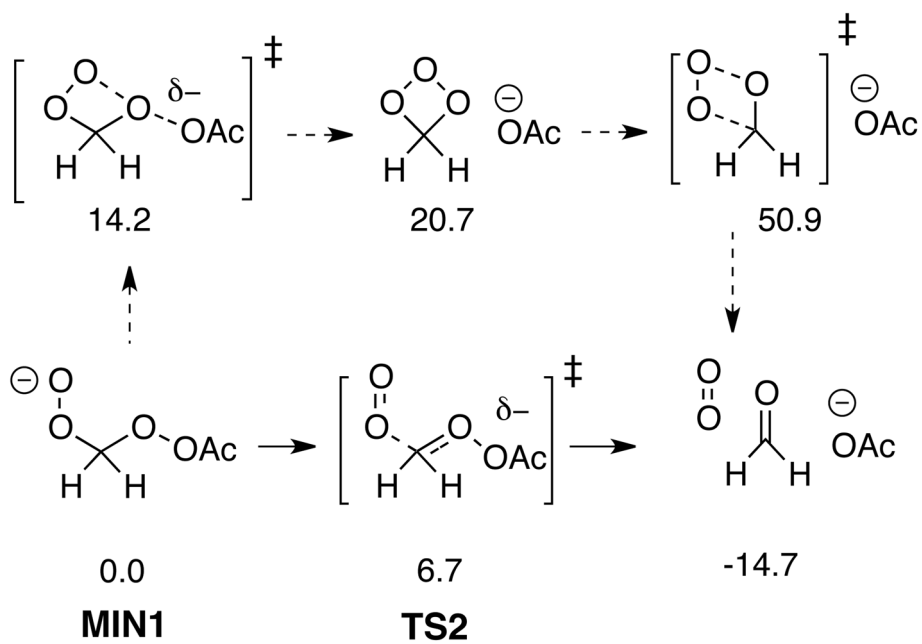
Scheme 6.
Available pathways and predicted relative energies (kcal/mol) for fragmentation of a deprotonated monoester.
[a]Energetics are based on the most stable conformer of each structure.
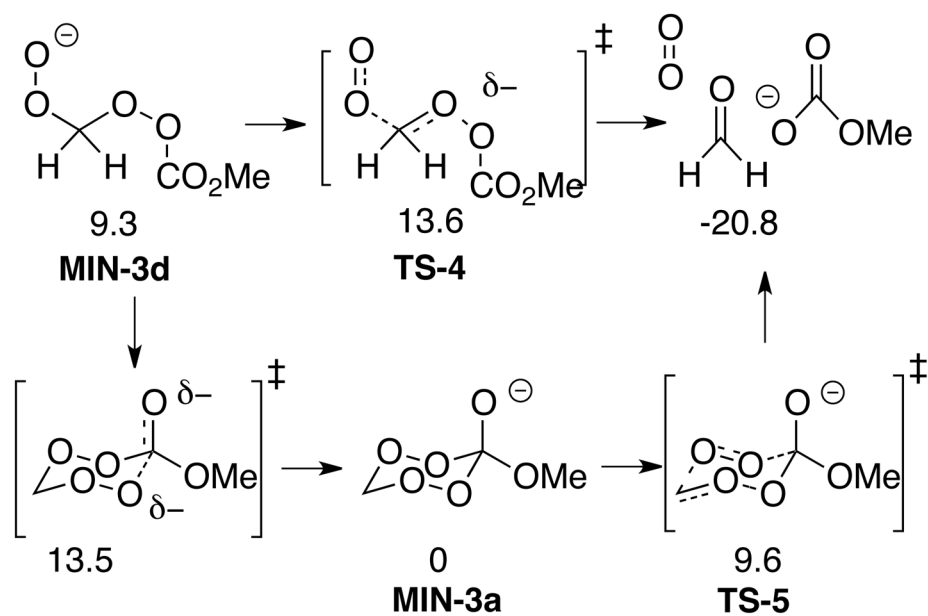
Scheme 7.
Calculated relative energies (kcal/mol) for selected intermediates (MIN) and transition states (TS) in fragmentation of percarbonates
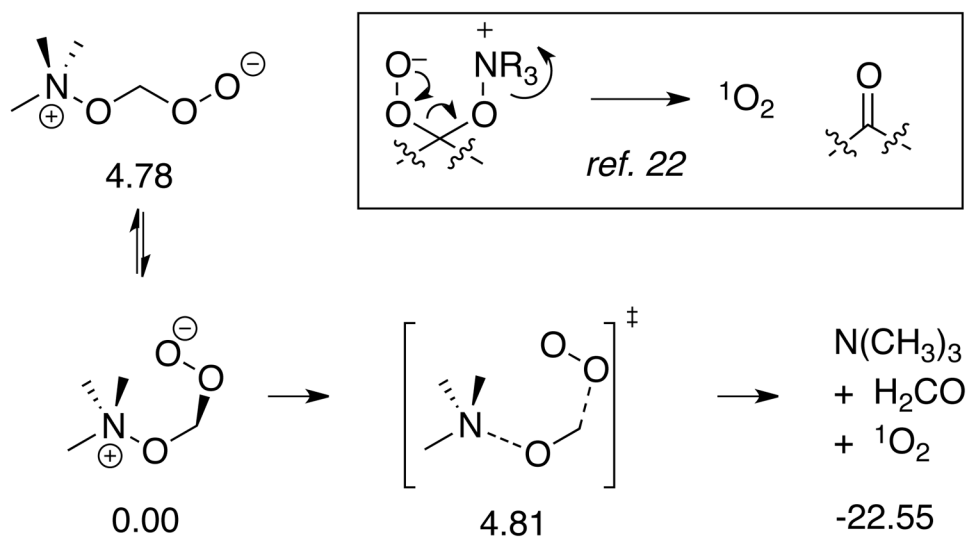
Scheme 8.
Calculated energies for decompositions of zwitterionic peroxyacetals.
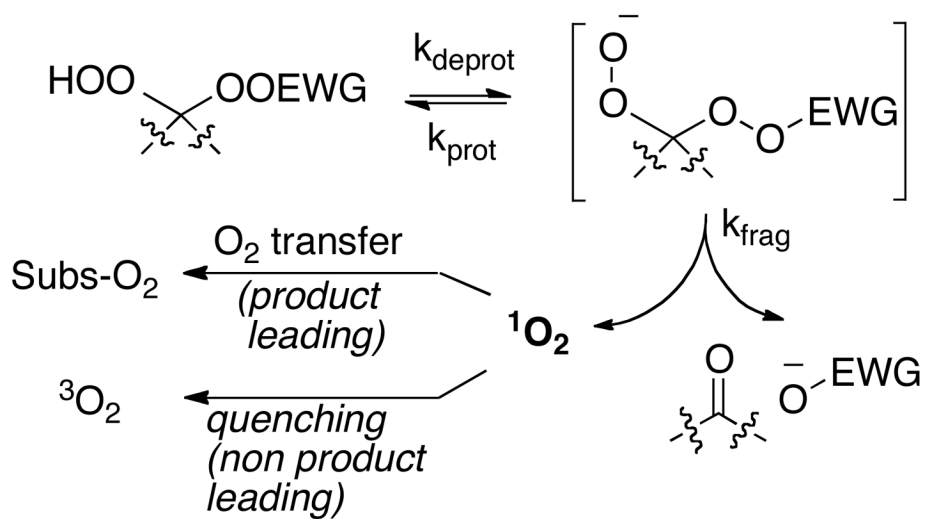
Scheme 9.
Mechanistic overview

Table 1

Influence of peroxyacetal backbone

monoperester or bisOOH	yield T-O$_2$[a]
1b	26%
2b	26%
3b	23%
4b	31%
5b	27%
7b	24%
8b	23%
1a	NR

[a] Yield of **T-O$_2$** relative to monoperester

Table 2

Influence of solvent on trapped $^1O_2$

1b (1.0 equiv)   *n*-Bu$_4$NF (1.2 eq, in THF)
      +   CH$_3$CN, 0 °C, 0.16h   → **T-O$_2$**
T (0.5 equiv)

solvent	base	yield T-O$_2$[a]
CH$_3$CN	*n*-Bu$_4$NF	26%
CHCl$_3$	*n*-Bu$_4$NF	17%
CDCl$_3$	*n*-Bu$_4$NF	35%
Acetone-d$_6$	*n*-Bu$_4$NF	33%
C$_6$D$_6$	*n*-Bu$_4$NF	30%
C$_6$F$_6$	*n*-Bu$_4$NF	7 %[b]
C$_6$F$_6$	KOtBu	1 %[b]
C$_6$F$_6$/CH$_3$CN (9:1)	*n*-Bu$_4$NF	24 %
C$_6$F$_6$/CH$_3$CN (1:1)	*n*-Bu$_4$NF	36 %
C$_6$F$_{14}$/CH$_3$CN (1:1)[c]	*n*-Bu$_4$NF	28 %
Freon-113/CH$_3$CN (1:1)	*n*-Bu$_4$NF	39 %

[a]Yield of **T-O$_2$** based upon **1b**;

[b]Limited reagent solubility;

[c]biphasic

Table 3

Influence of order of addition of reagents

$$\textbf{1b} \text{ (1.0 equiv)} + \textbf{T} \text{ (0.5 equiv)} \xrightarrow[\substack{\text{solvent,} \\ \text{r.t., 0.08h}}]{\text{base (1.2eq)}} \textbf{T-O}_2$$

conditions	yield T-O$_2$
Add n-Bu$_4$NF to solution of **1b** and **T**	35%
Add **1b** to solution of n-Bu$_4$NF and **T**	38%

[a]Based upon **T-O$_2$** vs. starting peroxide

Table 4

Investigation of other peracyl activating groups

1c: X = Ph
1d: X = OEt
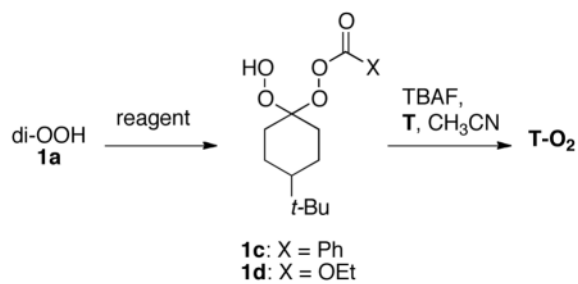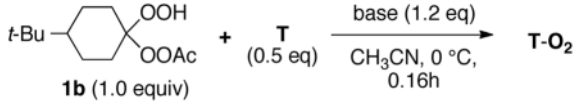
reagent	yield of 1c or 1d	yield T-O$_2$[a]
PhCOCl	**1c** (37%)	24%
EtOC(O)Cl	**1d** (76%)	20%
PhNCO	decomp	-
TsCl	decomp	-

[a]Based upon **T-O$_2$** vs. stoichiometry of **1c or 1d**

Table 5

Influence of Base

base	yield T-O$_2$[a]
KOtBu	30%
LiN(SiMe$_3$)$_2$ (in THF)	4.1%
nBu$_4$NF (in THF)	35%

[a] relative to stoichometry of perester

Table 6

Influence of temperature and rate of addition
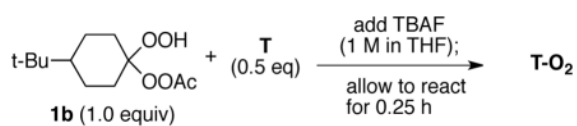
entry	T (°C)	solvent	addition mode	yield T-O$_2$[a]
1	rt	THF	b	10%
2	0	THF	b	13%
3	− 40	THF	b	19%
4	− 78	THF	b	24%
5	rt	CH$_3$CN	b	24%
6	rt	CH$_3$CN	c	42%

[a] relative to perester;

[b] syringe ($\leq 10^{-3}$ h);

[c] syringe pump. (0.25 h)

Table 7

Fragmentation of silylated dihydroperoxide monoesters

subs	SiR_3	t (min)	trap	yield[a]
9a	$SiEt_3$	5	**D**	33%
9b	TBS	5	**D**	29%
9b	TBS	5	**T**	25%
9b	TBS	10	**D**	25%
10	$SiEt_3$	30	**D**	34%
11	$SiEt_3$	20	**D**	37%
12	$SiEt_3$	10	**D**	41%
13	$SiEt_3$	16	**D**	38%
14	$SiEt_3$	5	**D**	28%

[a]Yield of **T-O2** or **D-O2** relative to peroxide starting material.

Table 8

Investigation of electrophiles for activation/fragmentation

activator	KOtBu (eq)	t (h)	convs[a]
CCl_3CN	2.0	0.75	incomplete
CCl_3CN	4.0	≤ 0.1	complete
triazene	2.0	>12	incomplete
triazene	4.0	≤ 0.1	complete
p-TsCl	2.0	0.3	incomplete
p-TsCl	4.0	≤ 0.1	complete
Ac_2O	2.0	0.5	incomplete
Ac_2O	4.0	0.25	complete

[a]Consumption of **1a** (TLC, NMR)

Table 9

Oxygen transfer via in-situ activation

activator	t (min)	yield D-O$_2$[a]
CCl$_3$CN	5	36%
triazene	5	39.5%
p-TsCl	5	39%
Ac$_2$O	5	31%

[a] relative to dihydroperoxide **1a**

Table 10

Investigation of preparative oxygenations

subs (eq)	trap	reagents (eq)	t (min)	product, yield[a]
1b (5)	**T**	TBAF (5)	10	**T-O$_2$** (83%)
1b (6)	**T**	TBAF (6)	10	**T-O$_2$** (100%)
1b (2.5)	**D**	TBAF (2.5)	5	**D-O$_2$** (100%)
1a (5)	**T**	triazine (5), KOtBu (20)	15	**T-O$_2$** (69%)
1a (7)	**T**	triazine (7), KOtBu (28)	15	**T-O$_2$** (100%)
8b (6)	**T**	TBAF (6)	10	**T-O$_2$** (100%)

[a]yield of **T-O$_2$** or **D-O$_2$**

Supporting Information: Experimental Procedures

Generation of singlet oxygen from fragmentation of monoactivated 1,1-dihydroperoxides

Jiliang Hang, Prasanta Ghorai, Solaire A. Finkenstaedt-Quinn, Ilhan Findik, Emily Sliz, Keith T.

Kuwata, Patrick H. Dussault*

pdussault1@unl.edu

<u>General Experimental Conditions</u>: All reagents and solvents were used as supplied commercially, except CH_2Cl_2 and THF, which were distilled from CaH_2, and Na/benzophenone, respectively. All reactions were conducted under an atmosphere of N_2 except where noted; "RBF" indicates round-bottom flask. Thin layer chromatography (TLC) was performed on 0.25 mm hard-layer silica G plates. Developed TLC plates were visualized with a hand-held UV lamp or by staining: 1% ceric sulfate and 10% ammonium molybdate in 10% H_2SO_4 (general stain, after charring); 1% N,N'-dimethyl-p-phenylenediamine solution in 1:20:100 acetic acid/water/methanol (specific for peroxides);[1] Melting points are uncorrected. Unless noted, NMR spectra were acquired at 400 MHz (^{1}H) or 100 MHz (^{13}C) in $CDCl_3$. IR spectra were recorded as neat films on a ZrSe crystal with selected absorbances reported in cm^{-1}.

<u>Calculation Methods:</u>

1. Methodology: The B3LYP/6-31+G(d,p) model chemistry was used in all calculations. Differences in electronic energies were corrected by inclusion of zero-point vibrational energies scaled by 0.9806. Because B3LYP is based on a single Slater determinant, it cannot rigorously describe either singlet molecular oxygen or transition structures in which singlet O_2 is a distinct moiety. The standard approximate treatment is to relax the restriction that and orbitals be identical. While this allows B3LYP to provide a qualitatively correct description of the electronic structure, this treatment also introduces triplet character into the wave function. We corrected for this spin contamination using the approach of Houk and co-workers.[2] This approach predicts a singlet-triplet gap for molecular oxygen of 20.8 kcal/mol, in fair agreement with the experimental value of 22.5 kcal/mol.[3] Individual conformers within the monoperacetate and monopercarbonate systems are illustrated in the Supporting Information.

2. Conformational Analysis of the Acetate System

SCHEME 1S

MIN-1a: **0.0**   MIN-1b: **1.7**   MIN-1c: **8.3**

MIN-1d: **8.4**   MIN-1e: **8.8**   MIN-1f: **10.1**

MIN-1g: **10.4**   MIN-1h: **11.3**   MIN-1i: **11.7**

MIN-1j: **13.0**   MIN-1k: **13.2**   MIN-1l: **13.2**
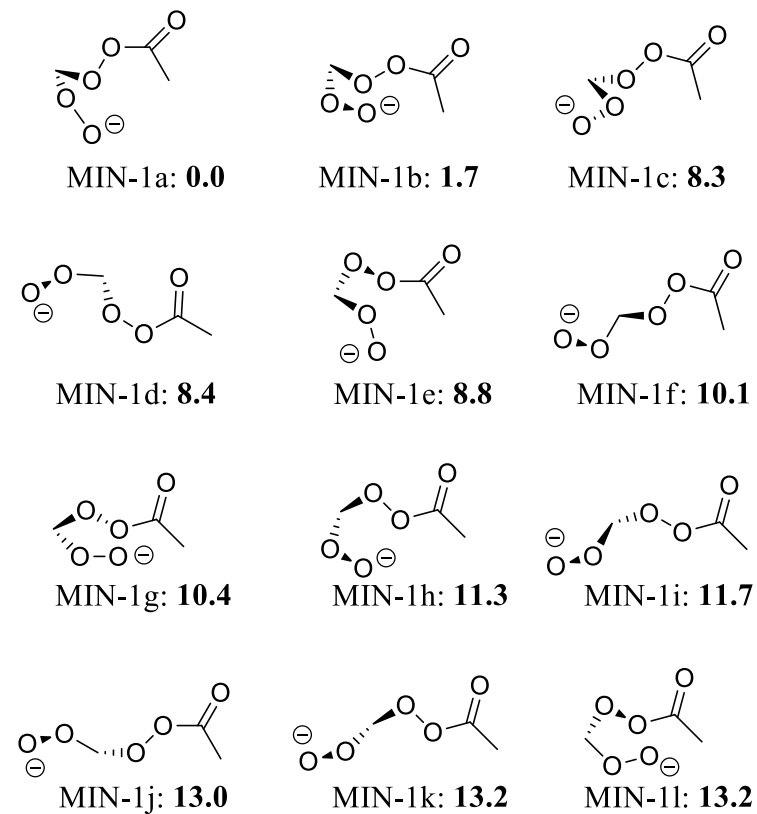
3. Conformational Analysis of the Carbonate Peroxyanion

SCHEME 2S
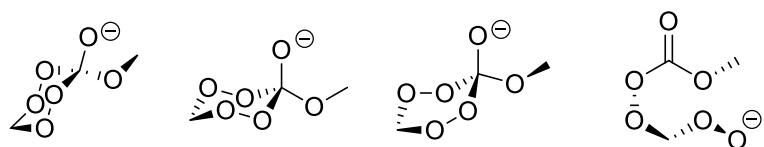
MIN-3a: **0.0**   MIN-3b: **5.2**   MIN-3c: **7.1**   MIN-3d: **9.3**
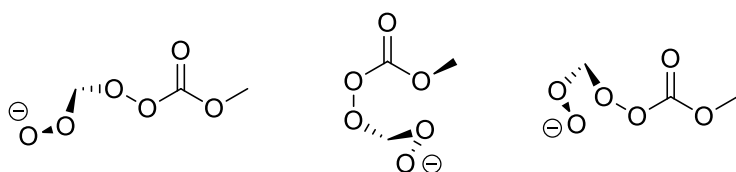
MIN-3e: **14.6**   MIN-3f: **14.7**   MIN-3g: **14.9**
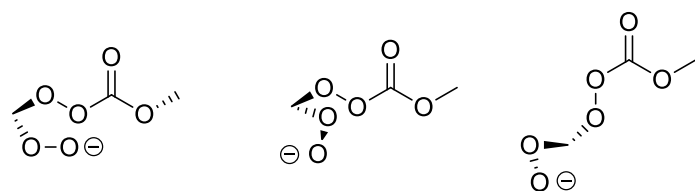
MIN-3h: **15.5**   MIN-3i: **16.3**   MIN-3j: **16.5**

4. Optimized Coordinates of All Structures Labeled in the Manuscript

MIN-1a

```
-------------------------------------------------------------------
Center     Atomic     Atomic          Coordinates (Angstroms)
Number     Number     Type        X           Y           Z
-------------------------------------------------------------------
   1          6          0        1.545657   -1.027806   -0.157278
   2          8          0        1.784942    0.267046   -0.458797
   3          8          0        0.280450   -1.309963    0.529615
   4          8          0       -0.808554   -0.983912   -0.387424
   5          6          0       -1.372644    0.247968   -0.128065
   6          8          0       -2.244246    0.588322   -0.909713
   7          1          0        2.248386   -1.430062    0.589585
```

8	1	0	1.541699	-1.598735	-1.097410
9	8	0	2.061630	1.009662	0.793303
10	6	0	-0.900731	0.999741	1.070427
11	1	0	-1.485217	1.919332	1.142196
12	1	0	0.200622	1.202077	1.011221
13	1	0	-1.036332	0.388195	1.969178

MIN-1b

Center Number	Atomic Number	Atomic Type	Coordinates (Angstroms) X	Y	Z
1	6	0	-1.814891	0.387658	-0.232287
2	8	0	-2.933365	1.094644	-0.500733
3	8	0	-1.018589	0.026717	-1.431315
4	8	0	0.268103	0.733936	-1.445155
5	6	0	0.306811	1.799161	-2.317803
6	8	0	1.385937	2.363073	-2.388995
7	1	0	-2.130003	-0.598763	0.140736
8	1	0	-1.129958	0.909121	0.447679
9	8	0	-2.590060	2.528168	-0.615367
10	6	0	-0.948210	2.171635	-3.023743
11	1	0	-0.727162	2.984965	-3.717547
12	1	0	-1.691455	2.473251	-2.232729
13	1	0	-1.381823	1.313031	-3.543097

MIN-1c

```
---------------------------------------------------------------------

Center     Atomic     Atomic          Coordinates (Angstroms)

Number     Number     Type         X          Y           Z

---------------------------------------------------------------------

  1          6          0       1.574247   -0.913104   -0.191240

  2          8          0       1.786145    0.434079   -0.305703

  3          8          0       0.356650   -1.182998    0.548247

  4          8          0      -0.795999   -0.996321   -0.345077

  5          6          0      -1.489056    0.153762   -0.095320

  6          8          0      -2.501188    0.321497   -0.749130

  7          1          0       2.328113   -1.405138    0.450953

  8          1          0       1.522491   -1.415144   -1.169442

  9          8          0       3.116340    0.475747   -0.987989

 10          6          0      -0.959633    1.095032    0.950206

 11          1          0      -1.640622    1.945103    1.012090

 12          1          0       0.054211    1.406335    0.675232

 13          1          0      -0.886400    0.589444    1.917329

---------------------------------------------------------------------
```

MIN-1d

```
---------------------------------------------------------------------

Center     Atomic     Atomic          Coordinates (Angstroms)

Number     Number     Type         X          Y           Z

---------------------------------------------------------------------

  1          6          0       1.249348    0.397149   -0.127322

  2          8          0       2.657117    0.238349    0.223991
```

3	8	0	0.775246	-0.587622	0.660456
4	8	0	-1.184721	-1.002884	0.035985
5	6	0	-1.930315	0.039147	-0.012703
6	8	0	-1.609273	1.234868	0.084698
7	1	0	1.142156	0.245866	-1.209205
8	1	0	0.974565	1.417352	0.180026
9	8	0	3.375780	-0.445938	-0.673018
10	6	0	-3.430196	-0.304864	-0.203005
11	1	0	-3.884687	0.425377	-0.879242
12	1	0	-3.924432	-0.220793	0.771983
13	1	0	-3.572727	-1.319384	-0.583146

MIN-1e

Center Number	Atomic Number	Atomic Type	Coordinates (Angstroms) X	Y	Z

1	6	0	-0.000122	0.306045	0.202006
2	8	0	1.198638	0.911407	0.397842
3	8	0	-1.114791	1.204150	-0.134286
4	8	0	-1.308158	2.034764	1.051893
5	6	0	-0.616229	3.230995	0.929811
6	8	0	-0.521884	3.860767	-0.100229
7	1	0	-0.278633	-0.285974	1.081576
8	1	0	0.013088	-0.285800	-0.729816
9	8	0	1.521276	0.969811	1.851226
10	6	0	0.008523	3.540557	2.252195

11	1	0	0.370554	4.570596	2.279544
12	1	0	0.826596	2.776188	2.315637
13	1	0	-0.675331	3.337476	3.082196

MIN-1f

Center Number	Atomic Number	Atomic Type	Coordinates (Angstroms)		
			X	Y	Z

1	6	0	1.642007	-1.078422	-0.152775
2	8	0	2.750172	-0.884109	0.570710
3	8	0	0.469138	-0.753812	0.729927
4	8	0	-0.756625	-0.939501	-0.095185
5	6	0	-1.552267	0.150782	-0.062930
6	8	0	-2.604183	0.106091	-0.679139
7	1	0	1.521804	-2.117420	-0.479473
8	1	0	1.588840	-0.352717	-0.983066
9	8	0	3.148375	-2.146230	1.248417
10	6	0	-1.091867	1.339545	0.745938
11	1	0	-1.845543	2.123230	0.656011
12	1	0	-0.119541	1.691301	0.391819
13	1	0	-0.950058	1.055123	1.792033

MIN-1g

| Center | Atomic | Atomic | Coordinates (Angstroms) | | |

Number	Number	Type	X	Y	Z
1	6	0	-0.810136	-2.333546	-2.054104
2	8	0	0.333062	-2.705031	-1.451981
3	8	0	-2.008687	-2.198491	-1.166980
4	8	0	-1.643332	-1.351290	-0.042914
5	6	0	-1.515491	-0.035983	-0.361546
6	8	0	-1.966146	0.504754	-1.349198
7	1	0	-1.195114	-3.145210	-2.694524
8	1	0	-0.691204	-1.385720	-2.589225
9	8	0	1.097656	-1.473318	-1.081395
10	6	0	-0.678424	0.615761	0.710286
11	1	0	-0.769004	1.701772	0.645106
12	1	0	0.344742	0.277822	0.493271
13	1	0	-0.950092	0.259748	1.708373

MIN-1h

Center	Atomic	Atomic	Coordinates (Angstroms)		
Number	Number	Type	X	Y	Z
1	6	0	1.615607	-1.387080	0.168795
2	8	0	2.724347	-0.739326	0.542795
3	8	0	0.402462	-1.210167	1.026492
4	8	0	-0.162974	0.116899	0.811553
5	6	0	-1.126802	0.142382	-0.127112
6	8	0	-1.564201	-0.801116	-0.754644

7	1	0	1.736573	-2.470673	0.339059
8	1	0	1.320576	-1.139974	-0.857821
9	8	0	2.773695	0.580810	-0.148080
10	6	0	-1.613689	1.573931	-0.276731
11	1	0	-1.683368	1.802040	-1.343292
12	1	0	-0.940062	2.279380	0.211893
13	1	0	-2.615829	1.655249	0.157985

MIN-1i

| Center | Atomic | Atomic | | Coordinates (Angstroms) | |
| Number | Number | Type | X | Y | Z |

1	6	0	1.963010	-0.750778	-0.083265
2	8	0	2.651617	-0.296562	-1.132575
3	8	0	0.581993	-1.263977	-0.331484
4	8	0	-0.238417	-0.139393	-0.760606
5	6	0	-1.149703	0.230062	0.160079
6	8	0	-1.301113	-0.231601	1.271728
7	1	0	1.848873	0.059564	0.653916
8	1	0	2.389100	-1.673118	0.343177
9	8	0	3.161335	-1.451318	-1.923576
10	6	0	-2.007723	1.340572	-0.425973
11	1	0	-3.021832	0.955188	-0.573545
12	1	0	-1.615056	1.701699	-1.378108
13	1	0	-2.059338	2.159998	0.295876

MIN-1j

```
---------------------------------------------------------------------

Center      Atomic      Atomic              Coordinates (Angstroms)

Number      Number      Type          X           Y           Z

---------------------------------------------------------------------

   1          6           0        0.327619    -2.231703    1.165952

   2          8           0        0.754531    -3.292260    0.430491

   3          8           0        0.358449    -0.991205    0.405516

   4          8           0       -0.786853    -0.960043   -0.521717

   5          6           0       -1.625132     0.067804   -0.245182

   6          8           0       -2.564205     0.246242   -0.998574

   7          1           0        1.027012    -1.978132    1.987280

   8          1           0       -0.689908    -2.374935    1.570449

   9          8           0        0.765511    -4.353696    1.489147

  10          6           0       -1.337364     0.921825    0.967443

  11          1           0       -2.118904     1.679712    1.035354

  12          1           0       -0.353577     1.390608    0.882412

  13          1           0       -1.318771     0.309583    1.872868

---------------------------------------------------------------------
```

MIN-1k

```
---------------------------------------------------------------------

Center      Atomic      Atomic              Coordinates (Angstroms)

Number      Number      Type          X           Y           Z

---------------------------------------------------------------------

   1          6           0        1.738089    -0.778737   -0.094178

   2          8           0        1.662349     0.530603    0.203657
```

3	8	0	0.447970	-1.469934	-0.403283
4	8	0	-0.423567	-0.455296	-0.955954
5	6	0	-1.417331	-0.145006	-0.050680
6	8	0	-1.941008	-0.932061	0.700644
7	1	0	2.087045	-1.413385	0.738464
8	1	0	2.374480	-0.867069	-0.989807
9	8	0	0.890673	0.711387	1.457681
10	6	0	-1.773983	1.310102	-0.212050
11	1	0	-2.780393	1.497074	0.169297
12	1	0	-1.681040	1.638286	-1.251697
13	1	0	-1.017215	1.830106	0.391885

MIN-1l

Center Number	Atomic Number	Atomic Type	Coordinates (Angstroms) X	Y	Z
1	6	0	1.738089	-0.778737	-0.094178
2	8	0	1.662349	0.530603	0.203657
3	8	0	0.447970	-1.469934	-0.403283
4	8	0	-0.423567	-0.455296	-0.955954
5	6	0	-1.417331	-0.145006	-0.050680
6	8	0	-1.941008	-0.932061	0.700644
7	1	0	2.087045	-1.413385	0.738464
8	1	0	2.374480	-0.867069	-0.989807
9	8	0	0.890673	0.711387	1.457681
10	6	0	-1.773983	1.310102	-0.212050

11	1	0	-2.780393	1.497074	0.169297
12	1	0	-1.681040	1.638286	-1.251697
13	1	0	-1.017215	1.830106	0.391885

TS-2

| Center | Atomic | Atomic | Coordinates (Angstroms) | | |
| Number | Number | Type | X | Y | Z |

1	6	0	1.733188	-0.943000	0.168225
2	8	0	3.295922	-0.905126	0.614313
3	8	0	1.361398	-0.001836	0.972531
4	8	0	-0.794916	-0.751001	-0.305428
5	6	0	-1.790947	0.045679	-0.222290
6	8	0	-2.879336	-0.139252	-0.814787
7	1	0	1.443891	-1.981144	0.377360
8	1	0	1.812466	-0.720263	-0.908619
9	8	0	3.662450	-1.841208	1.420880
10	6	0	-1.614468	1.277006	0.674056
11	1	0	-2.470997	1.948858	0.567432
12	1	0	-0.681191	1.791448	0.429267
13	1	0	-1.526348	0.953585	1.717051

TS-2*

Center	Atomic	Atomic	Coordinates (Angstroms)

Number	Number	Type	X	Y	Z
1	6	0	1.539531	-0.935548	-0.232515
2	8	0	2.353381	0.145568	0.042384
3	8	0	0.468005	-0.994021	0.692467
4	8	0	-0.988271	-1.084186	-0.105798
5	6	0	-1.674441	0.065490	-0.035880
6	8	0	-2.761780	0.095859	-0.606363
7	1	0	2.171425	-1.826772	-0.077602
8	1	0	1.140565	-0.888083	-1.255662
9	8	0	1.818865	1.317679	-0.571195
10	6	0	-1.078344	1.223131	0.714917
11	1	0	-1.775072	2.062364	0.660553
12	1	0	-0.095396	1.481061	0.282726
13	1	0	-0.893371	0.943003	1.756433

MIN-3a

Center Number	Atomic Number	Atomic Type	Coordinates (Angstroms)		
			X	Y	Z
1	6	0	1.546563	-0.734064	-0.303429
2	8	0	1.275456	0.580308	0.091233
3	8	0	0.717229	-1.665543	0.334789
4	8	0	-0.643114	-1.424981	-0.206559
5	6	0	-1.121879	-0.068165	0.109862
6	8	0	-2.205050	0.166645	-0.471431

7	1	0	2.562820	-0.953511	0.049287
8	1	0	1.449771	-0.828253	-1.395329
9	8	0	-0.072485	0.875524	-0.455608
10	8	0	-1.046820	0.018750	1.536732
11	6	0	-1.592266	1.223081	2.036328
12	1	0	-1.568600	1.146777	3.129590
13	1	0	-0.998005	2.093735	1.722389
14	1	0	-2.627634	1.361791	1.697915

MIN-3b

Center Number	Atomic Number	Atomic Type	Coordinates (Angstroms)		
			X	Y	Z

1	6	0	1.659021	-0.692222	-0.181884
2	8	0	1.326882	0.178244	0.865638
3	8	0	0.603569	-1.550766	-0.519835
4	8	0	-0.426971	-0.687120	-1.101626
5	6	0	-0.933802	0.232996	0.015912
6	8	0	-1.505182	-0.298420	0.977342
7	1	0	2.458158	-1.337129	0.205820
8	1	0	1.970144	-0.114668	-1.065140
9	8	0	0.311582	1.078671	0.313654
10	8	0	-1.623508	1.183896	-0.810540
11	6	0	-2.959418	1.415080	-0.401467
12	1	0	-3.009755	1.814821	0.619198
13	1	0	-3.365417	2.149536	-1.106410

```
   14             1            0        -3.560590    0.497749   -0.435460

  ----------------------------------------------------------------------
```

MIN-3c

```
----------------------------------------------------------------------

  Center      Atomic      Atomic               Coordinates (Angstroms)

  Number      Number      Type         X            Y            Z

----------------------------------------------------------------------

    1            6            0        1.954908    -0.726550   -0.249784

    2            8            0        1.666550     0.630220   -0.015520

    3            8            0        0.823486    -1.548132   -0.075776

    4            8            0       -0.310078    -0.806569   -0.591503

    5            6            0       -0.677133     0.238274    0.462619

    6            8            0       -1.443450    -0.084235    1.390031

    7            1            0        2.689120    -1.141207    0.462235

    8            1            0        2.344989    -0.747134   -1.281745

    9            8            0        0.652812     0.640878    1.047356

   10            8            0       -1.088698     1.265803   -0.458916

   11            6            0       -1.946696     2.223840    0.127631

   12            1            0       -2.283490     2.876612   -0.686349

   13            1            0       -2.809342     1.748786    0.610250

   14            1            0       -1.419840     2.831765    0.880040

----------------------------------------------------------------------
```

MIN-3d

```
----------------------------------------------------------------------

  Center      Atomic      Atomic               Coordinates (Angstroms)

  Number      Number      Type         X            Y            Z
```

1	6	0	1.498572	-1.121721	-0.046344
2	8	0	1.527438	-0.149082	-0.980698
3	8	0	0.470524	-0.996404	1.003019
4	8	0	-0.823896	-1.096565	0.326398
5	6	0	-1.268937	0.109284	-0.135220
6	8	0	-2.114119	0.121805	-1.009486
7	1	0	2.402294	-1.132422	0.581420
8	1	0	1.307547	-2.079356	-0.553993
9	8	0	2.226203	1.051416	-0.443152
10	8	0	-0.779683	1.143995	0.530602
11	6	0	-0.531703	2.357393	-0.221053
12	1	0	-1.263604	2.456942	-1.027206
13	1	0	-0.642984	3.175748	0.494312
14	1	0	0.507432	2.269999	-0.575592

MIN-3e

| Center | Atomic | Atomic | | Coordinates (Angstroms) | |
| Number | Number | Type | X | Y | Z |

1	6	0	-1.576651	0.634404	0.357205
2	8	0	-2.485554	-0.334451	0.256274
3	8	0	-0.401051	0.582872	-0.570358
4	8	0	0.431820	-0.554440	-0.194890
5	6	0	1.524438	-0.146705	0.464529
6	8	0	1.833887	0.964243	0.833533

7	1	0	-1.149299	0.635410	1.371803
8	1	0	-1.961345	1.617852	0.041978
9	8	0	-3.342931	-0.078614	-0.934679
10	8	0	2.278240	-1.262721	0.663756
11	6	0	3.487073	-1.040385	1.395785
12	1	0	3.968122	-2.017643	1.462136
13	1	0	4.134833	-0.330395	0.873385
14	1	0	3.271703	-0.653795	2.396439

MIN-3f

| Center | Atomic | Atomic | Coordinates (Angstroms) | | |
| Number | Number | Type | X | Y | Z |

1	6	0	-1.456993	-0.935924	0.191617
2	8	0	-1.567953	0.356141	-0.243813
3	8	0	-0.231794	-1.130863	0.938920
4	8	0	0.883018	-1.078232	-0.019844
5	6	0	1.321691	0.181580	-0.268611
6	8	0	2.022300	0.382841	-1.239634
7	1	0	-1.501663	-1.649923	-0.644371
8	1	0	-2.203220	-1.203182	0.965225
9	8	0	-2.827435	0.323667	-1.049959
10	8	0	0.997282	1.067108	0.674939
11	6	0	0.924389	2.432522	0.234757
12	1	0	0.832016	3.026154	1.145204
13	1	0	1.823749	2.711990	-0.320117

| 14 | 1 | 0 | 0.029611 | 2.545378 | -0.383381 |

MIN-3g

| Center | Atomic | Atomic | Coordinates (Angstroms) | | |
| Number | Number | Type | X | Y | Z |

1	6	0	-1.571762	-0.505700	0.485322
2	8	0	-2.513819	0.401597	0.223230
3	8	0	-0.758557	-1.003909	-0.675044
4	8	0	0.279946	-0.044400	-1.053997
5	6	0	1.419132	-0.282008	-0.392838
6	8	0	1.651738	-1.100823	0.470412
7	1	0	-2.039714	-1.476469	0.724169
8	1	0	-0.862572	-0.164627	1.248010
9	8	0	-1.951496	1.763930	0.431026
10	8	0	2.331098	0.597710	-0.885886
11	6	0	3.599289	0.570532	-0.225565
12	1	0	4.201688	1.330336	-0.726473
13	1	0	3.489287	0.812415	0.835558
14	1	0	4.069381	-0.413126	-0.319591

MIN-3h

| Center | Atomic | Atomic | Coordinates (Angstroms) | | |
| Number | Number | Type | X | Y | Z |

```
----------------------------------------------------------------------
    1          6           0        -1.421332    -0.864462     0.196817

    2          8           0        -1.804771     0.415142     0.035493

    3          8           0        -0.361259    -1.344908    -0.757246

    4          8           0         0.599160    -0.280234    -0.959175

    5          6           0         1.295655    -0.009938     0.176942

    6          8           0         1.414636    -0.711138     1.155327

    7          1           0        -2.229339    -1.553431    -0.098786

    8          1           0        -1.044123    -1.046821     1.207588

    9          8           0        -0.919489     1.266786     0.887661

   10          8           0         1.983913     1.128746    -0.072510

   11          6           0         2.255369     1.891897     1.110806

   12          1           0         2.875892     1.322041     1.809862

   13          1           0         2.787038     2.782561     0.768994

   14          1           0         1.301970     2.159459     1.575774

----------------------------------------------------------------------
```

MIN-3i

```
----------------------------------------------------------------------
Center     Atomic      Atomic              Coordinates (Angstroms)

Number     Number      Type             X            Y            Z

----------------------------------------------------------------------
    1          6           0         1.602683    -0.443827     0.392481

    2          8           0         1.368718     0.236885    -0.762485

    3          8           0         0.427882    -1.181510     0.826195

    4          8           0        -0.522248    -0.194783     1.343014

    5          6           0        -1.679384    -0.253490     0.659969

    6          8           0        -2.032835    -1.042561    -0.181617
```

Center Number	Atomic Number	Atomic Type	X	Y	Z
7	1	0	1.936743	0.218860	1.206279
8	1	0	2.313801	-1.285924	0.273316
9	8	0	2.688802	0.915867	-0.974037
10	8	0	-2.439940	0.762251	1.147985
11	6	0	-3.726897	0.883004	0.532565
12	1	0	-4.201092	1.735673	1.021151
13	1	0	-3.624878	1.066252	-0.540523
14	1	0	-4.319788	-0.023849	0.685178

MIN-3j

Center Number	Atomic Number	Atomic Type	Coordinates (Angstroms) X	Y	Z
1	6	0	-1.577180	0.403678	0.200277
2	8	0	-2.345284	-0.631192	0.636844
3	8	0	-0.297647	0.461500	0.886525
4	8	0	0.578854	-0.612544	0.381074
5	6	0	1.515668	-0.180685	-0.476015
6	8	0	2.364015	-0.944737	-0.895777
7	1	0	-1.988808	1.392352	0.486076
8	1	0	-1.402863	0.375136	-0.888265
9	8	0	-3.606143	-0.366220	-0.129813
10	8	0	1.422156	1.119987	-0.805227
11	6	0	2.399543	1.564977	-1.754651
12	1	0	2.183573	2.622532	-1.911564
13	1	0	3.411226	1.433484	-1.360847

| 14 | 1 | 0 | 2.306170 | 1.011667 | -2.693024 |

TS-4

| Center | Atomic | Atomic | Coordinates (Angstroms) | | |
| Number | Number | Type | X | Y | Z |

1	6	0	1.269297	-0.596152	-0.093764
2	8	0	2.189102	0.126227	0.642310
3	8	0	0.279476	-0.906446	0.868712
4	8	0	-1.173574	-1.321502	0.115609
5	6	0	-1.991774	-0.321550	-0.214546
6	8	0	-2.829704	-0.507981	-1.088043
7	1	0	1.769829	-1.512564	-0.445825
8	1	0	0.859875	-0.000307	-0.920033
9	8	0	1.868532	1.512867	0.639190
10	8	0	-1.942655	0.870995	0.401148
11	6	0	-1.276933	1.125605	1.665305
12	1	0	-0.232151	1.398896	1.494305
13	1	0	-1.842254	1.957863	2.095669
14	1	0	-1.337654	0.252519	2.317033

TS-5

| Center | Atomic | Atomic | Coordinates (Angstroms) | | |
| Number | Number | Type | X | Y | Z |

1	6	0	1.954243	-0.551770	-0.372806
2	8	0	1.969954	0.786153	-0.687419
3	8	0	0.853181	-1.279742	-0.886746
4	8	0	-0.256712	-1.522194	0.307806
5	6	0	-1.148074	-0.536324	0.387652
6	8	0	-1.824320	-0.399242	1.397600
7	1	0	2.018542	-0.700425	0.715516
8	1	0	2.817048	-0.993952	-0.901899
9	8	0	1.259340	1.516240	0.328606
10	8	0	-1.281419	0.185963	-0.733173
11	6	0	-1.807914	1.510691	-0.563158
12	1	0	-2.117497	1.832374	-1.560415
13	1	0	-2.661379	1.506703	0.120940
14	1	0	-0.994316	2.139163	-0.187454

Investigations of Reaction Order and Reaction Kinetics

Part I. Fixed monoperester concentration unchanged, variable [TBAF].
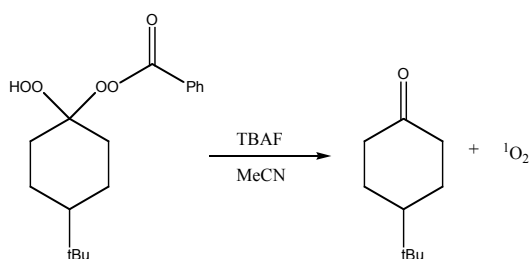
Conditions: 0.5mM monoperester 3mL, TBAF 15μL: Rapidly stirred THF solutions (0.5 mM) of

dihydroperoxide monoester **1c** in a cuvette were individually treated with a series of THF

solutions of TBAF ranging in concentration from 0.5 to 2.00 mM. The reaction solutions were

mixed and the cuvettes then placed in the UV spectrophotometer, with the absorbence at 272 nm

monitored for 1.0 minute.

$$V_0 = k \cdot [\text{Monoperester}]_0^m \cdot [\text{TBAF}]_0^n$$

$$-\frac{d[\text{Monoperester}]_0}{dt} = k \cdot [\text{Monoperester}]_0^m \cdot [\text{TBAF}]_0^n$$

$$\text{Abs} = \varepsilon \cdot b \cdot [\text{Monoperester}]$$

$$-\frac{d(\text{Abs})_0}{dt} = k \cdot [\text{Monoperester}]_0^m \cdot \varepsilon \cdot b \cdot [\text{TBAF}]_0^n$$

$$K_1 = k \cdot [\text{Monoperester}]_0^m \cdot \varepsilon \cdot b$$

$$-\frac{d(\text{Abs})_0}{dt} = K_1 \cdot [\text{TBAF}]_0^n$$

$$\text{Lg}\left(-\frac{d(\text{Abs})_0}{dt}\right) = n \cdot \text{Lg}\left([\text{TBAF}]_0\right) + \text{Lg}(K_1)$$

At the initial point, V_0 is the initial rate, $(\text{Abs})_0$ is the initial absorbance, $[\text{Monoperester}]_0$ and

$[\text{TBAF}]_0$ are the initial concentration

[TBAF]$_0$/mM	-d(Abs)$_0$/dt	Lg([TBAF]$_0$)	Lg(-d(Abs)$_0$/dt)
0.50	0.0302	-0.301	-1.520
0.75	0.0339	-0.125	-1.470
1.00	0.0524	0.000	-1.281
1.25	0.0647	0.097	-1.189
1.50	0.0789	0.176	-1.103
1.75	0.0845	0.243	-1.073
2.00	0.1055	0.301	-0.977

Then plot Lg(-d(Abs)$_0$/dt) vs Lg([TBAF]$_0$)
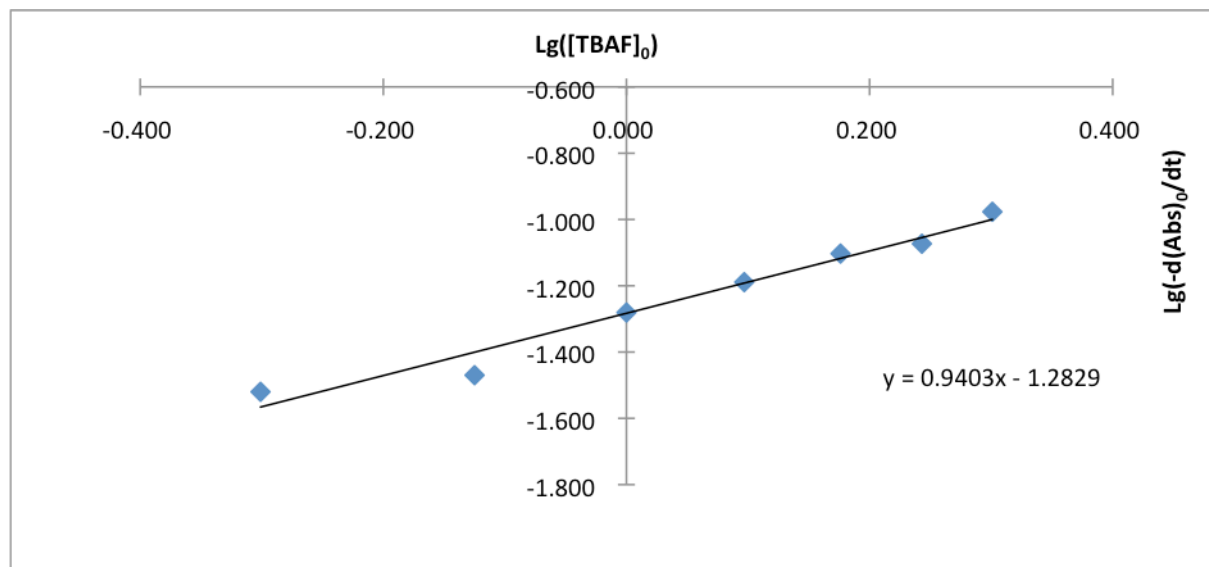
n = 0.9403. This indicates the reaction is a first order reaction to TBAF reactant

$K_1 = 0.05213 \ L \cdot mmol^{-1} \cdot s^{-1}$

Part II. Fixed TBAF concentration unchanged, variable [Monoperester]
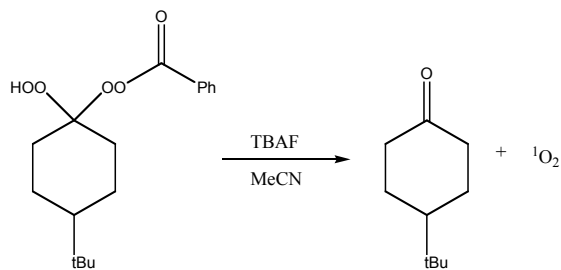
Conditions: Monoperester 3mL, TBAF 0.3M 15 μ L: The experiment described above was repeated except that the concentration of TBAF was held constant while the concentration of **1c** was varied.

$$V_0 = k \cdot [\text{Monoperester}]_0^m \cdot [\text{TBAF}]_0^n$$

$$-\frac{d[\text{Monoperester}]_0}{dt} = k \cdot [\text{Monoperester}]_0^m \cdot [\text{TBAF}]_0^n$$

$$\text{Abs} = \varepsilon \cdot b \cdot [\text{Monoperester}]$$

$$-\frac{d(\text{Abs})_0}{dt} = k \cdot [\text{Monoperester}]_0^m \cdot \varepsilon \cdot b \cdot [\text{TBAF}]_0^n$$

$$K_2 = k \cdot [\text{TBAF}]_0^n \cdot \varepsilon \cdot b$$

$$-\frac{d(\text{Abs})_0}{dt} = K_2 \cdot [\text{Monoperester}]_0^m$$

$$\text{Lg}\left(-\frac{d(\text{Abs})_0}{dt}\right) = m \cdot \text{Lg}\left([\text{Monoperester}]_0\right) + \text{Lg}(K_2)$$

At the initial point, V_0 is the initial rate, $(\text{Abs})_0$ is the initial absorbance, $[\text{Monoperester}]_0$ and

$[\text{TBAF}]_0$ are the initial concentration

[Monoperester]$_0$/mM	-d(Abs)$_0$/dt	Lg([Monoperester]$_0$)	Lg(-d(Abs)$_0$/dt)
0.3	0.0352	-0.523	-1.453
0.4	0.0551	-0.398	-1.259
0.5	0.0695	-0.301	-1.158
0.6	0.0824	-0.222	-1.084
0.7	0.111	-0.155	-0.955
0.8	0.113	-0.097	-0.947
0.9	0.133	-0.046	-0.876
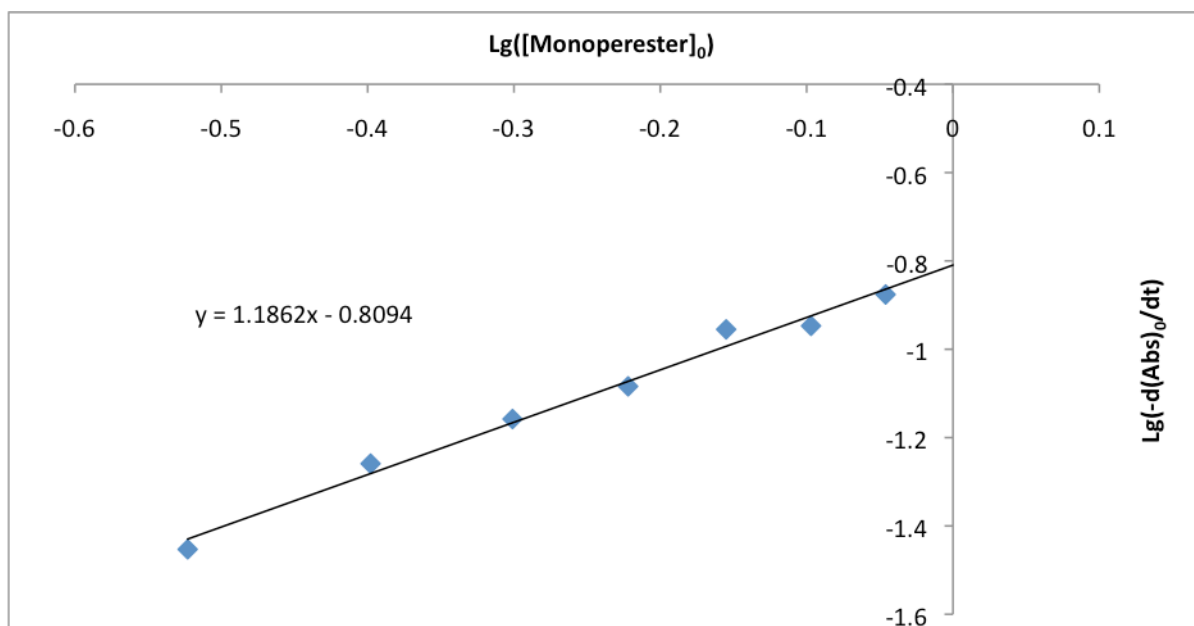
m = 1.1862. This indicates the reaction is a first order reaction to Peroxide reactant

$K_2 = 0.1551 \ L \cdot mmol\text{-}1 \cdot s\text{-}1$

Part III. Calculation of apparent rate constant.

$Abs = \varepsilon \cdot b \cdot [\text{Monoperester}]$

[Monoperester]/mM	Abs
0.3	0.323
0.4	0.405
0.5	0.511
0.6	0.612
0.7	0.732
0.8	0.827
0.9	0.927
1.0	1.036
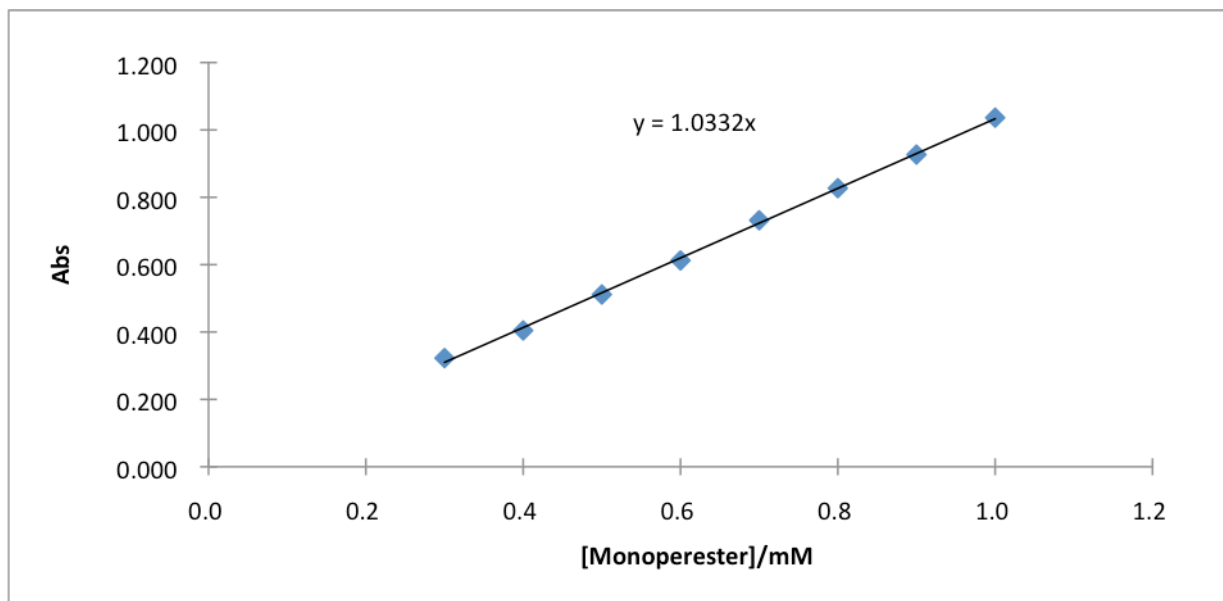
$\varepsilon \cdot b = 1.0332\ \text{L} \cdot \text{mmol}^{-1}$

With Part I result:

$K_1 = 0.05213\ \text{L} \cdot \text{mmol}^{-1} \cdot \text{s}^{-1}$, $[\text{Monoperester}]_0 = 0.5\ \text{mmol} \cdot \text{L}^{-1}$

$K_1 = k \cdot [\text{Monoperester}]_0 \cdot \varepsilon \cdot b$

$k = 0.101\ \text{L} \cdot \text{mmol}^{-1} \cdot \text{s}^{-1}$

With Part II result

$K_2 = 0.1551\ \text{L} \cdot \text{mmol}^{-1} \cdot \text{s}^{-1}$, $[\text{TBAF}]_0 = 1.5\ \text{mmol} \cdot \text{L}^{-1}$

$K_2 = k \cdot [\text{TBAF}]_0 \cdot \varepsilon \cdot b$

$k = 0.100\ \text{L} \cdot \text{mmol}^{-1} \cdot \text{s}^{-1}$

Therefore the reaction constant k is $0.101\ \text{L} \cdot \text{mmol}^{-1} \cdot \text{s}^{-1}$

Thermal stability of **1a** and **1d**
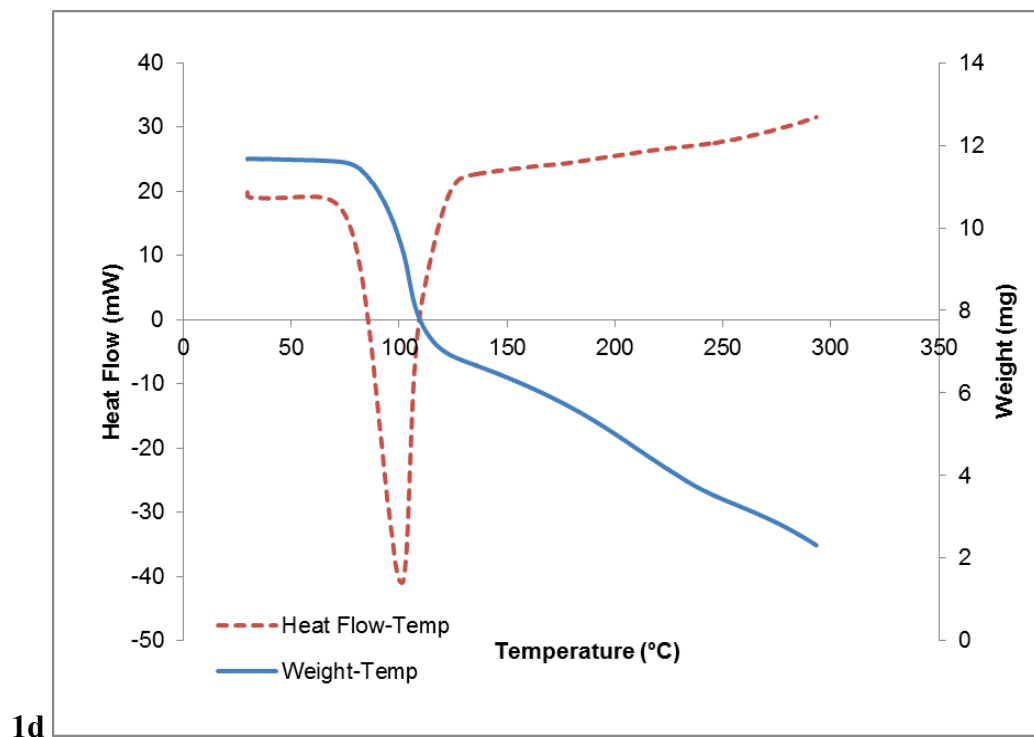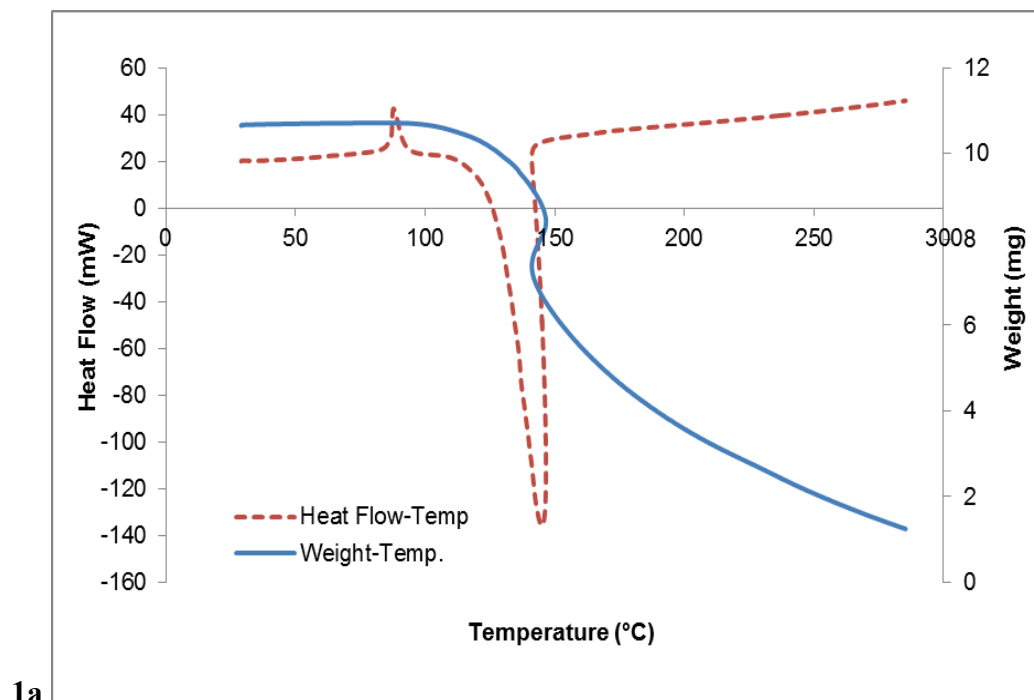
1a

1d

References

1) Smith L.; Hill F. L.; *J. Chrom. A* **1972**, *66*, 101

2) Goldstein, E.; Beno, B.; Houk, K. N. *J. Am. Chem. Soc.* **1996**, *118*, 6036.

3) Foote, C. S.; Clennan, E. L. In *Active Oxygen in Chemistry*; Foote, C. S., Valentine, J. S., Greenberg, A., Liebman, J. F., Eds.; Blackie: London, **1995**.

Supporting information (NMR spectra)

Generation of singlet oxygen from fragmentation of monoactivated 1,1-"
dihydroperoxides

Jiliang Hang, Prasanta Ghorai, Solaire A. Finkenstaedt-Quinn, Ilhan Findik, Emily
Sliz, Keith T. Kuwata, Patrick H. Dussault*

pdussault1@unl.edu

"

Contents	Page

SpinWorks 3: 1D Proton NMR

PPM

1.991

7a

file: ...\data\nmr\notebook7\jh-7-27\1\fid   expt: <zg30>
transmitter freq.: 400.132471 MHz
time domain size: 65536 points
width: 8278.15 Hz = 20.6885 ppm = 0.126314 Hz/pt
number of scans: 16

freq. of 0 ppm: 400.130000 MHz
processed size: 32768 complex points
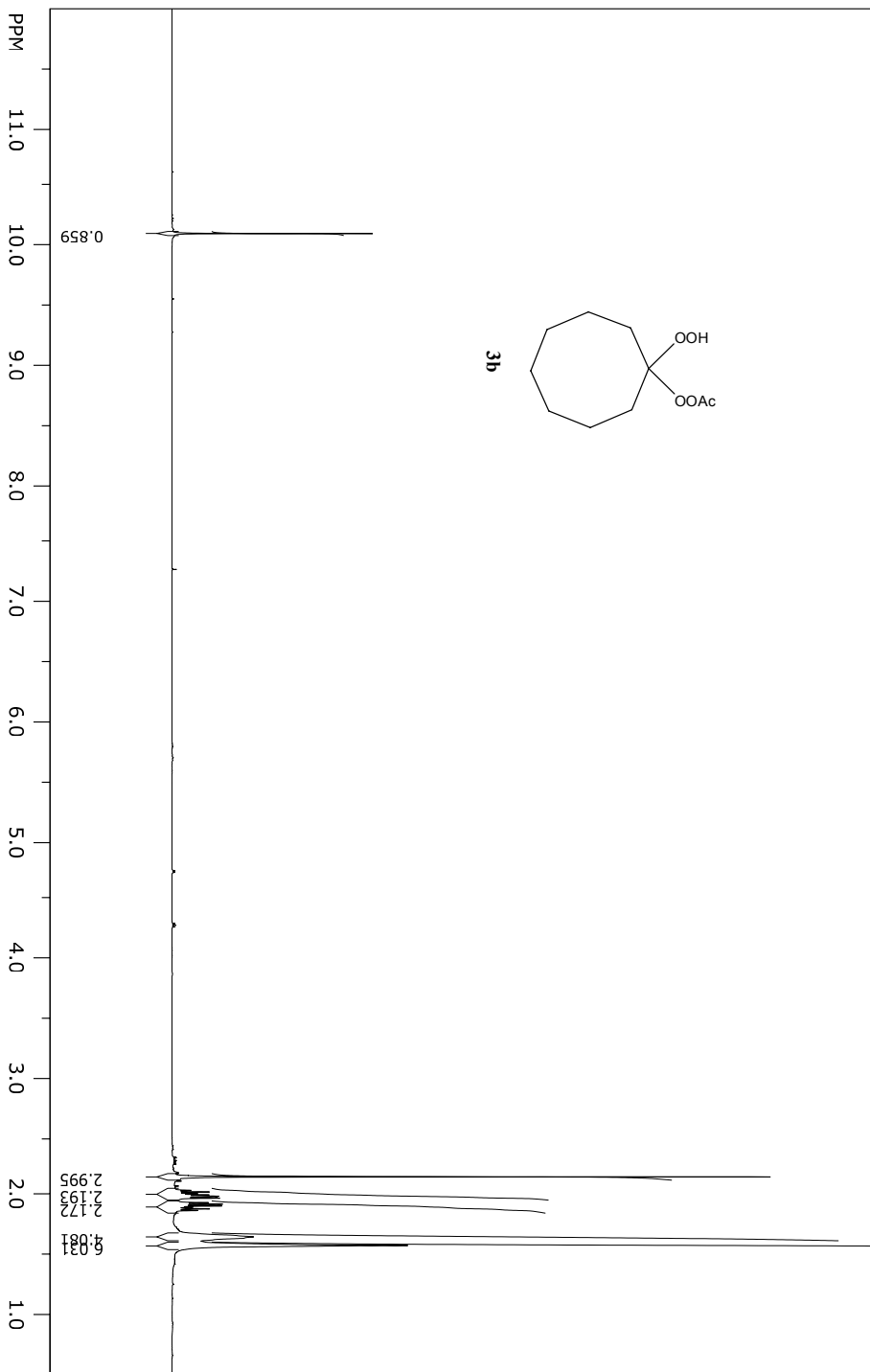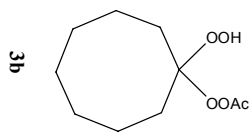LB: 0.300   GF: 0.0000
Hz/cm: 195.104   ppm/cm: 0.48760
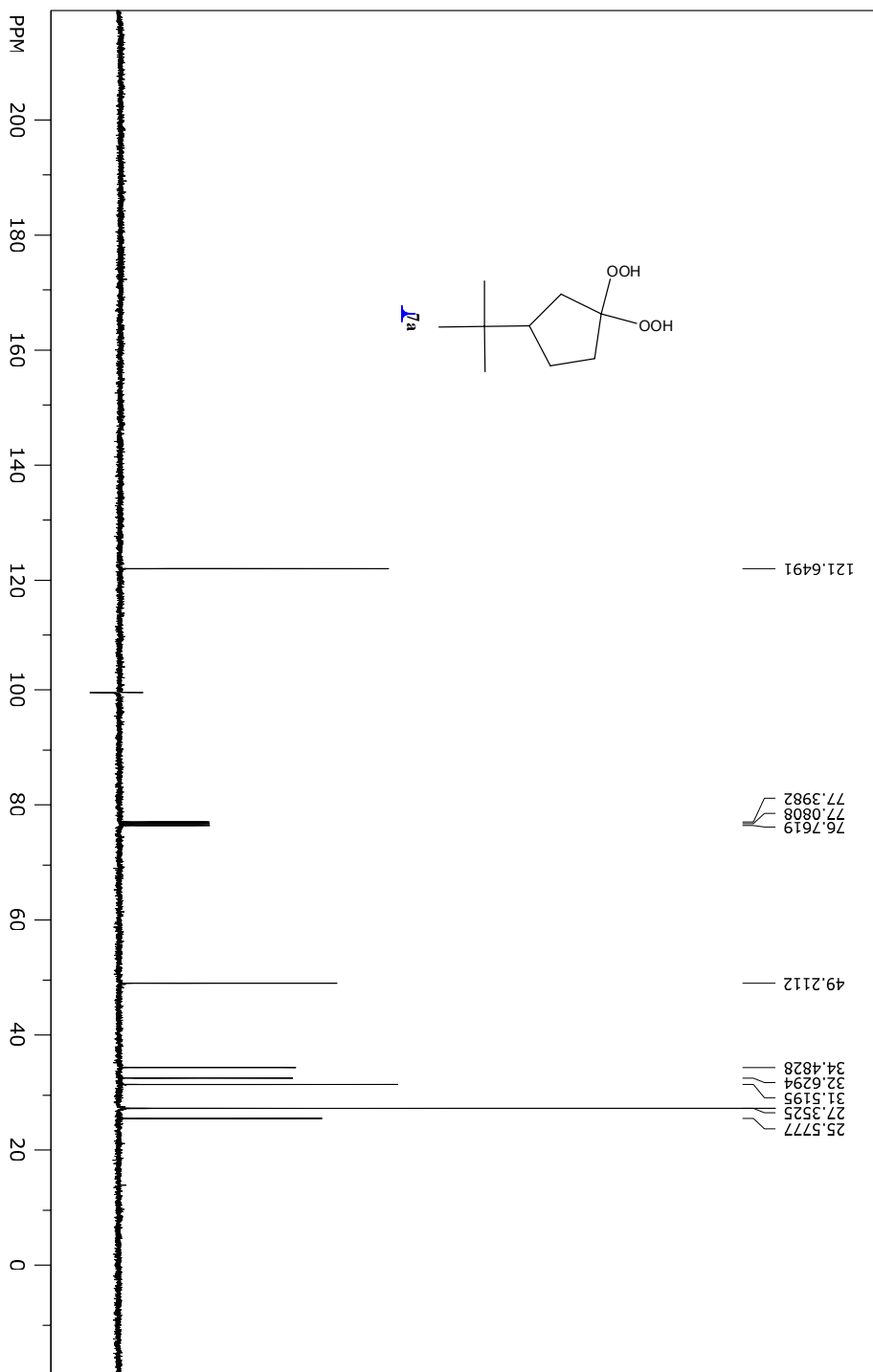
2.079
2.018
2.005
1.014
8.999

SpinWorks 3: 13C

PPM

file: ...\data\nmr\notebook7\jh-7-27\2\fid   expt: <zgpg30>
transmitter freq.: 100.622830 MHz
time domain size: 65536 points
width: 23980.82 Hz = 238.3238 ppm = 0.365918 Hz/pt
number of scans: 25

freq. of 0 ppm: 100.612769 MHz
processed size: 32768 complex points
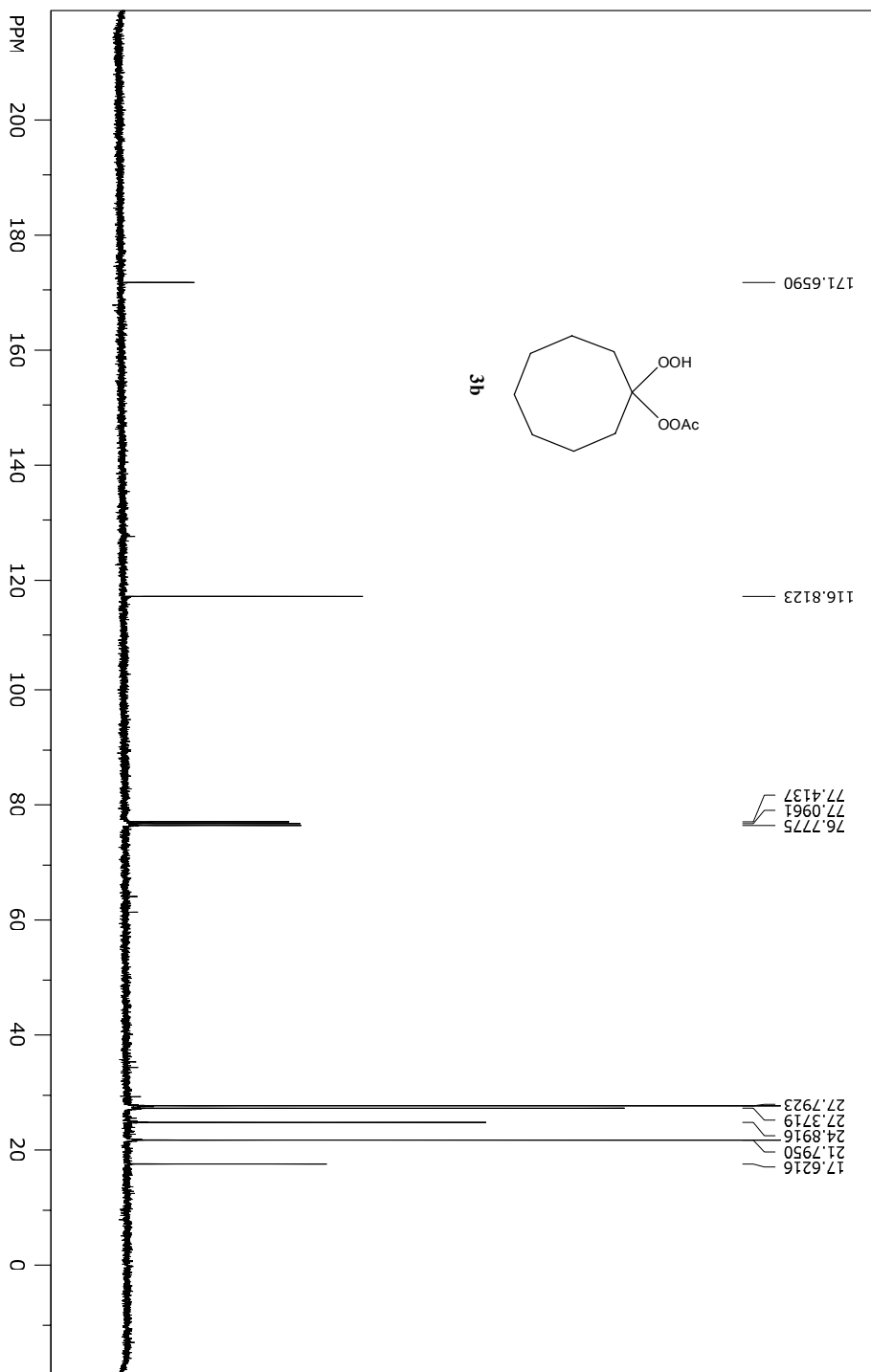LB: 1.000   GF: 0.0000
Hz/cm: 959.233   ppm/cm: 9.53295

121.6491

77.3982
77.0808
76.7619

49.2112

34.4828
32.6294
31.5195
27.3525
25.5777

2b

PPM

0.938

2.997
4.067
8.532

10.0 9.0 8.0 7.0 6.0 5.0 4.0 3.0 2.0 1.0
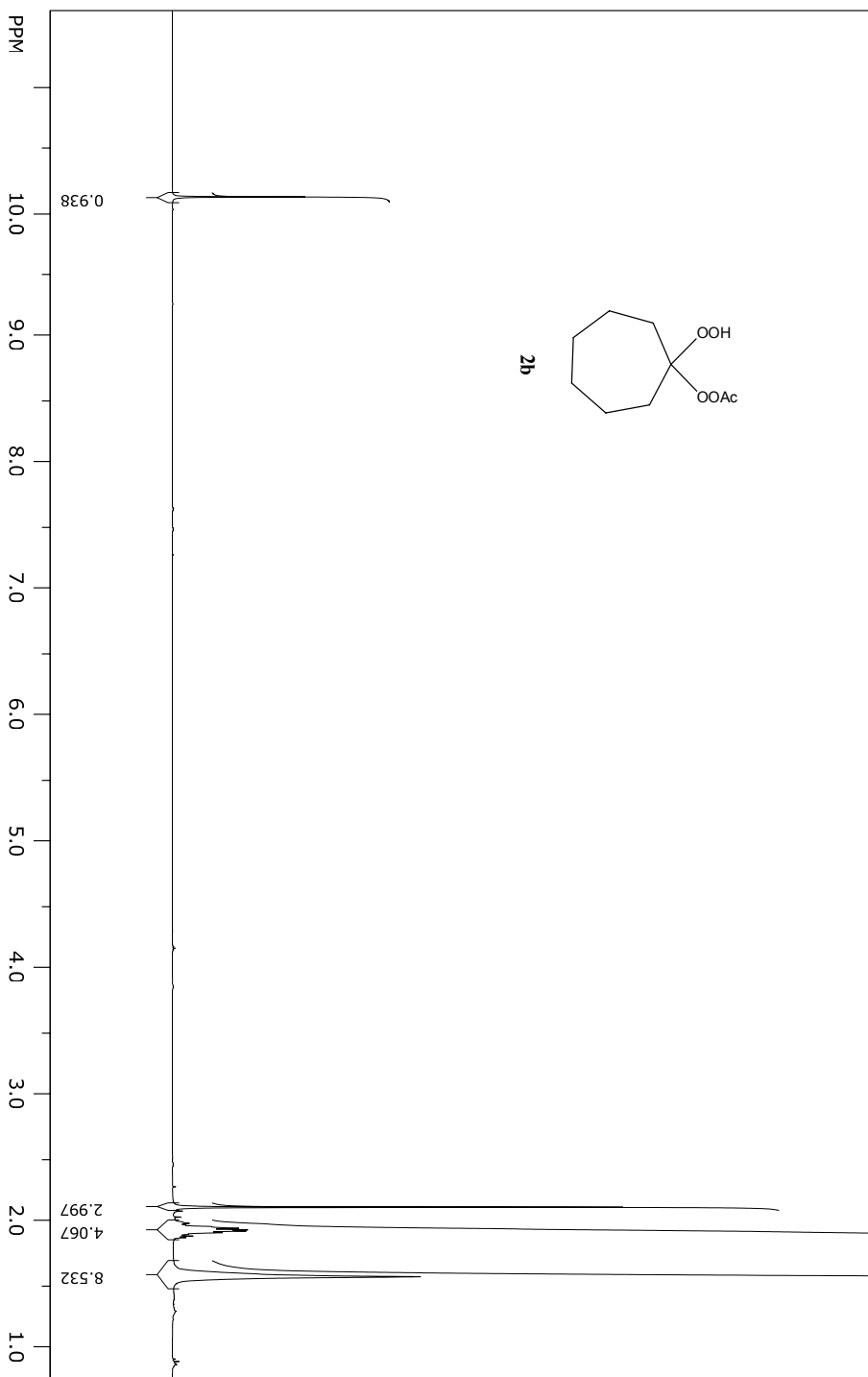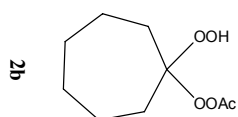
file: ...\data\nmr\notebook3\jh-3-96\1\fid   expt: <zg30>
transmitter freq.: 400.132471 MHz
time domain size: 65536 points
width: 8278.15 Hz = 20.6885 ppm = 0.126314 Hz/pt
number of scans: 16

freq. of 0 ppm: 400.130000 MHz
processed size: 32768 complex points
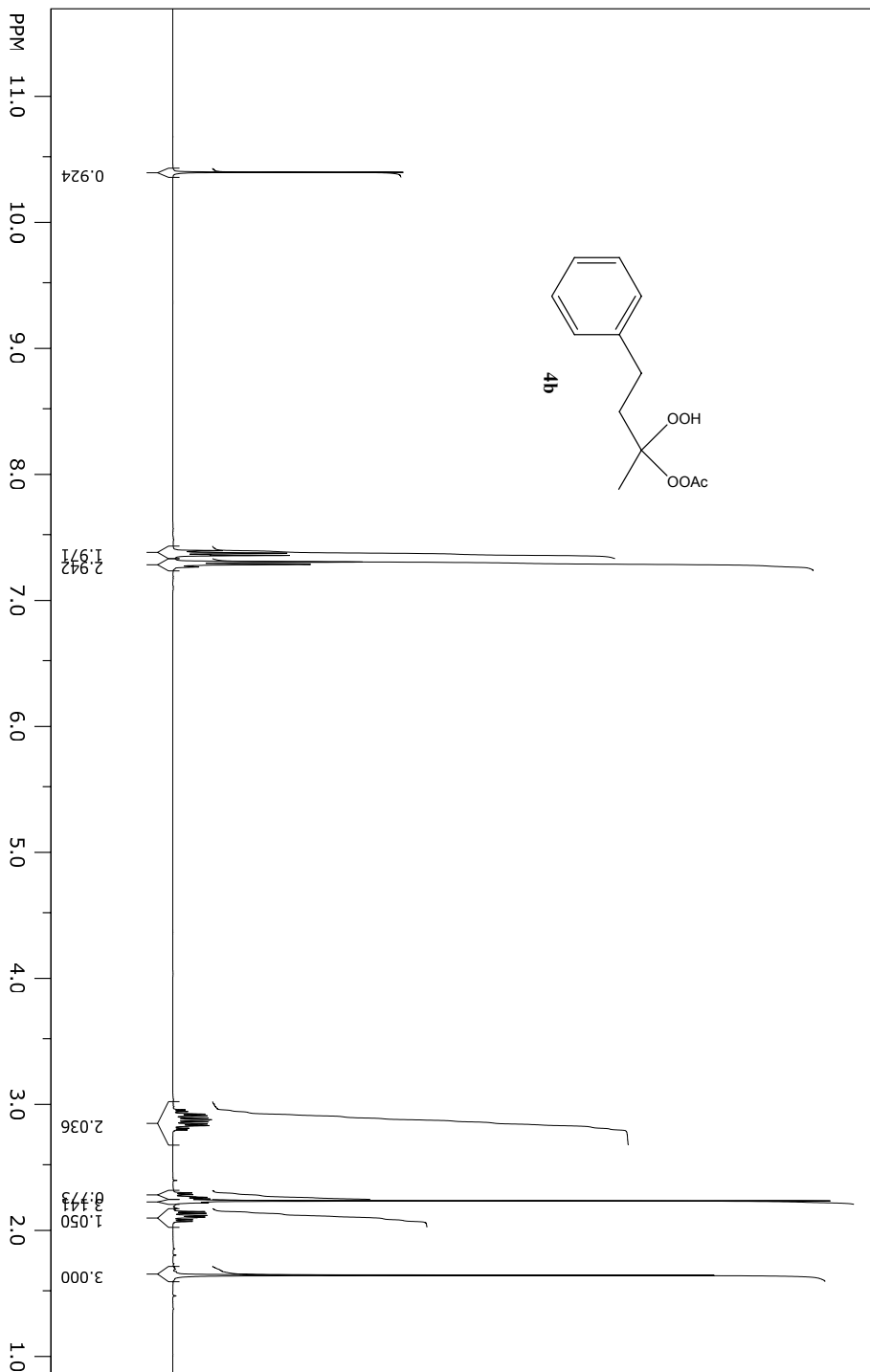LB: 0.300   GF: 0.0000
Hz/cm: 174.360   ppm/cm: 0.43575

SI_Spectra-5 ...
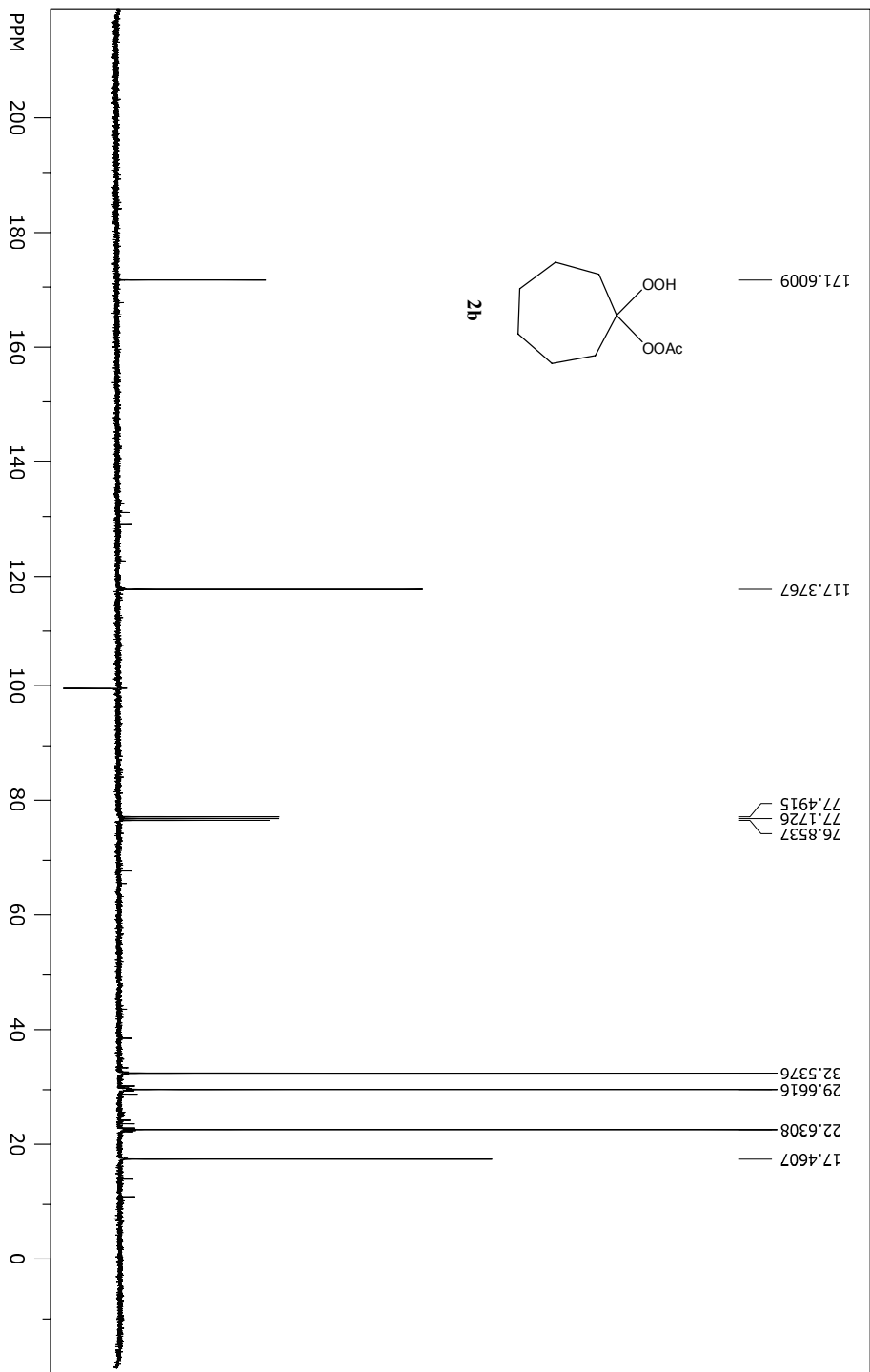
Hang, et al: "Generation of singlet oxygen from fragmentation of monoactivated 1,1- dihydroperoxides"

PPM

200 180 160 140 120 100 80 60 40 20 0

171.6009

117.3767

77.4915
77.1726
76.8537

32.5376
29.6616
22.6308

17.4607

2b

OOH

OOAc

file: ...:\data\nmr\notebook3\jh-3-96\2\fid   expt: <zgpg30>
transmitter freq.: 100.622830 MHz
time domain size: 65536 points
width: 23980.82 Hz = 238.3238 ppm = 0.365918 Hz/pt
number of scans: 35

freq. of 0 ppm: 100.612769 MHz
processed size: 32768 complex points
LB: 1.000   GF: 0.0000
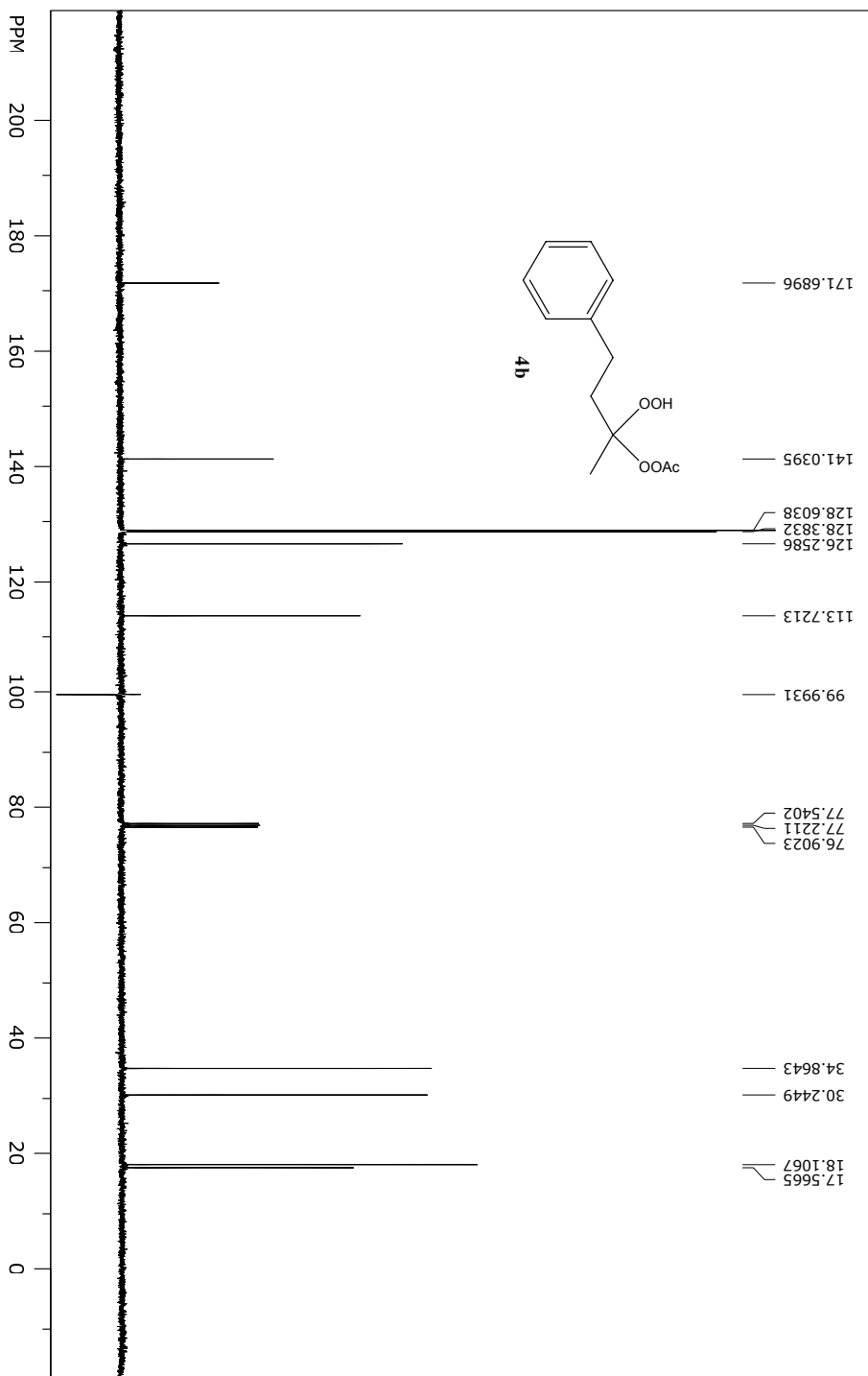Hz/cm: 959.233   ppm/cm: 9.53295

Hang, et al: "Generation of singlet oxygen from fragmentation of monoactivated 1,1- dihydroperoxides"

3b

PPM

0.859

2.995
2.193
2.172
4.081
6.031

Hang, et al: "Generation of singlet oxygen from fragmentation of monoactivated 1,1- dihydroperoxides"

171.6590

116.8123

77.4137
77.0961
76.7775

27.7923
27.3719
24.8916
21.7950
17.6216

3b

PPM   200   180   160   140   120   100   80   60   40   20   0
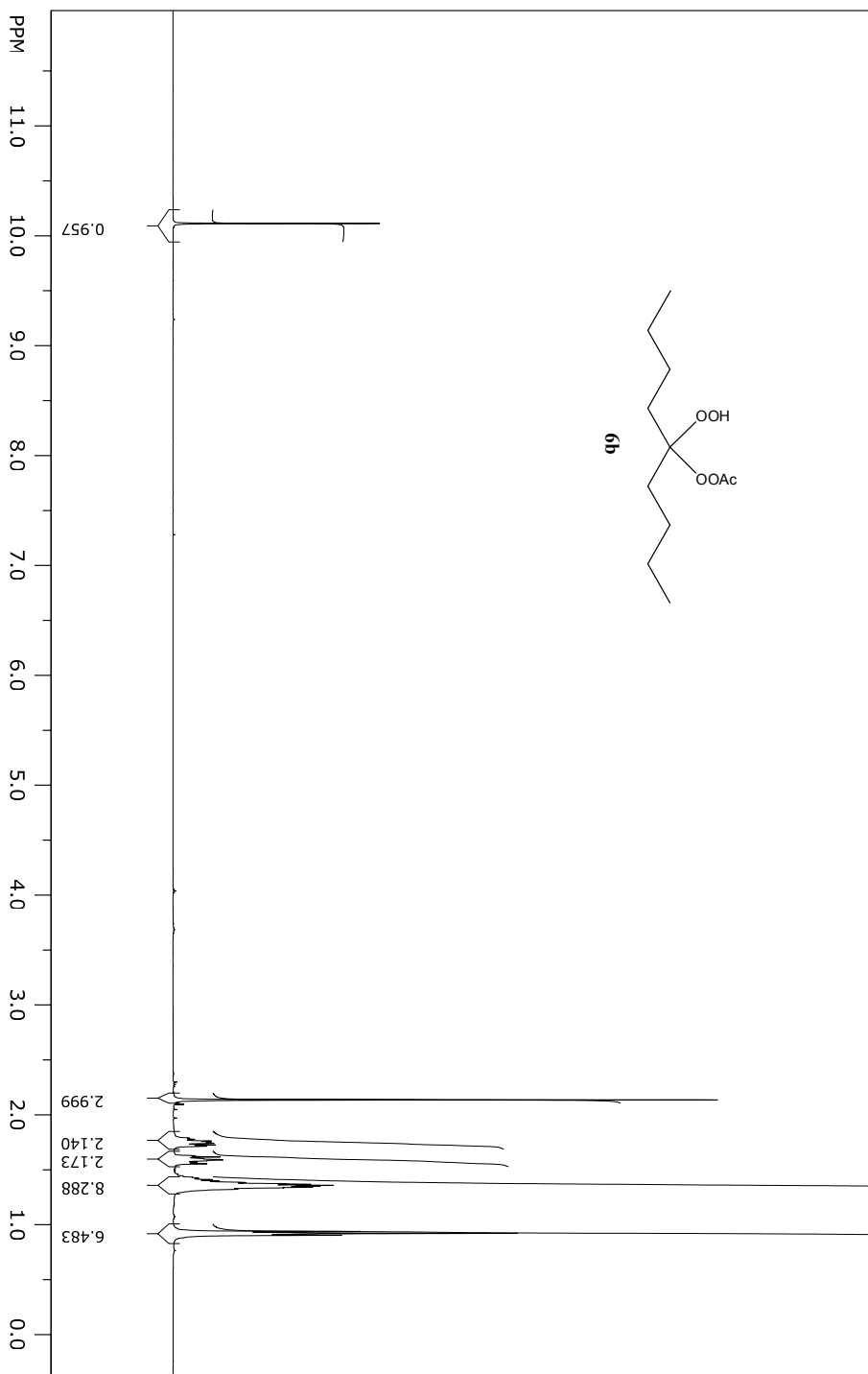
file: ...\data\nmr\notebook4\jh-4-18\2\fid   expt: <zgpg30>
transmitter freq.: 100.622830 MHz
time domain size: 65536 points
width: 23980.82 Hz = 238.3238 ppm = 0.365918 Hz/pt
number of scans: 46

freq. of 0 ppm: 100.612769 MHz
processed size: 32768 complex points
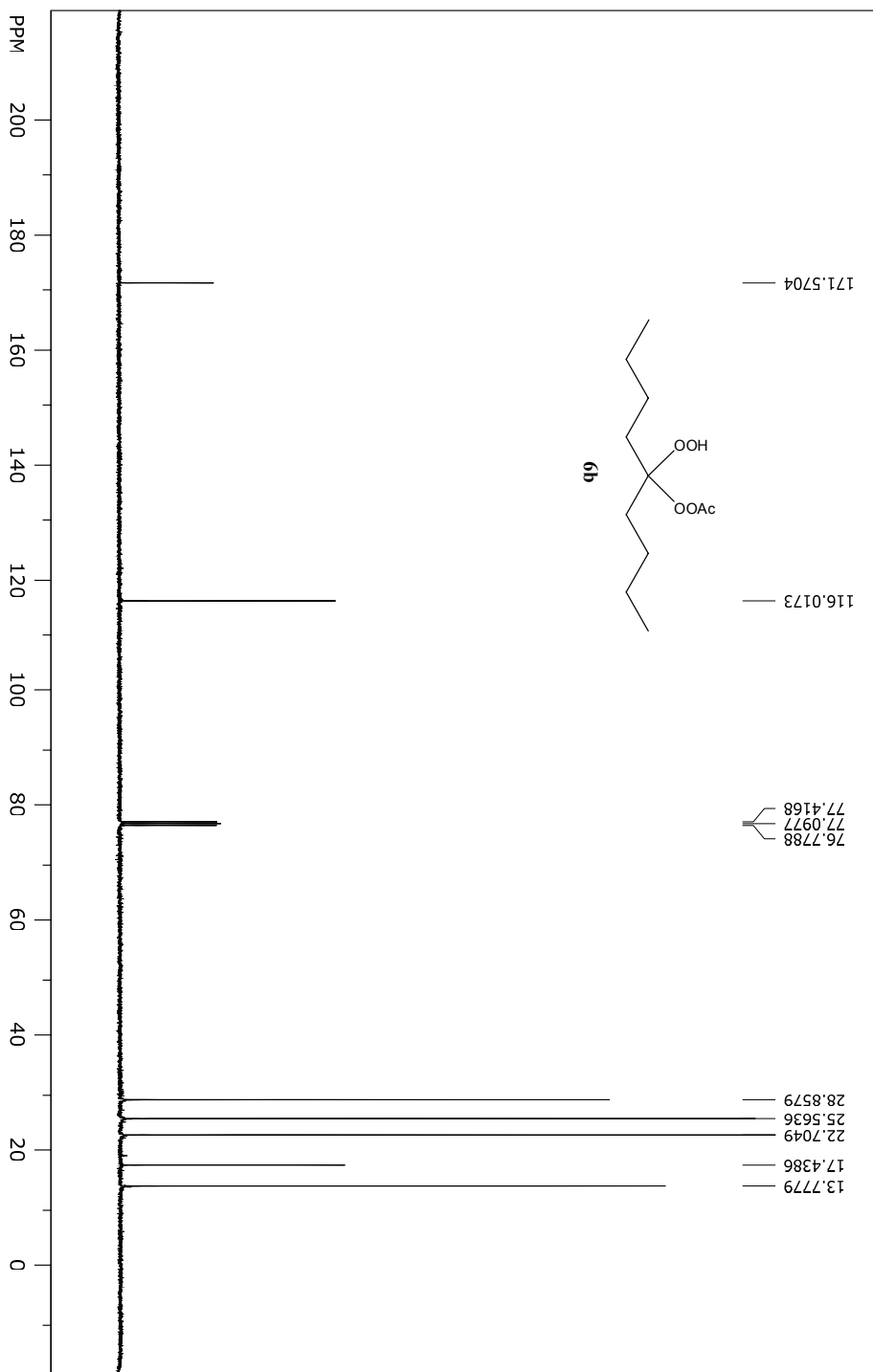LB: 1.000   GF: 0.0000
Hz/cm: 959.233   ppm/cm: 9.53295

.

Hang, et al: "Generation of singlet oxygen from fragmentation of monoactivated 1,1- dihydroperoxides"

SpinWorks 3: 1D Proton NMR

4b

OOH

OOAc

PPM 11.0 10.0 9.0 8.0 7.0 6.0 5.0 4.0 3.0 2.0 1.0

0.924

1.971
2.942

2.036

0.773
3.141
1.050

3.000

SI_Spectra-9

Hang, et al: "Generation of singlet oxygen from fragmentation of monoactivated 1,1- dihydroperoxides"

SpinWorks 3: 13C

4b

Structure label with OOH and OOAc substituents on a phenethyl chain.

Peaks:
171.6896
141.0395
128.6038
128.3832
126.2586
113.7213
99.9931
77.5402
77.2211
76.9023
34.8643
30.2449
18.1067
17.5665

PPM: 200 180 160 140 120 100 80 60 40 20 0

file: E:\data\nmr\notebook4\jh-4-2\2\fid   expt: <zgpg30>
transmitter freq.: 100.622830 MHz
time domain size: 65536 points
width: 23980.82 Hz = 238.3238 ppm = 0.365918 Hz/pt
number of scans: 19

freq. of 0 ppm: 100.612769 MHz
processed size: 32768 complex points
LB: 1.000   GF: 0.0000
Hz/cm: 959.233   ppm/cm: 9.53295

.

Hang, et al: "Generation of singlet oxygen from fragmentation of monoactivated 1,1- dihydroperoxides"

6b

OOH
OOAc

PPM   11.0   10.0   9.0   8.0   7.0   6.0   5.0   4.0   3.0   2.0   1.0   0.0

0.957

2.999
2.140
2.173
8.288
6.483

file: E:\data\nmr\notebook4\jh-4-9\1\fid   expt: <zg30>
transmitter freq.: 400.132471 MHz
time domain size: 65536 points
width: 8278.15 Hz = 20.6885 ppm = 0.126314 Hz/pt
number of scans: 16

freq. of 0 ppm: 400.130000 MHz
processed size: 32768 complex points
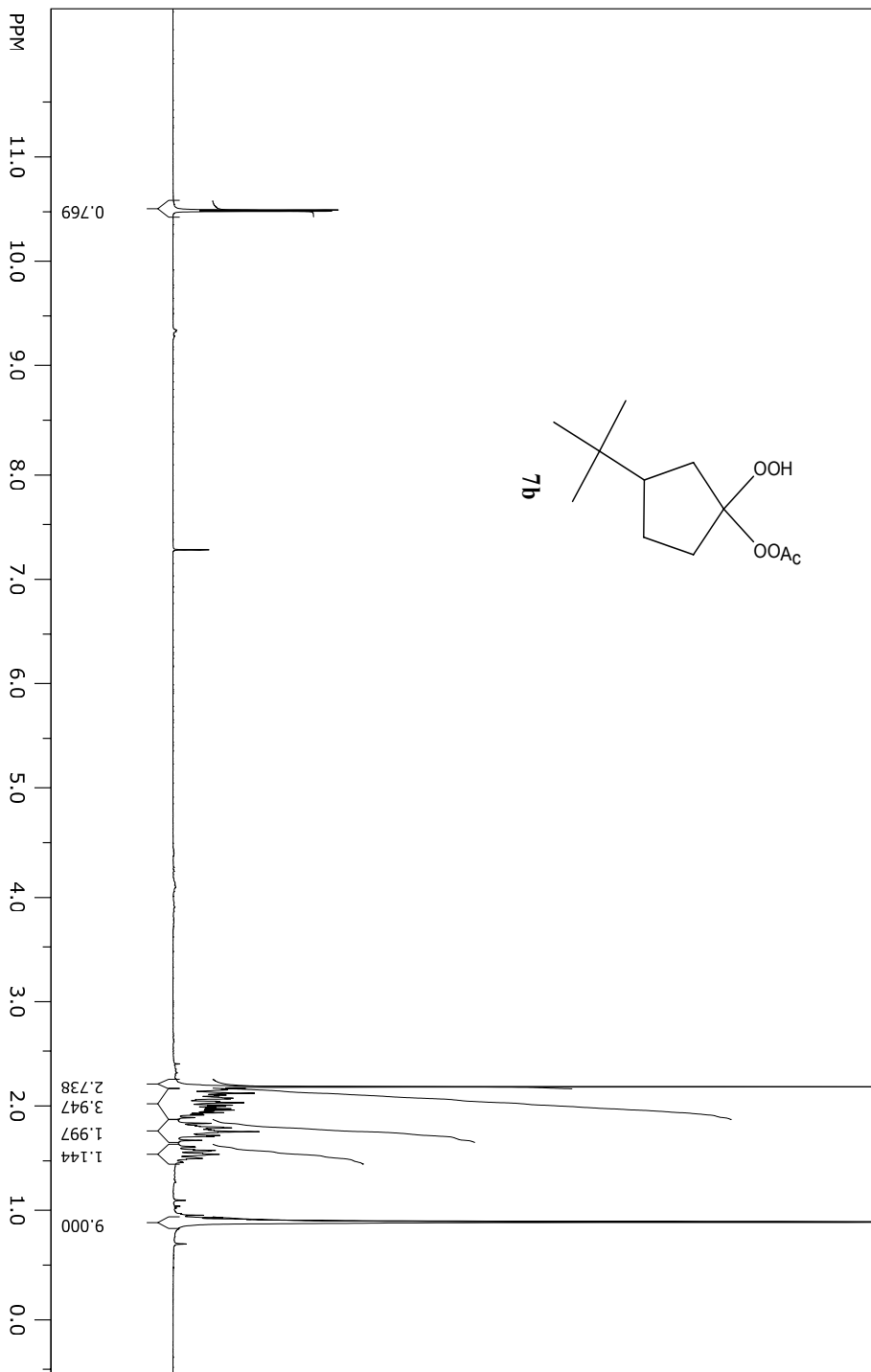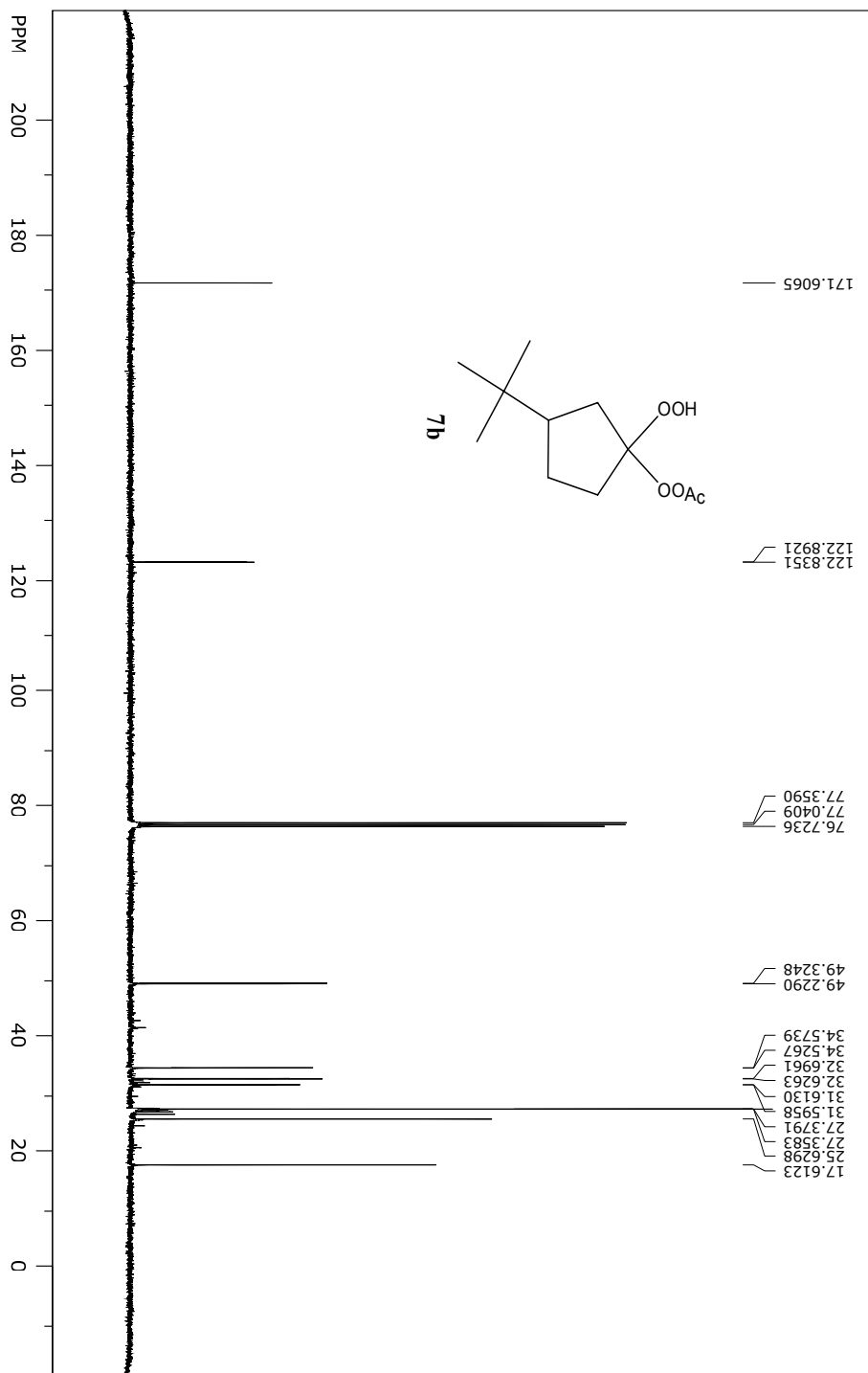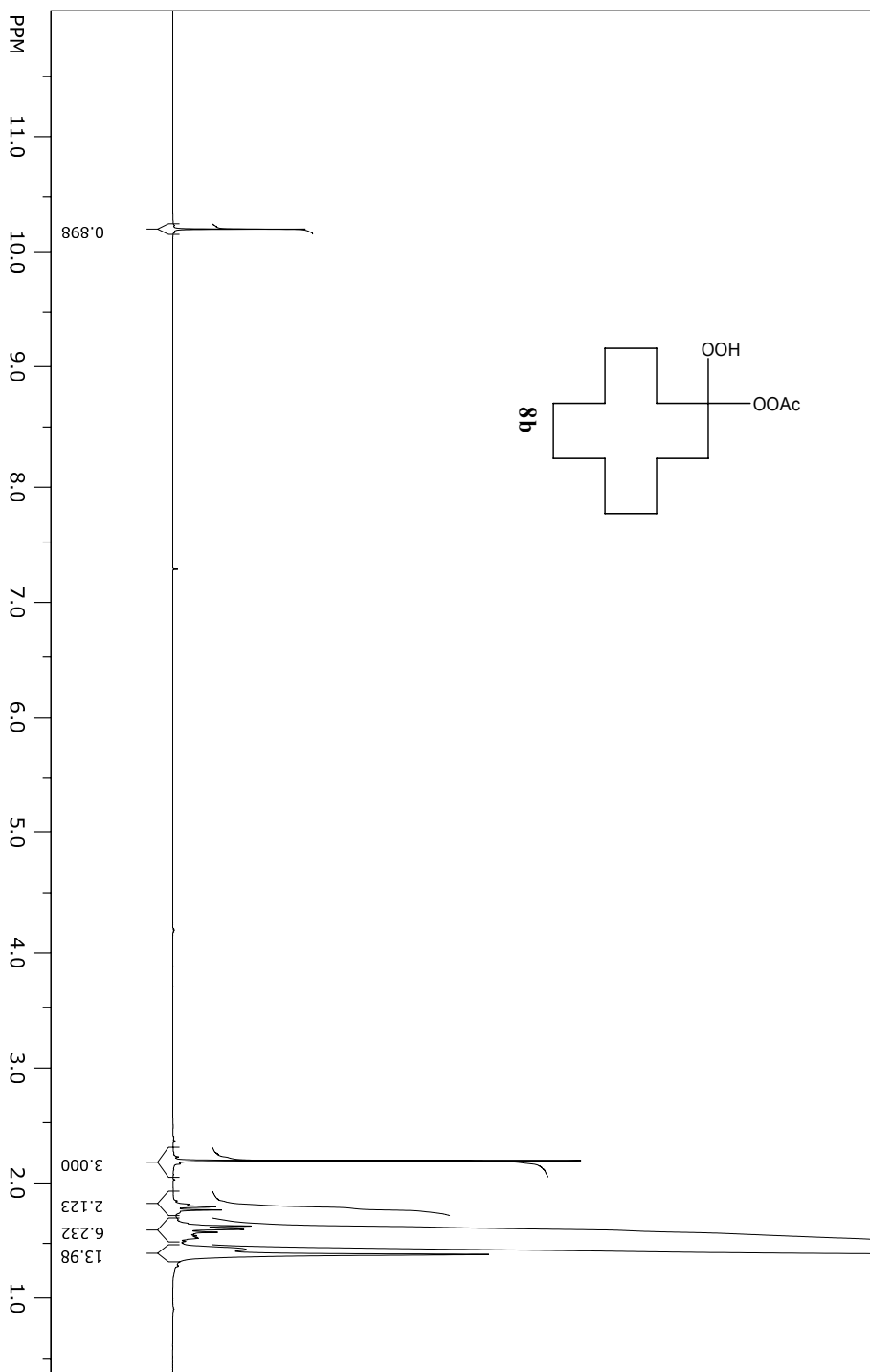LB: 0.300   GF: 0.0000
Hz/cm: 200.093   ppm/cm: 0.50007

SpinWorks 3: 13C

171.5704

116.0173

9b

OOH
OOAc

77.4168
77.0977
76.7788

28.8579
25.5636
22.7049
17.4386
13.7779

PPM   200   180   160   140   120   100   80   60   40   20   0

file: E:\data\nmr\notebook4\jh-4-9\2\fid   expt: <zgpg30>
transmitter freq.: 100.622830 MHz
time domain size: 65536 points
width: 23980.82 Hz = 238.3238 ppm = 0.365918 Hz/pt
number of scans: 26

freq. of 0 ppm: 100.612769 MHz
processed size: 32768 complex points
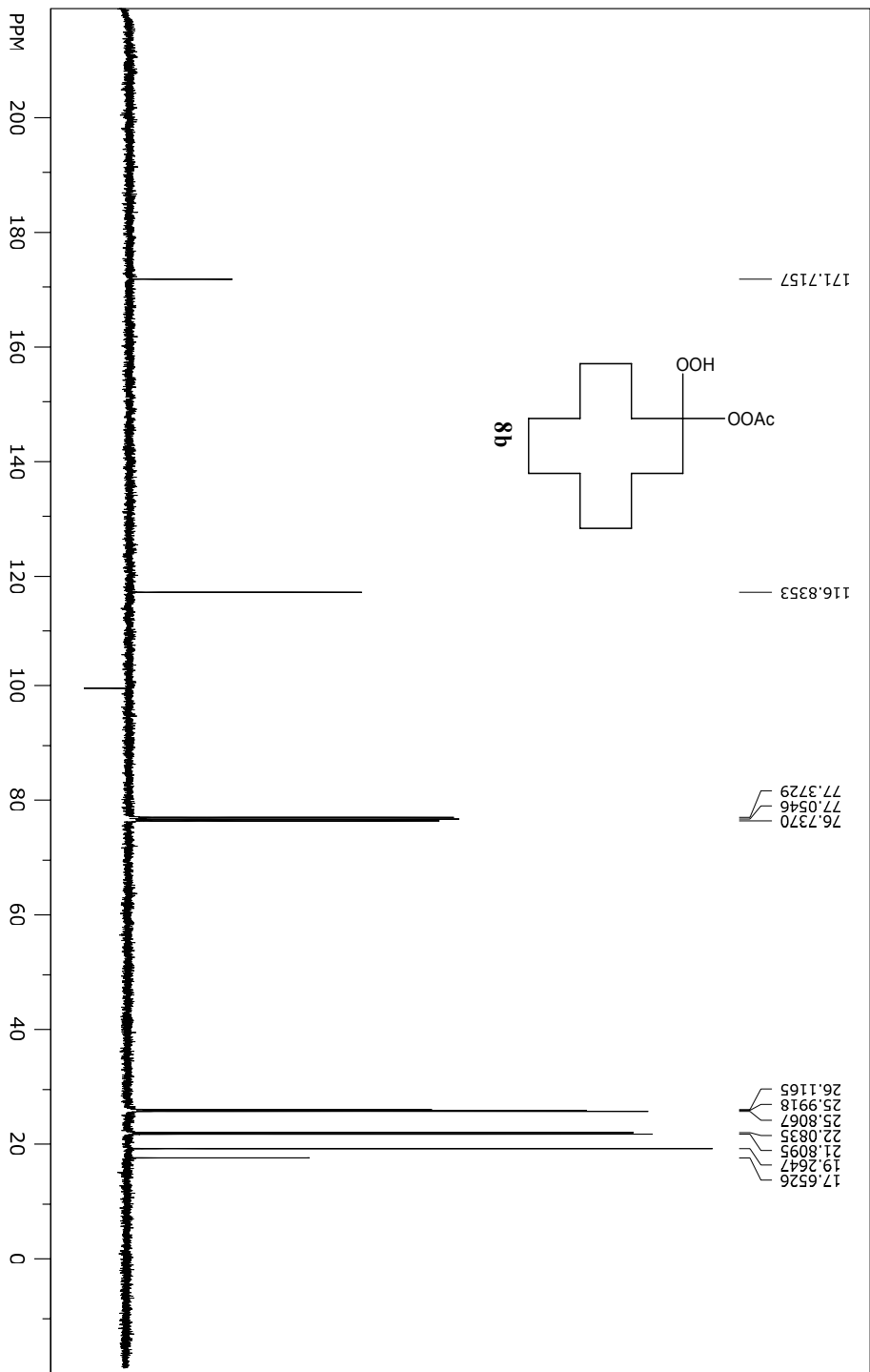LB: 1.000   GF: 0.0000
Hz/cm: 959.233   ppm/cm: 9.53295

SI_Spectra-12 .

Hang, et al: "Generation of singlet oxygen from fragmentation of monoactivated 1,1- dihydroperoxides"

7b

0.769

2.738
3.947
1.997
1.144

9.000

PPM   11.0   10.0   9.0   8.0   7.0   6.0   5.0   4.0   3.0   2.0   1.0   0.0

file: ...:\data\nmr\notebook4\jh-4-91\1\fid   expt: <zg30>
transmitter freq.: 300.131853 MHz
time domain size: 65536 points
width: 6172.84 Hz = 20.5671 ppm = 0.094190 Hz/pt
number of scans: 16

freq. of 0 ppm: 300.130000 MHz
processed size: 32768 complex points
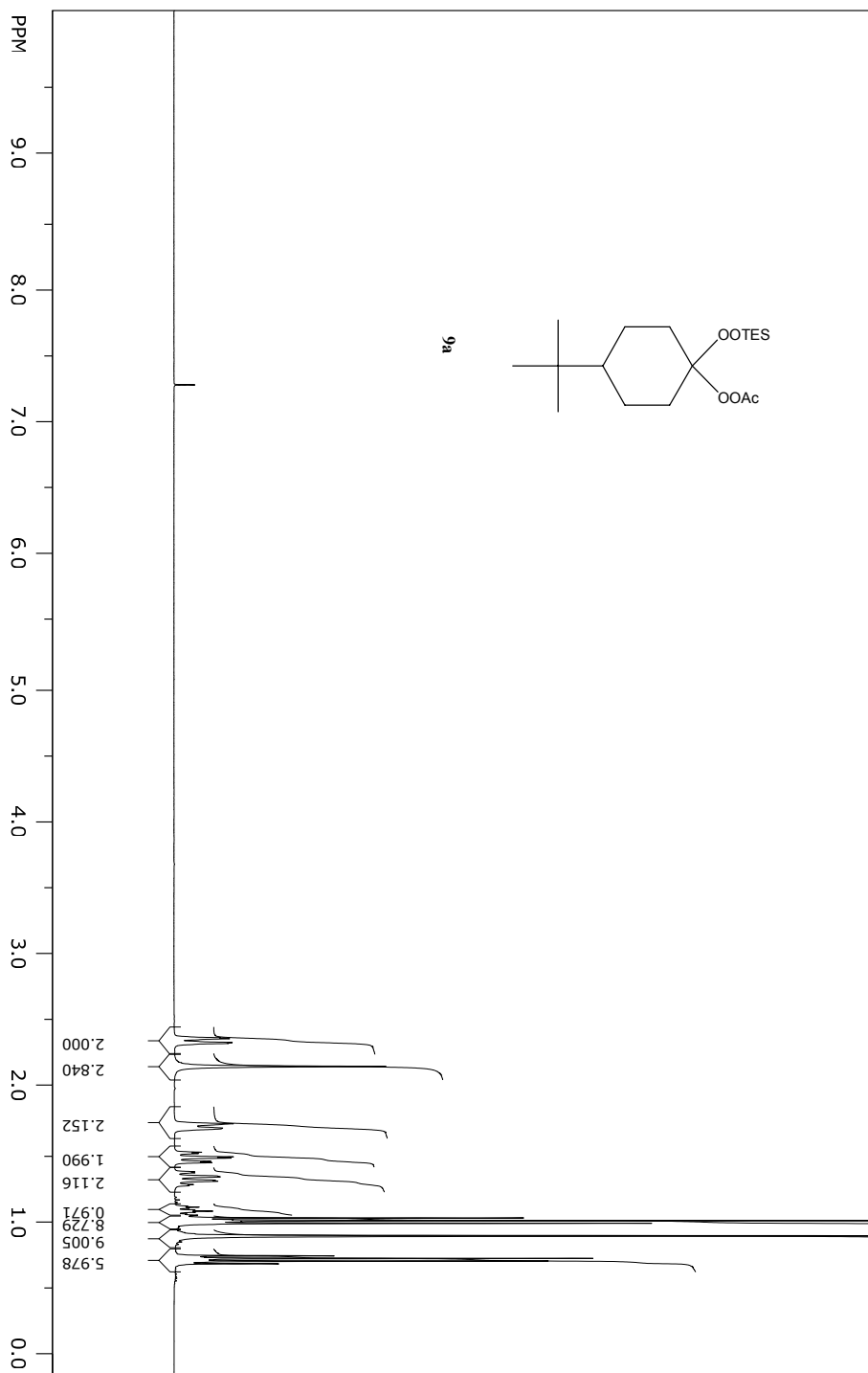LB: 0.300   GF: 0.0000
Hz/cm: 156.059   ppm/cm: 0.51997
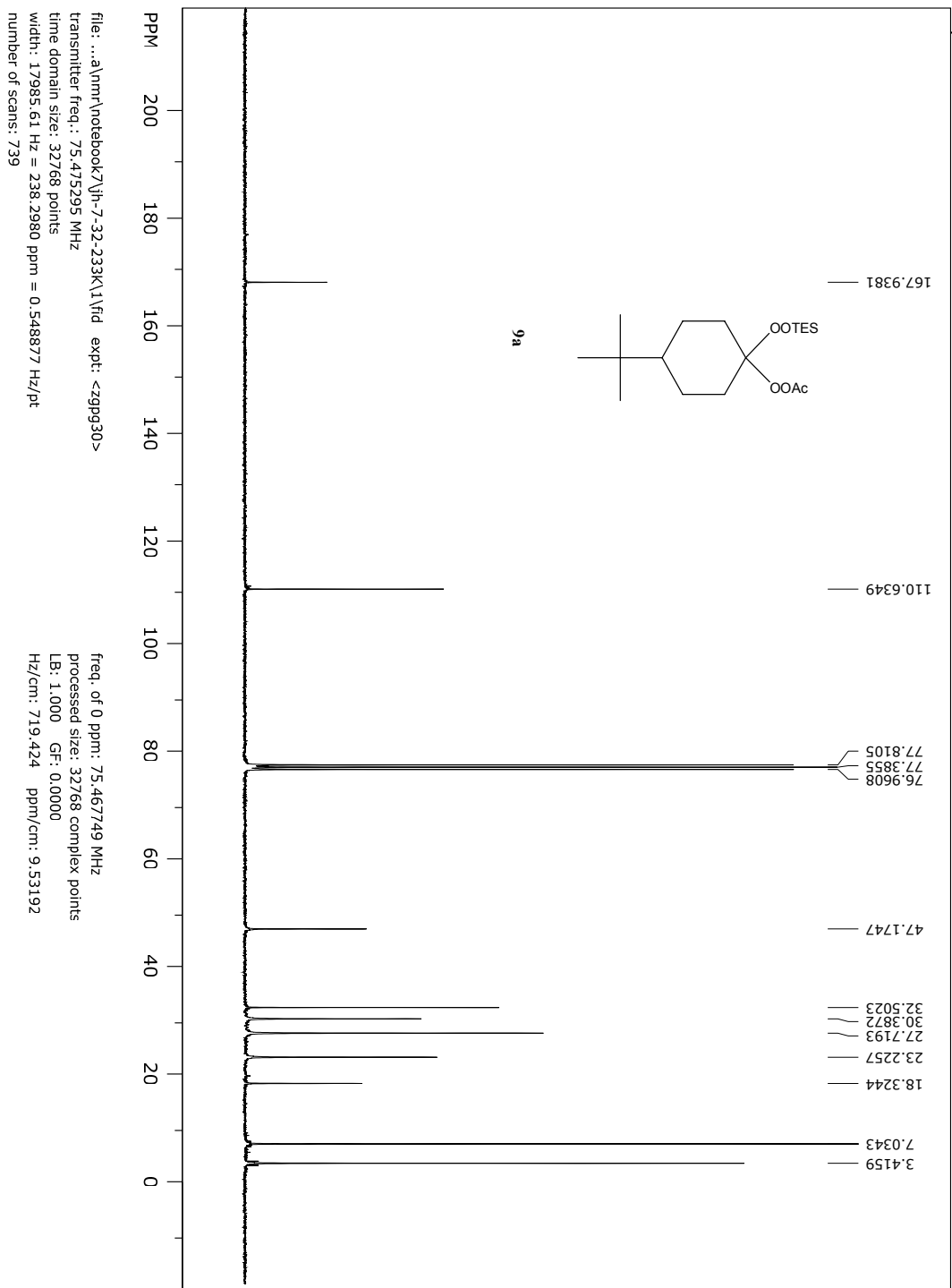
SpinWorks 3: 13C

171.6065

122.8921
122.8351

77.3590
77.0409
76.7236

49.3248
49.2290

34.5739
34.5267
32.6961
32.6263
31.6130
31.5958
27.3791
27.3583
25.6298
17.6123

7b

OOH

OOAc

PPM 200 180 160 140 120 100 80 60 40 20 0

PPM

OOH

OOAc

8b

0.898

11.0   10.0   9.0   8.0   7.0   6.0   5.0   4.0   3.0   2.0   1.0

3.000
2.123
6.232
13.98

SI_Spectra-15

Hang, et al: "Generation of singlet oxygen from fragmentation of monoactivated 1,1- dihydroperoxides"

SpinWorks 3: 13C

171.7157

OOH

OOAc

8b

116.8353

77.3729
77.0546
76.7370

26.1165
25.9918
25.8067
22.0835
21.8095
19.2647
17.6526

PPM   200   180   160   140   120   100   80   60   40   20   0

.

.

.

SI_Spectra-16 .

Hang, et al: "Generation of singlet oxygen from fragmentation of monoactivated 1,1- dihydroperoxides"

9a

OOTES

OOAc

PPM   9.0   8.0   7.0   6.0   5.0   4.0   3.0   2.0   1.0   0.0

2.000
2.840
2.152
1.990
2.116
0.971
8.729
9.005
5.978

SI_Spectra-17 .

Hang, et al: "Generation of singlet oxygen from fragmentation of monoactivated 1,1- dihydroperoxides"

167.9381

OOTES

9a

OOAc

110.6349

77.8105
77.3855
76.9608

47.1747

32.5023
30.3872
27.7193
23.2257

18.3244

7.0343
3.4159

PPM   200   180   160   140   120   100   80   60   40   20   0

9b

OOTBS

OOAc

PPM 7.6 7.2 6.8 6.4 6.0 5.6 5.2 4.8 4.4 4.0 3.6 3.2 2.8 2.4 2.0 1.6 1.2 0.8 0.4 0.0 -0.4

2.134
2.999
2.163
1.890
2.174
1.182
9.261
9.577
6.070
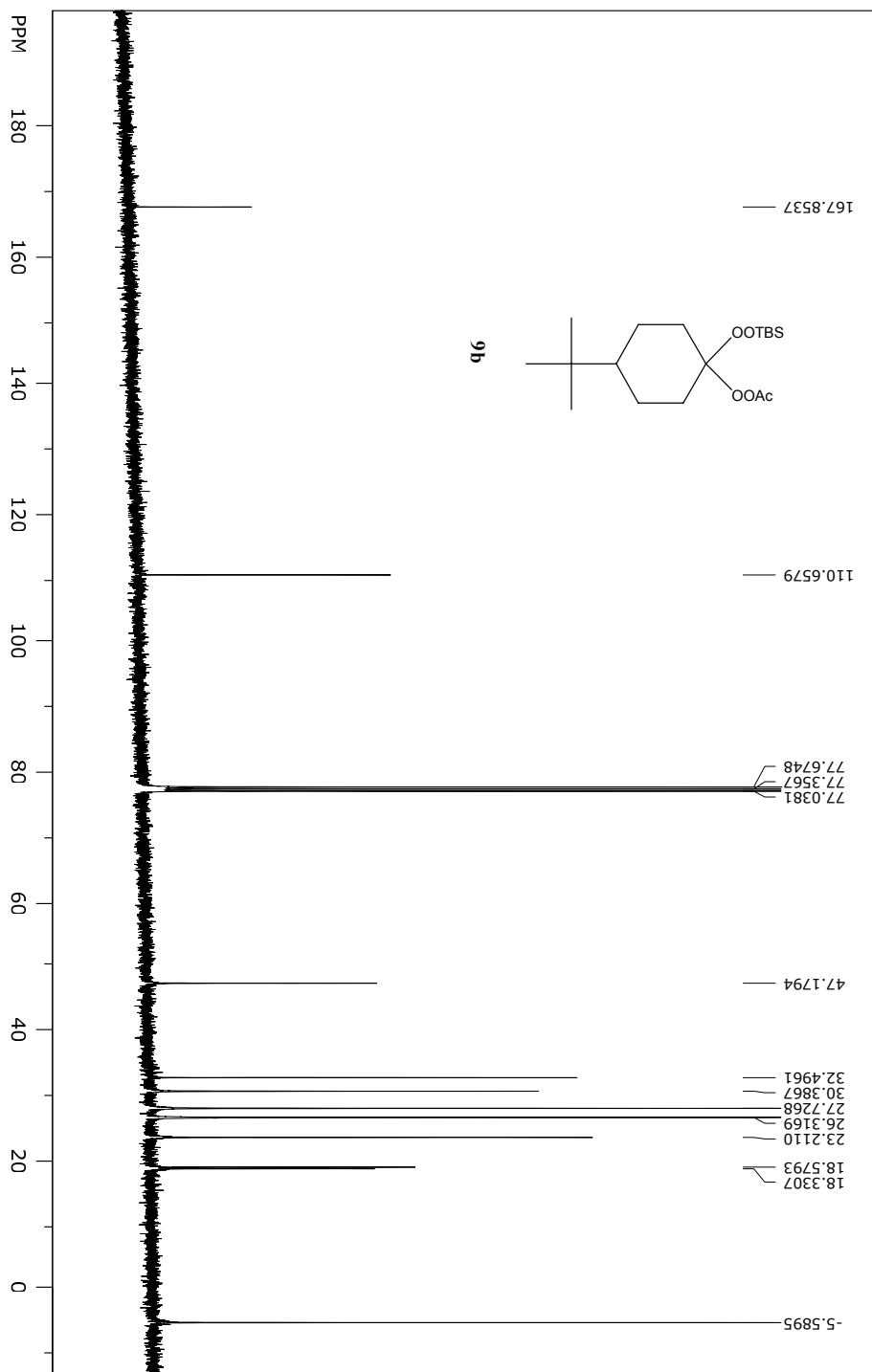
file: ...\data\nmr\notebook7\jh-7-31\1\fid   expt: <zg30>
transmitter freq.: 400.132471 MHz
time domain size: 65536 points
width: 8278.15 Hz = 20.6885 ppm = 0.126314 Hz/pt
number of scans: 16

freq. of 0 ppm: 400.130000 MHz
processed size: 32768 complex points
LB: 0.300   GF: 0.0000
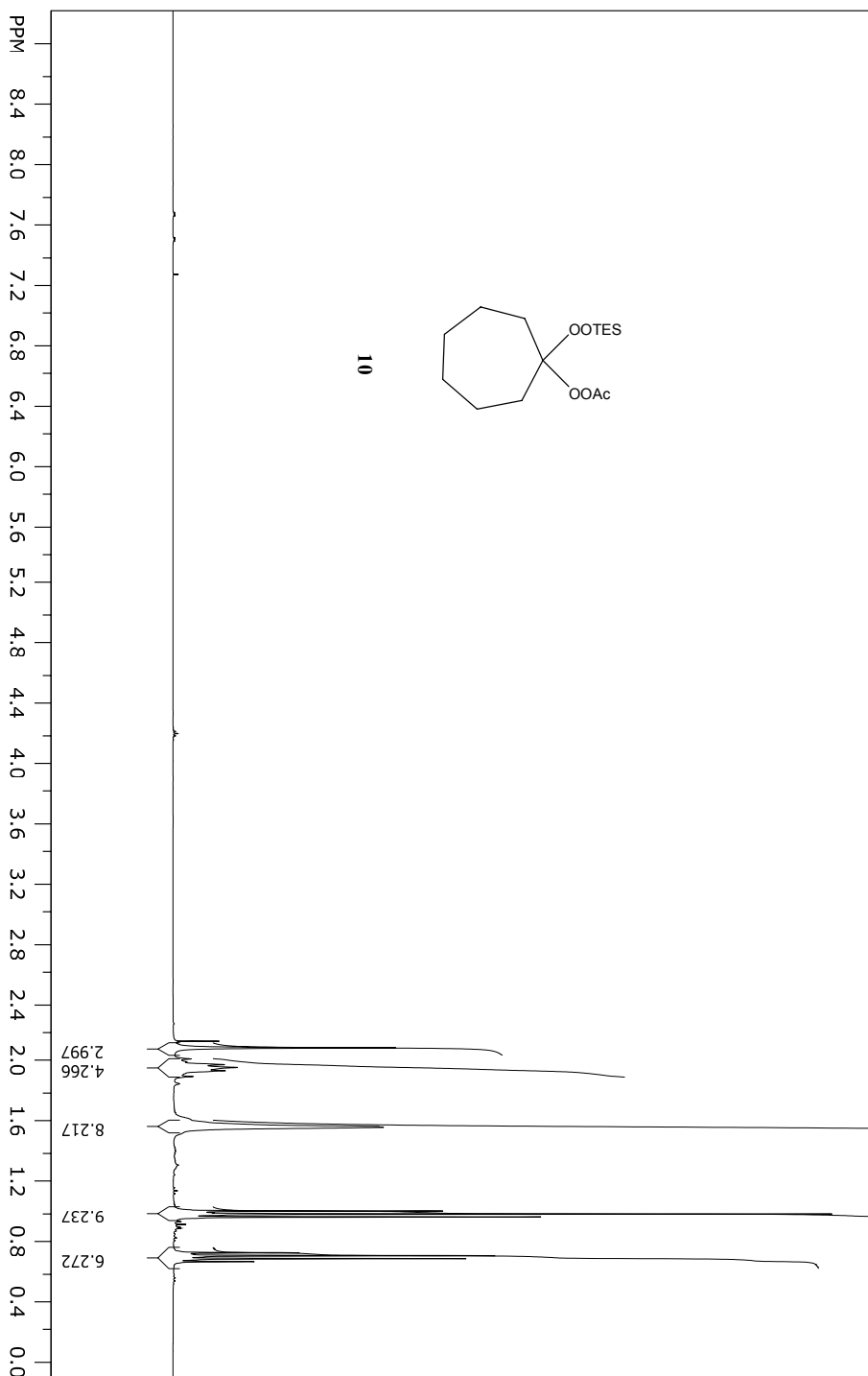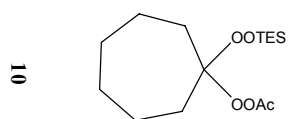Hz/cm: 144.687   ppm/cm: 0.36160

167.8537

110.6579

77.6748
77.3567
77.0381

47.1794

32.4961
30.3867
27.7268
26.3169
23.2110

18.5793
18.3307

-5.5895

9b

OOTBS

OOAc

PPM   180   160   140   120   100   80   60   40   20   0

SI_Spectra-20 .

Hang, et al: "Generation of singlet oxygen from fragmentation of monoactivated 1,1- dihydroperoxides"

10

OOTES

OOAc

2.997
4.266
8.217
9.237
6.272

PPM 8.4 8.0 7.6 7.2 6.8 6.4 6.0 5.6 5.2 4.8 4.4 4.0 3.6 3.2 2.8 2.4 2.0 1.6 1.2 0.8 0.4 0.0

SI_Spectra-21 .

Hang, et al: "Generation of singlet oxygen from fragmentation of monoactivated 1,1- dihydroperoxides"

PPM

200　180　160　140　120　100　80　60　40　20　0

10

OOTES

OOAc

115.9400

77.3984
77.0807
76.7623

32.9739
30.1730
22.7562
17.8387
6.6105
3.6898

SI_Spectra-22 .

Hang, et al: "Generation of singlet oxygen from fragmentation of monoactivated 1,1- dihydroperoxides"

11

OOTES

OOAc

PPM 8.8 8.4 8.0 7.6 7.2 6.8 6.4 6.0 5.6 5.2 4.8 4.4 4.0 3.6 3.2 2.8 2.4 2.0 1.6 1.2 0.8 0.4

3.000
4.229
10.47
9.030
6.166

file: ...\data\nmr\notebook4\jh-4-19\1\fid   expt: <zg30>
transmitter freq.: 400.132471 MHz
time domain size: 65536 points
width: 8278.15 Hz = 20.6885 ppm = 0.126314 Hz/pt
number of scans: 16

freq. of 0 ppm: 400.130000 MHz
processed size: 32768 complex points
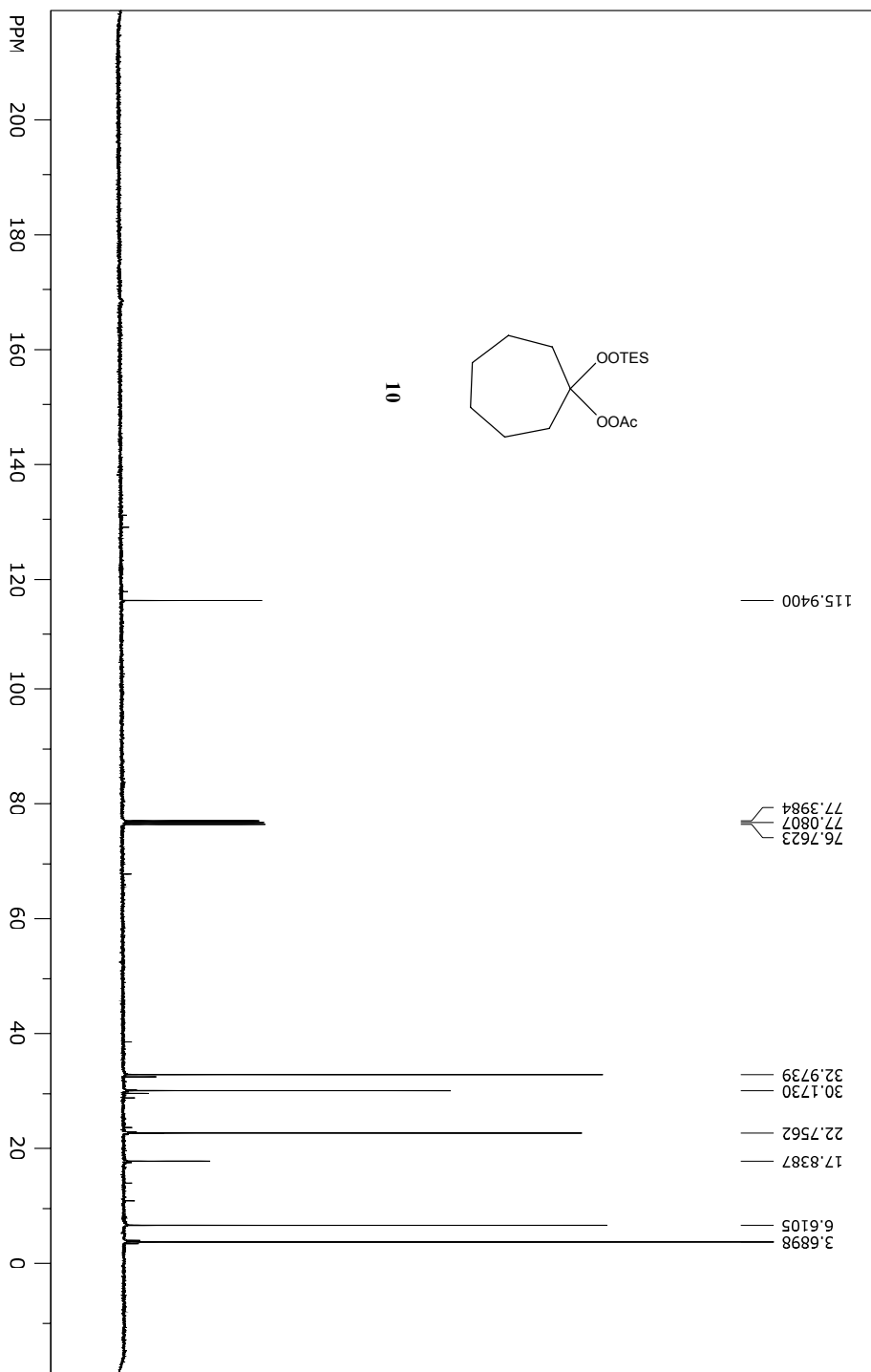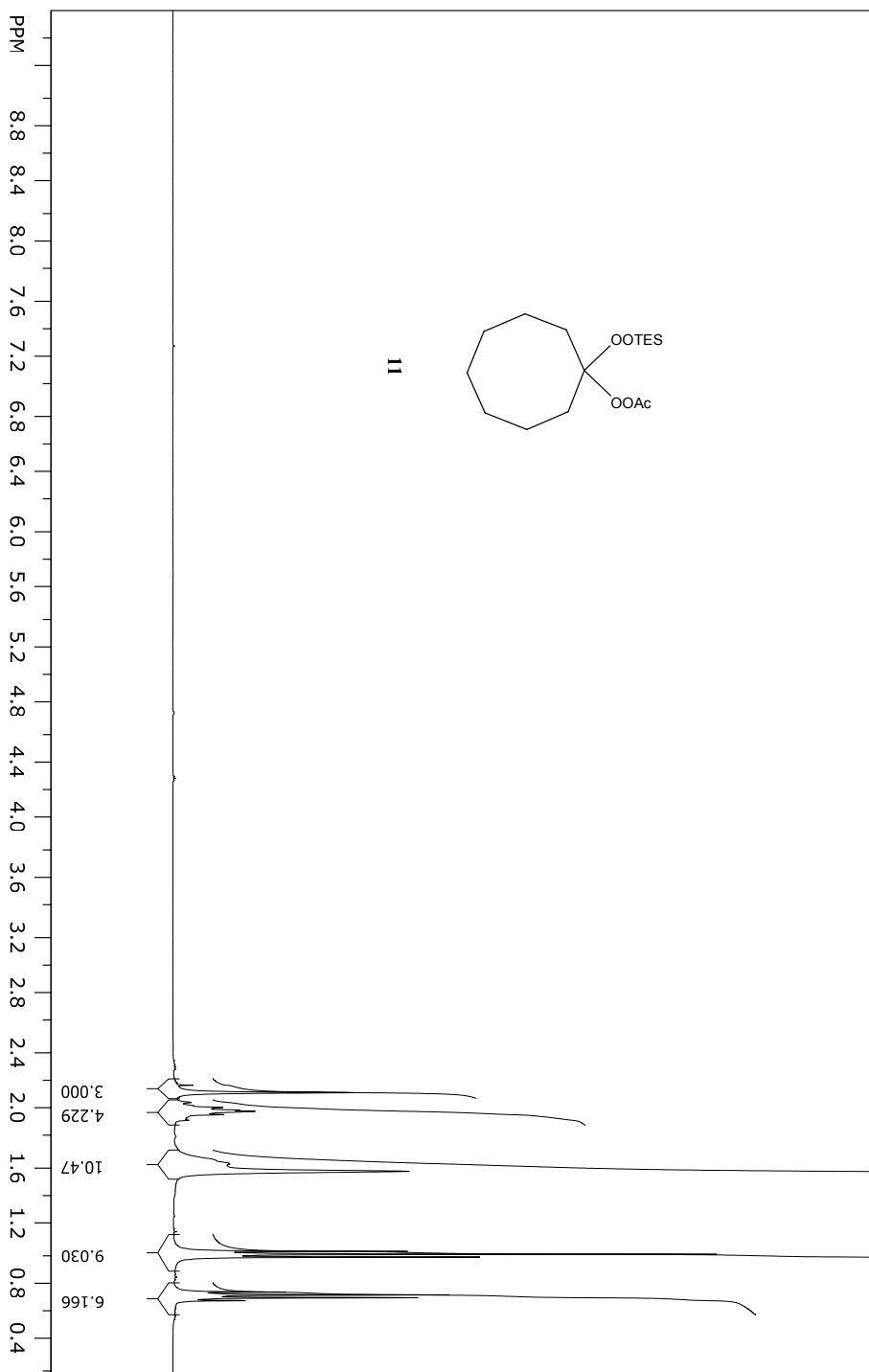LB: 0.300   GF: 0.0000
Hz/cm: 151.777   ppm/cm: 0.37932

SI_Spectra-23

Hang, et al: "Generation of singlet oxygen from fragmentation of monoactivated 1,1- dihydroperoxides"

PPM

180   160   140   120   100   80   60   40   20   0

168.0850

115.0308

77.6946
77.3758
77.0573

27.8421
27.2127
24.6628
21.9830
18.1862

6.9783
3.3991

11

OOTES

OOAc

SI_Spectra-24

12

OOTES

OOAc

PPM

9.0   8.0   7.0   6.0   5.0   4.0   3.0   2.0   1.0   0.0
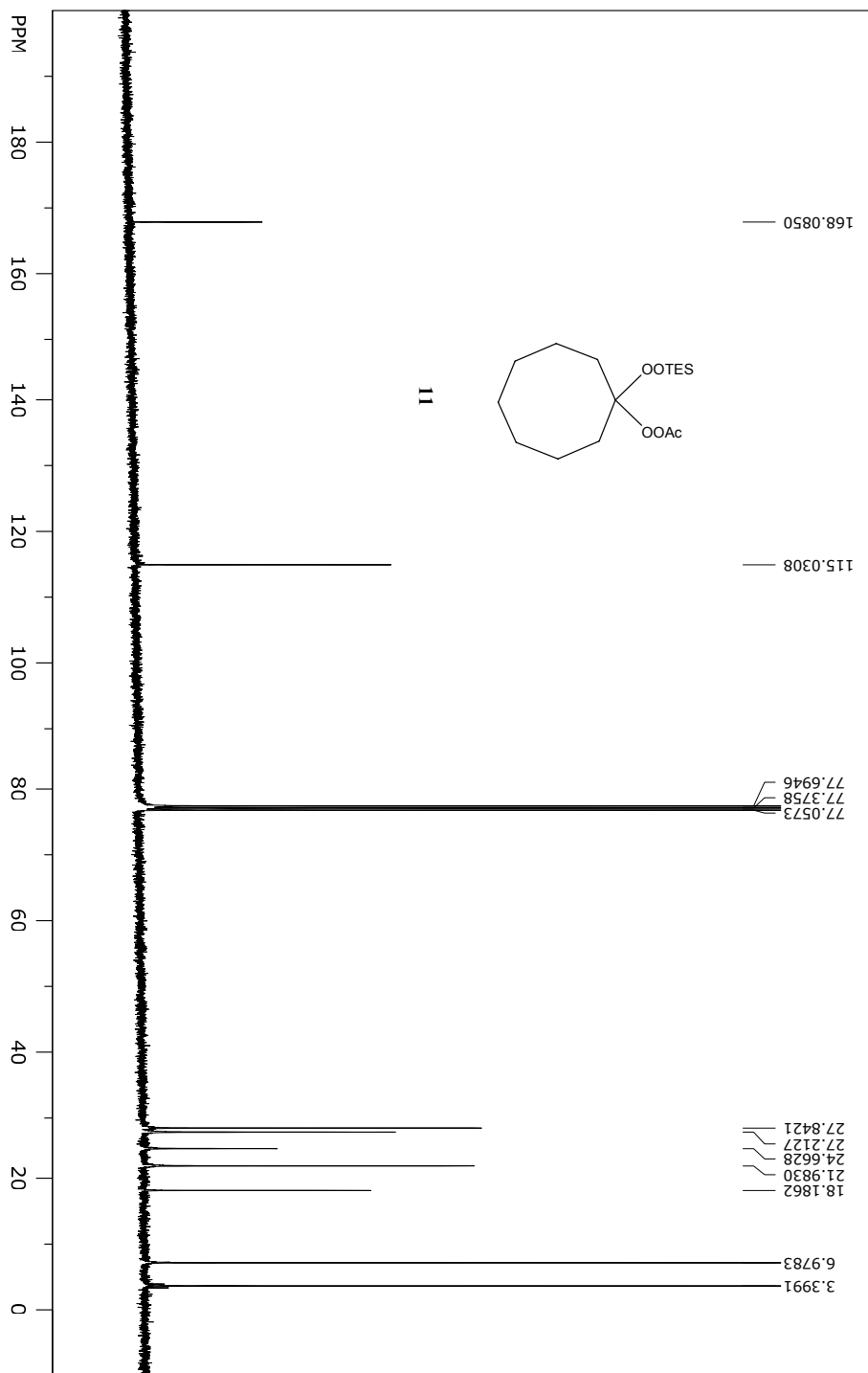
2.110
3.106

2.059

5.089

3.085

9.116

5.998

file: E:\data\nmr\notebook4\jh-4-3\1\fid   expt: <zg30>
transmitter freq.: 400.132471 MHz
time domain size: 65536 points
width: 8278.15 Hz = 20.6885 ppm = 0.126314 Hz/pt
number of scans: 16

freq. of 0 ppm: 400.130000 MHz
processed size: 32768 complex points
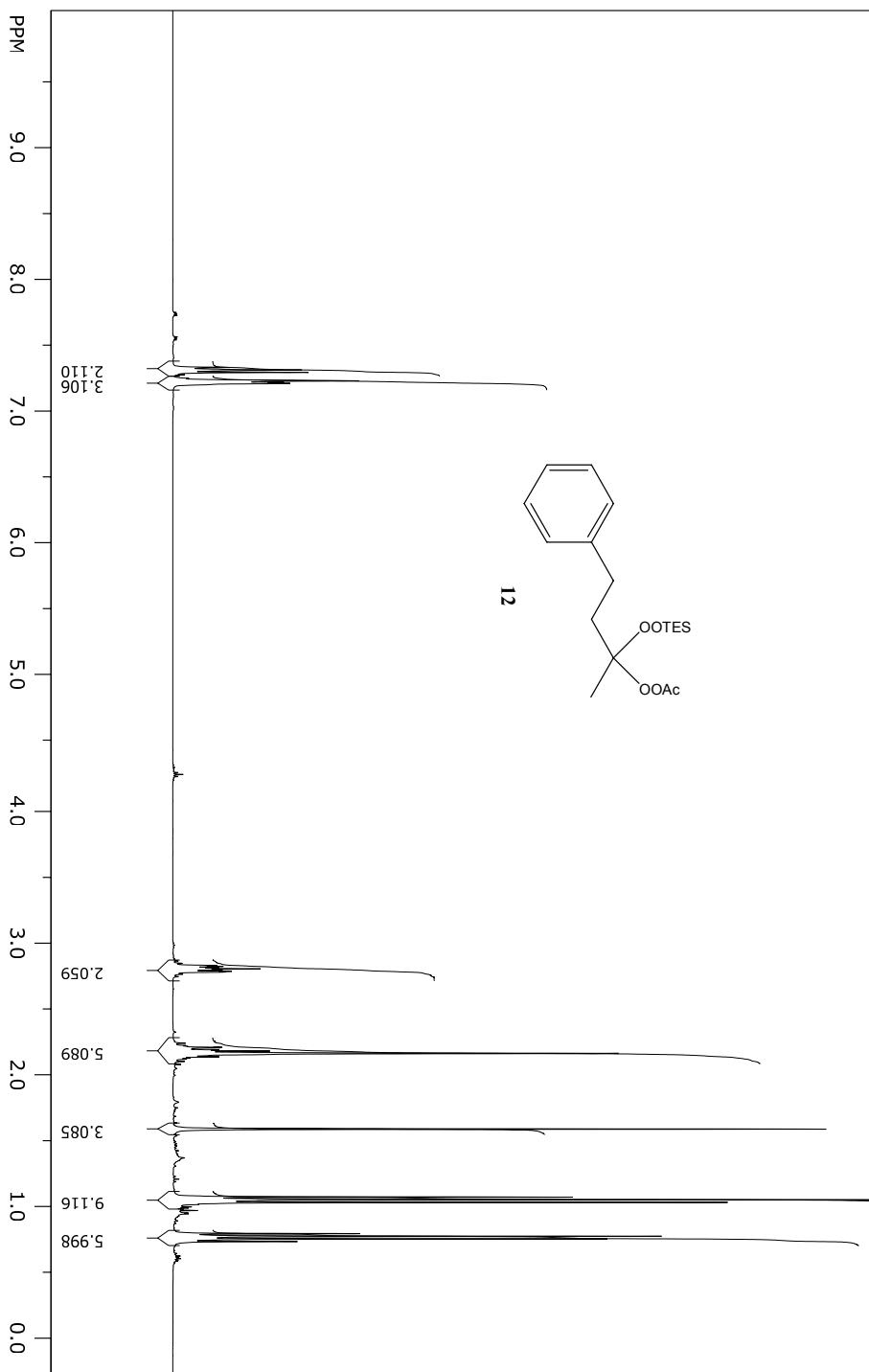LB: 0.300   GF: 0.0000
Hz/cm: 165.432   ppm/cm: 0.41344

SI_Spectra-25 .

Hang, et al: "Generation of singlet oxygen from fragmentation of monoactivated 1,1- dihydroperoxides"

SpinWorks 3: 13C

PPM

200 180 160 140 120 100 80 60 40 20 0

141.2659

128.5055
128.3132
126.1018

111.9391

77.4360
77.1181
76.7997

35.5343

30.3452

18.4709
17.8161

6.6915
3.7438

12

OOTES

OOAc

file: E:\data\nmr\notebook4\jh-4-3\2\fid   expt: <zgpg30>
transmitter freq.: 100.622830 MHz
time domain size: 65536 points
width: 23980.82 Hz = 238.3238 ppm = 0.365918 Hz/pt
number of scans: 46

freq. of 0 ppm: 100.612769 MHz
processed size: 32768 complex points
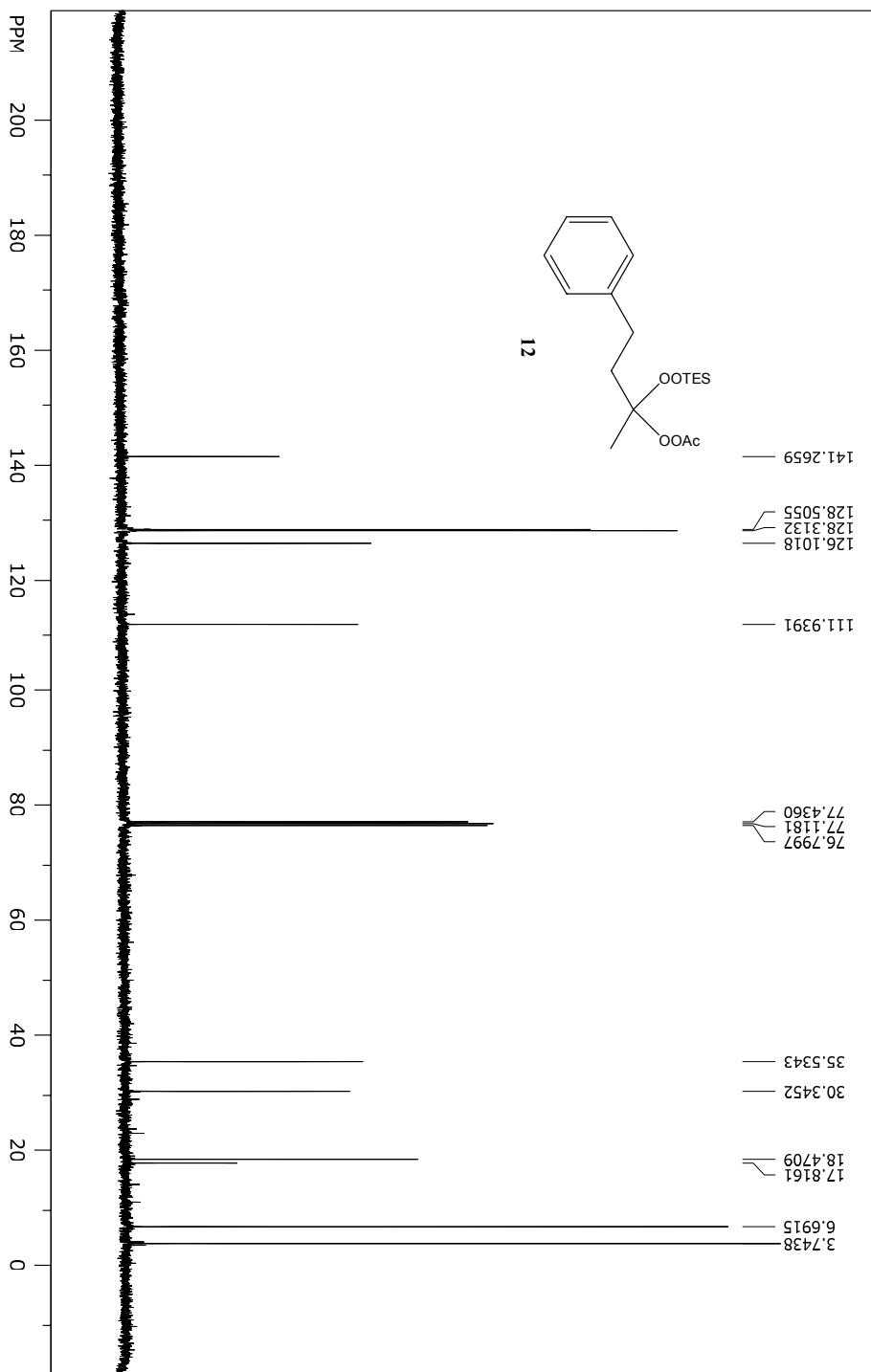LB: 1.000   GF: 0.0000
Hz/cm: 959.233   ppm/cm: 9.53295

SI_Spectra-26 .

Hang, et al: "Generation of singlet oxygen from fragmentation of monoactivated 1,1- dihydroperoxides"

13

OOTES

OOAc

PPM

8.4 8.0 7.6 7.2 6.8 6.4 6.0 5.6 5.2 4.8 4.4 4.0 3.6 3.2 2.8 2.4 2.0 1.6 1.2 0.8 0.4

3.000

4.159

8.306

8.995

6.627

6.105

file: ...\data\nmr\notebook4\jh-4-10\1\fid   expt: <zg30>
transmitter freq.: 400.132471 MHz
time domain size: 65536 points
width: 8278.15 Hz = 20.6885 ppm = 0.126314 Hz/pt
number of scans: 16

freq. of 0 ppm: 400.130000 MHz
processed size: 32768 complex points
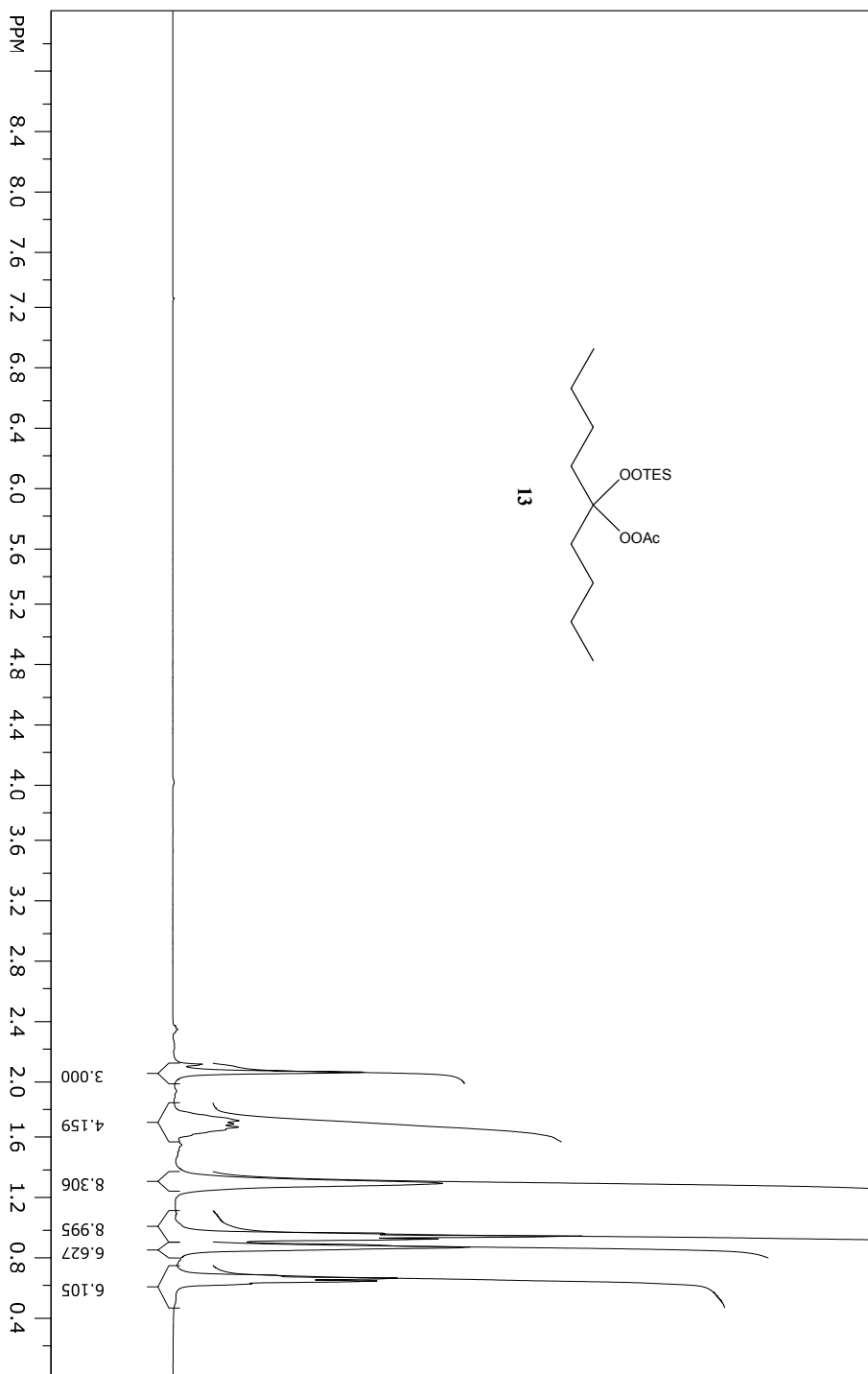LB: 0.300   GF: 0.0000
Hz/cm: 148.363   ppm/cm: 0.37079

SI_Spectra-27

Hang, et al: "Generation of singlet oxygen from fragmentation of monoactivated 1,1- dihydroperoxides"

PPM 200 180 160 140 120 100 80 60 40 20 0

114.0582

13

OOTES

OOAc

77.4286
77.1100
76.7914

29.5935
25.5295
22.7216
17.7170
13.7292
6.4911
3.6141

SI_Spectra-28 .

Hang, et al: "Generation of singlet oxygen from fragmentation of monoactivated 1,1- dihydroperoxides"

SpinWorks 3: 1D Proton NMR

14

OOTES

OOAc

PPM 10.0 9.0 8.0 7.0 6.0 5.0 4.0 3.0 2.0 1.0 0.0

3.103
4.580
18.30
8.949
5.999
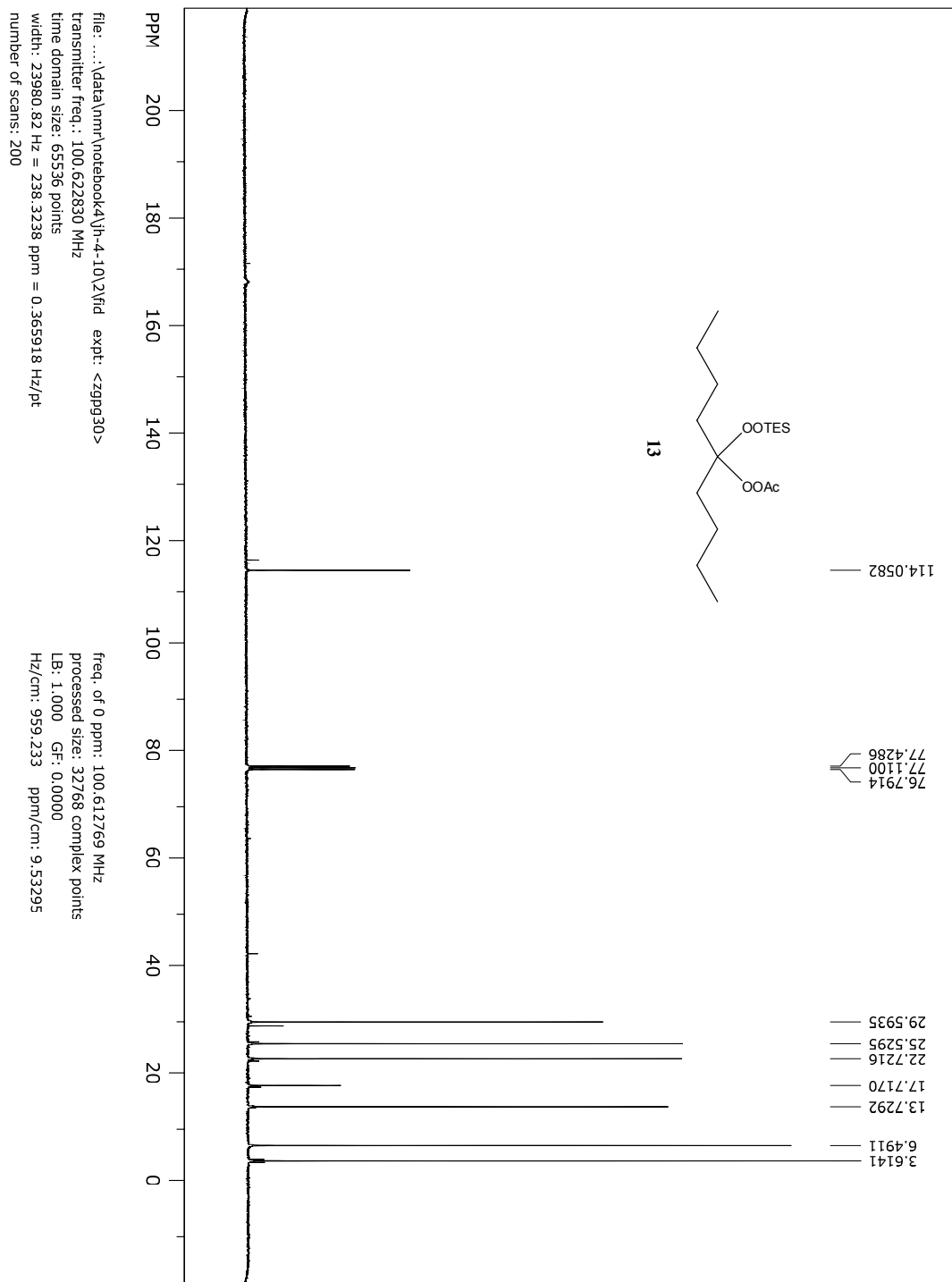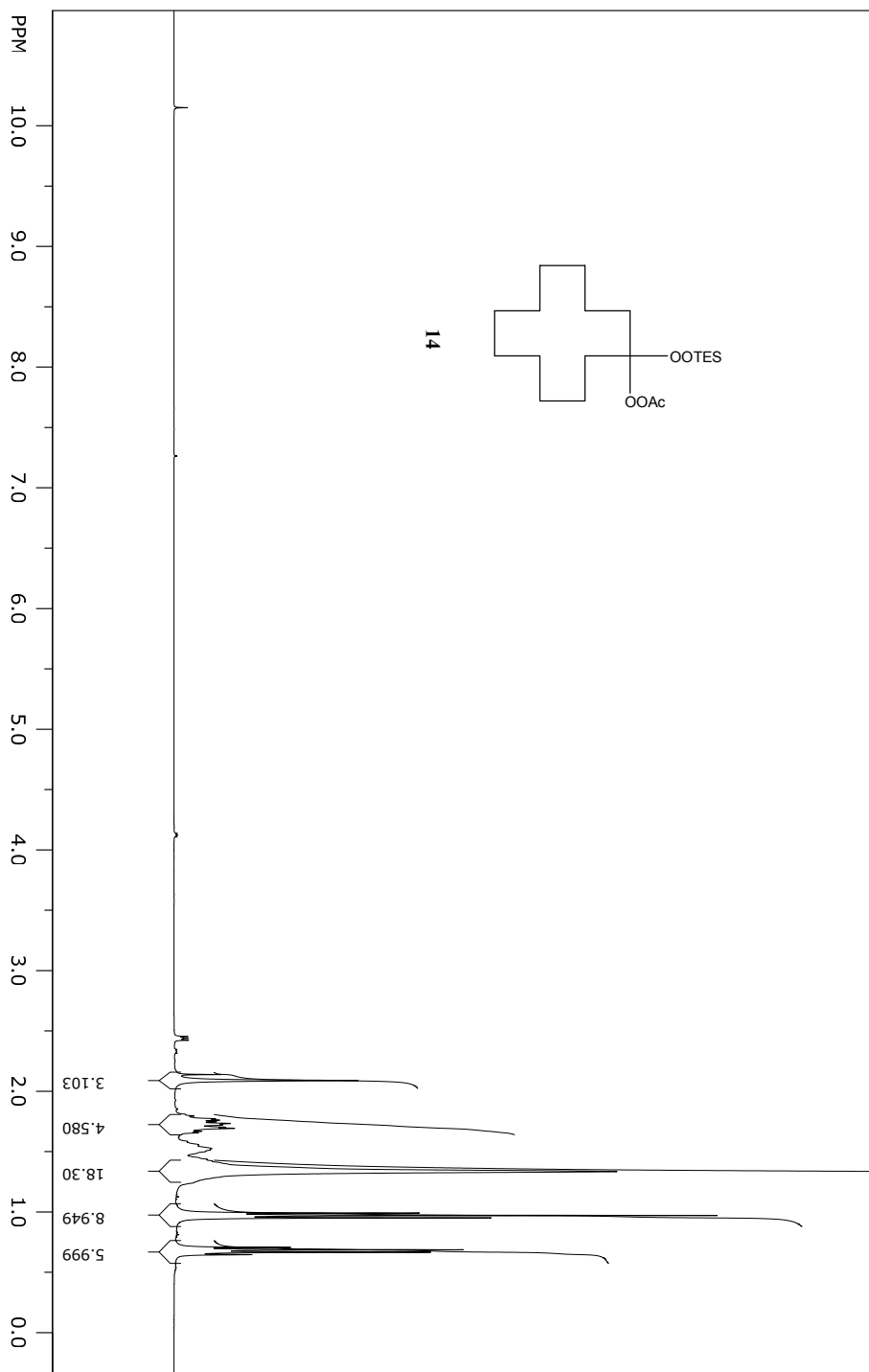
file: ...\data\nmr\notebook4\jh-4-44\1\fid   expt: <zg30>
transmitter freq.: 400.132471 MHz
time domain size: 65536 points
width: 8278.15 Hz = 20.6885 ppm = 0.126314 Hz/pt
number of scans: 16

freq. of 0 ppm: 400.130000 MHz
processed size: 32768 complex points
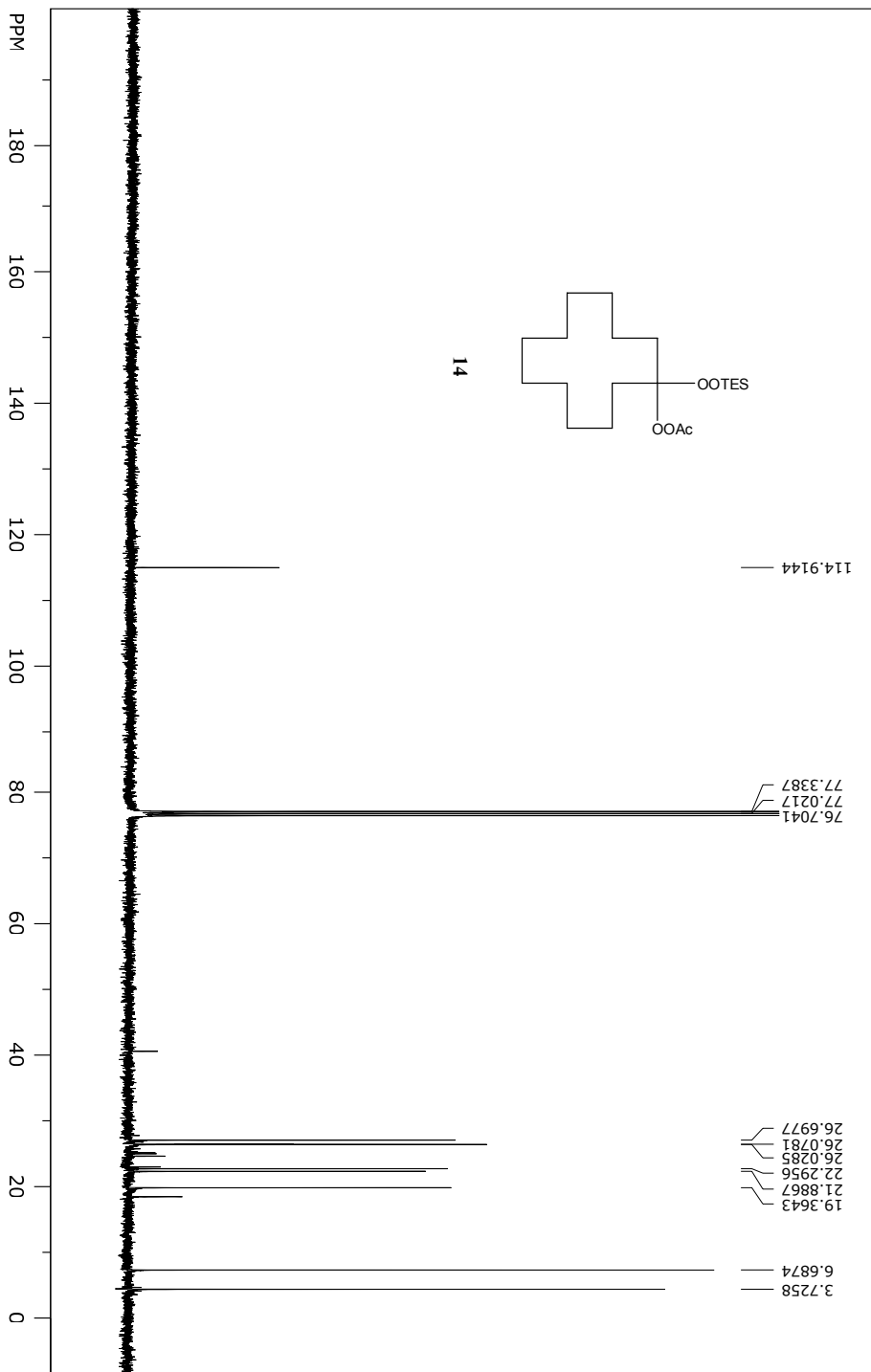LB: 0.300   GF: 0.0000
Hz/cm: 181.975   ppm/cm: 0.45479

SI_Spectra-29 .

Hang, et al: "Generation of singlet oxygen from fragmentation of monoactivated 1,1- dihydroperoxides"

PPM

180   160   140   120   100   80   60   40   20   0

14

OOTES

OOAc

114.9144

77.3387
77.0217
76.7041

26.6977
26.0781
26.0285
22.2956
21.8867
19.3643

6.6874

3.7258

file: ...a\nmr\notebook4\jh-4-44-pure\2\fid   expt: <zgpg30>
transmitter freq.: 100.622830 MHz
time domain size: 65536 points
width: 23980.82 Hz = 238.3238 ppm = 0.365918 Hz/pt
number of scans: 1024

freq. of 0 ppm: 100.612769 MHz
processed size: 32768 complex points
LB: 1.000   GF: 0.0000
Hz/cm: 845.890   ppm/cm: 8.40654

SI_Spectra-30 .

16

PPM 7.2 6.8 6.4 6.0 5.6 5.2 4.8 4.4 4.0 3.6 3.2 2.8 2.4 2.0 1.6 1.2 0.8 0.4 0.0

2.000 2.655 3.123 2.061 2.064 2.108 1.052 9.226

file: ...\data\nmr\notebook4\jh-4-52\1\fid   expt: <zg30>
transmitter freq.: 400.132471 MHz
time domain size: 65536 points
width: 8278.15 Hz = 20.6885 ppm = 0.126314 Hz/pt
number of scans: 16

freq. of 0 ppm: 400.130000 MHz
processed size: 32768 complex points
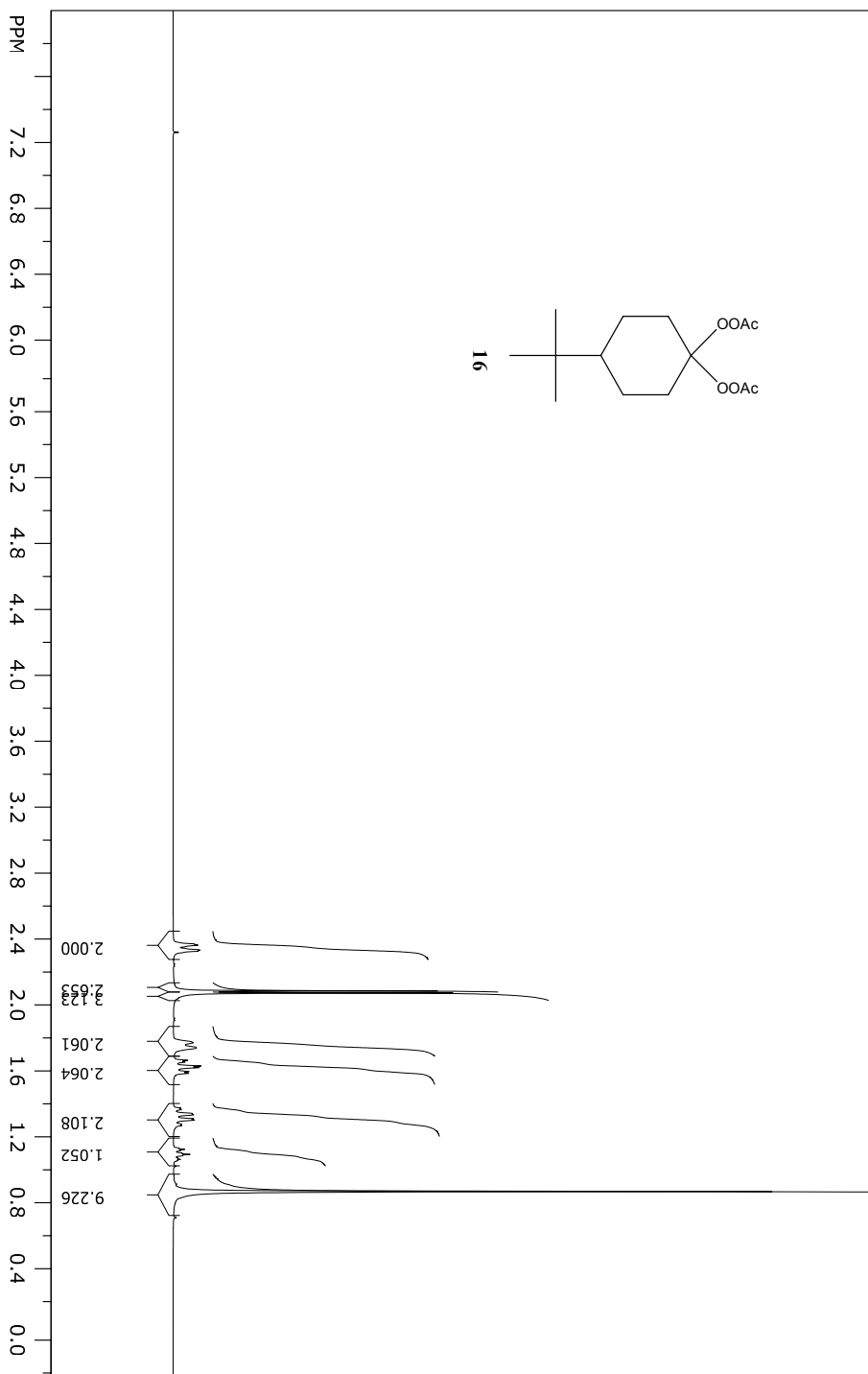LB: 0.300   GF: 0.0000
Hz/cm: 132.608   ppm/cm: 0.33141

SI_Spectra-31 .

Hang, et al: "Generation of singlet oxygen from fragmentation of monoactivated 1,1- dihydroperoxides"

167.4831
167.3791

OOAc
OOAc

111.5112

77.4387
77.1197
76.8008

47.0530

32.2313
30.1073
27.4833
23.1630

17.5471
17.4311

PPM   200   180   160   140   120   100   80   60   40   20   0

16

.

SI_Spectra-32

Hang, et al: "Generation of singlet oxygen from fragmentation of monoactivated 1,1- dihydroperoxides"